TECHNIQUES FOR CALCULATING Cw AND TDS FROM LOGS

Chapter 14

Assessment of ground-water quality from well logs usually centers around values for total dissolved solids (TDS) and specific conductance (Cw). Well logs are used to calculate Cw and then TDS is estimated from previously established TDS-Cw graphs. Sometimes other water properties such as chloride content and total hardness can be estimated from similar graphs. In some cases, TDS can be estimated directly from the log data. Unfortunately, trace elements such as iron, fluoride, and nitrates cannot be detected.

While it has been documented in other studies that determination of Cw and TDS from logging data is feasible (Chapter 1), many ground-water researchers have had little success applying the techniques. Both the cause and effect of this is the fact that most ground-water logging literature has only a cursory discussion of the subject.

This chapter is a discussion of seven techniques for calculating Cw and TDS from logging data. The first three (TDS-Ro Graphs, Ro_c-TDS Graphs, and Field Formation Factor) are empirical relationships that must be derived from the available data in a localized geographic areas (e.g. a county). The last four (Formation Factor Equation, Ro-Porosity Graphs, Resistivity Ratio Method, and SP) are stand-alone techniques that calculate Rw. This chapter also contains guidelines for accurate Cw calculations and a discussion of sources of logs in Texas.

Considerable variation exists in the logging literature for two terms important to this discussion. When reading logging literature, one should remember that:

1. Water that naturally saturates a formation is referred to as **formation water**, **connate water**, or **interstitial water**. The term formation water is used herein.

2. The term water resistivity (Rw), not water conductivity (Cw), is used in virtually all logging literature. This chapter also uses Rw. The relationship between the two terms is discussed in Chapter 2 and is restated here:

$$Rw\ (ohm\text{-}m) = \frac{10{,}000}{Cw}\ (\mu mhos/cm) \qquad (12\text{-}1)$$

GUIDELINES FOR Cw and TDS CALCULATIONS

The accuracy of Cw and TDS calculations will be greatly improved if:

1. The logging tools are suitable for the borehole conditions and the petrophysical properties of the aquifer being analyzed.

2. The technique for calculating Rw is compatible with the chemical composition of the water being analyzed and the available log data.

3. The logging data are accurate.

Suitable Tools and Techniques

Logging tools and water quality calculation techniques must be selected according to the chemical composition of the ground water, the petrophysical properties of the aquifer, and the borehole conditions. The choice of logging tools, especially for resistivity tools, has considerable bearing on the accuracy of the data. It also determines which analytical techniques can be used. It is essential for one to be familiar with the applications and limitations of the various resistivity tools (Chapters 8 and 9) and to remember that:

1. Most logging tools and techniques are designed for clean (shale-free), "normal" sedimentary rocks (quartz-rich sandstones, limestones, and dolomite). Analysis of shaly formations may require modifications to the techniques.

2. All resistivity tools are not created equal. They must be compatible with the type of aquifer and borehole being logged. For example, induction tools are not the best choice for logging aquifers with resistivities greater than 100 ohm-meters or zones (beds or porous intervals) less than 5 to10 feet thick. Guard or Latero tools provide better vertical resolution and more accurate resistivity values in such circumstances (Chapters 8 and 9).

3. The SP curve is good for quantitative work only in thick, clean sands. SP values are too low if the formation (sandstone or carbonate) is thin, shaly, highly resistive, or deeply invaded (see Guyod, 1966; Alger and Harrison, 1988; Sciacca, 1989; Chapter 12).

4. Most of the techniques for determining ground-water quality utilize either an SP or a deep resistivity curve. The techniques have been borrowed, with little or no modification, from the petroleum logging industry. Application of the techniques to ground-water studies has largely been unsuccessful because oilfield waters are radically different from ground waters. Petroleum logging techniques assume that formation waters have high salinities (more than 50,000 ppm TDS) with predominately monovalent NaCl ions. Ground waters, on the other hand, usually have much lower salinities and a significant concentration of divalent calcium and magnesium ions. The responses of SP and resistivity tools must be interpreted differently for each of the two water types (Chapter 12).

Accurate Log Data

Log data accuracy is a major area of weakness for the ground-water logging industry. The petroleum logging industry has devoted considerable attention to data accuracy (see any detailed logging text and in particular Helander, 1983; Bateman, 1985). Unfortunately, this expertise has not been sufficiently utilized by the ground-water industry. Ground-water logging articles that mention the subject provide little in the way of guidelines for correcting log values.

Log data accuracy was addressed as each tool was discussed in Chapters 8 to 13. The subject is so critical to Cw and TDS calculations that a few points need to be reemphasized:

1. The accuracy of log data will be greatly improved by running a logging suite which is compatible with the borehole conditions and the petrophysical properties of the aquifer.

2. Resistivity values may require corrections for bed thickness, borehole diameter, mud resistivity, and mud filtrate invasion (Chapters 8 and 9).

3. Tool calibration and quality control are essential for obtaining valid data. Merkel and Snyder (1977), Hallenburg (1980), Hill (1986), Hodges (1988), Collier (1988), and Sciacca (1989) discuss various aspects of these two important subjects.

4. The correct assumption must be made about what part of the borehole a particular resistivity tool is investigating. Most Cw and TDS calculations utilize Ro, which in water wells is equivalent to Rt. Variations in logging tool responses and borehole conditions mean that Ro is not always what is being measured. Either deep mud filtrate invasion (not likely to occur in shallow or highly porous clastic aquifers) or insufficient depth of investigation by the resistivity tool (more likely to be the case) is usually the reason an incorrect value is used for Ro. The Resistivity Ratio Method requires both Ro and Rxo (the resistivity of the flushed zone). In the case of Rxo, the resistivity tool is supposed to measure a thin zone very close to the borehole wall. If the tool reads too deep or too shallow, the resistivity will not be Rxo.

ACQUIRING LOGGING DATA

Fresh Water Aquifers

When studying the fresh water portion of Texas aquifers, most of the logs will be from water wells and most of the wells will have at least one water analysis. Virtually none of the logs will be hydrocarbon tests. Oil companies are required to set surface casing through fresh water aquifers and they generally do not log before setting surface casing. Openhole logs run through casing cannot be used to determine water quality.

Water well borehole geophysical logs are scattered throughout the files of the ground-water industry. Unfortunately, there is no single, easily accessible source. The following organizations are sources of logs:

1. **Texas Water Commission, Central Records, Ground-Water Technical File.** This is the largest collection of water well logs in Texas. Water well drilling contractors sometimes submit logs on a voluntary basis, so coverage is by no means complete. Data are filed by county and by complete or partial state well number. Without a state well number, data on a particular well are not

easily accessible. It can be very time consuming to track down large numbers of logs.

2. **Texas Water Commission, Watershed Management, Surface Casing Unit.** This file consists mainly of oilfield logs. However, it does contain a small number of fresh-water logs. Some are logs from water wells; the rest are oilfield logs that penetrated fresh water formations.

3. **Water well drilling contractors.** Irrigation and domestic wells are rarely logged. Conversely, virtually all municipal, rural water supply, and industrial wells are logged. Drilling contracts usually contain a clause requiring borehole geophysical logs. Drilling companies meet the requirement by subcontracting to a logging service company. Drilling contractors generally retain copies of these logs. The older drilling firms have amassed extensive log files. Access to the logs varies from company to company.

4. **Ground-water consulting firms.** These firms have a limited number of logs and generally consider their data proprietary.

5. **Petroleum Information Corporation (PI).** PI is the main broker for oilfield logs. They carry some water well logs, but the logs are not identified as such. Water well drilling contractors do not routinely release their logs to PI. They only release the ones that PI requests, which are usually the wells logged by the major commercial logging companies. Consequently, PI carries only a small percentage of available water well logs.

6. **Logging companies.** Major logging companies, except for Schlumberger, retain their logs for only a few months. Schlumberger started archiving tapes of logging jobs as of 1987. Presently, about 50 percent of all jobs are archived (at no fee to the client). The client may request that a logging job be archived. If the client releases the data, anyone can purchase a copy of the tape. However, Schlumberger does not archive hard copies of the logs and it takes sophisticated logging software to make a hard copy from a tape. Smaller logging companies sometimes keep hard copies of all their logs (e.g. Tejas). However, they do not make a practice of furnishing copies of the logs in their files. In

fact, the logs archived by any logging company are proprietary and cannot be released without the consent of the client.

Saline Water Aquifers

Log coverage of the saline water portions of Texas aquifers is much more complete. In fact, too much data will be the problem in some of the petroleum-producing areas of the state. Most of the logs will be from hydrocarbon tests and very few will have accompanying water analyses. When searching for logs, one should check the following sources:

1. **Petroleum Information Corporation (PI).** PI is the premier source of oilfield logs. They sell copies of the logs, or one may borrow logs from a PI log library. A membership is generally required to check out logs from the library.

2. **Petroleum log libraries.** Scattered around Texas are numerous public and private membership petroleum log libraries. Some libraries cover the entire state, while others only cover a particular geographic area. In public log libraries, logs can be examined in-house for a flat per-day fee or they may be checked out by members.

3. **Texas Water Commission, Watershed Management Division, Surface Casing Unit.** This agency has over 250,000 logs from throughout the state. The logs are filed by county and are keyed to county land and ownership maps. It is easy to locate logs from a particluar geographic area. Logs may be copied from the file, or they may be checked out to be copied and returned within 2 days.

4. **Bureau of Economic Geology, Geophysical Log Facility.** This agency is the repository for oilfield logs collected by the Railroad Commission of Texas. Since 1986, oil companies have been required to submit a log for each new well. The regulation is worded so that any wireline log is acceptable. Thus, the log which is submitted may be of a type that is of no value for water-quality calculations. The regulation further states that the log must be of the producing interval. Some operators, therefore, submit a partial log, rather than a log of the entire borehole. The end result is that many of these logs may not be suitable for ground-water studies.

The Geophysical Log Facility also has a large number of pre-1986 logs. These logs are from the Railroad Commission and the Bureau of Economic Geology files.

5. **Ground-water firms.** Water well drilling contractors and ground-water consulting firms have few such logs.

EMPIRICAL RELATIONSHIPS FOR ESTIMATING TDS AND RW

TDS-Ro Graphs

Under ideal conditions, it is possible to accurately estimate TDS directly from an Ro value. An Ro value is plotted on a previously established TDS-Ro graph and the corresponding TDS value is read directly off the graph. The procedure is as follows:

1. Construct a TDS-Ro graph using data from wells closest to the well being analyzed. Ideally, the data should also be from the same stratigraphic unit. In reality, well control is usually sparse and the stratigraphy of any aquifers from which water samples were analyzed is not always identified . For these reasons, the data collected during this project (Volume II, Section 5) were processed by counties. Data plotted by counties often has a high correlation coefficient because most of the wells are from the same aquifer (Figure 14-1).

2. Logarithmic scales are recommended. They allow a wider range of values to be plotted on a single graph (Figures 14-1 and 14-2) and the curve fit is a straight line.

3. The deepest reading resistivity curve (64" normal, deep induction, lateral, or deep laterolog) is used for Ro.

    a. An average Ro value is selected for the aquifer. Figures 8-25, 8-26, and 9-21 discuss how to select average resistivity values. If there is more than 10 percent variation in the resistivity of the zone, it may be worth plotting the highest and lowest average values, Ro High (Ro_H) and Ro Low (Ro_L). This was done, as necessary, for the graphs in Volume II, Section 5.

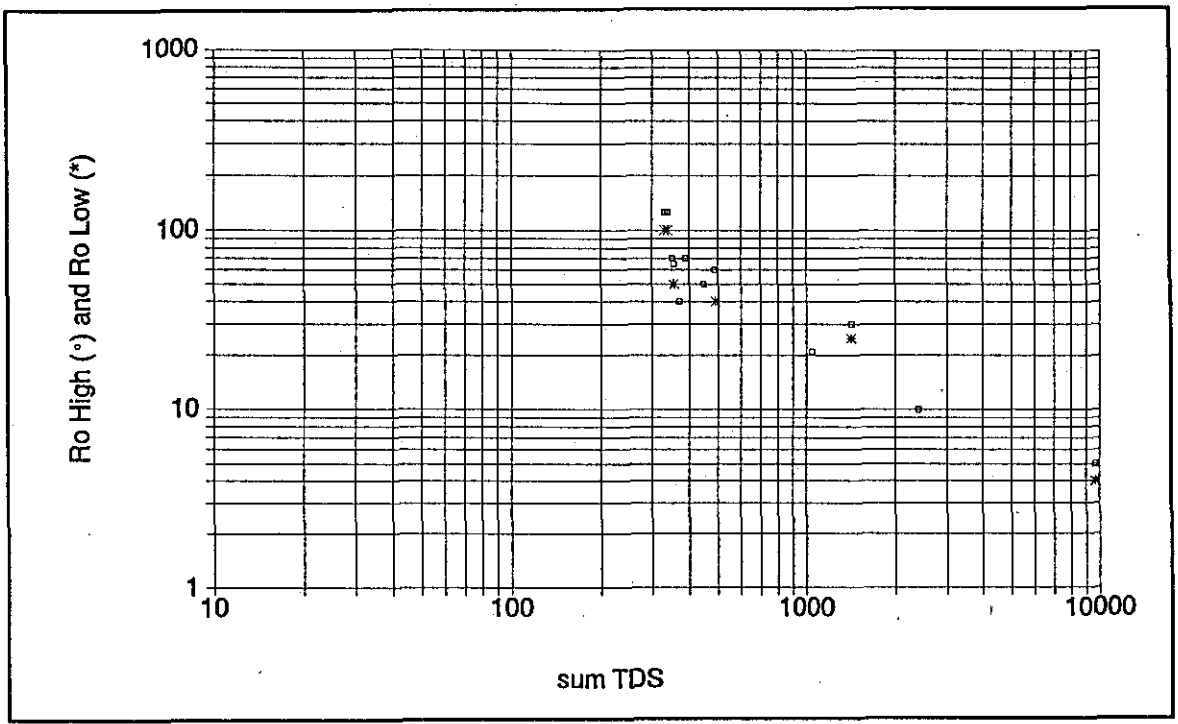

Figure 14-1. Ro-TDS graph that has a high correlation between Ro and TDS. Data are from Harris County. Sum TDS includes 100 percent of the bicarbonate value.

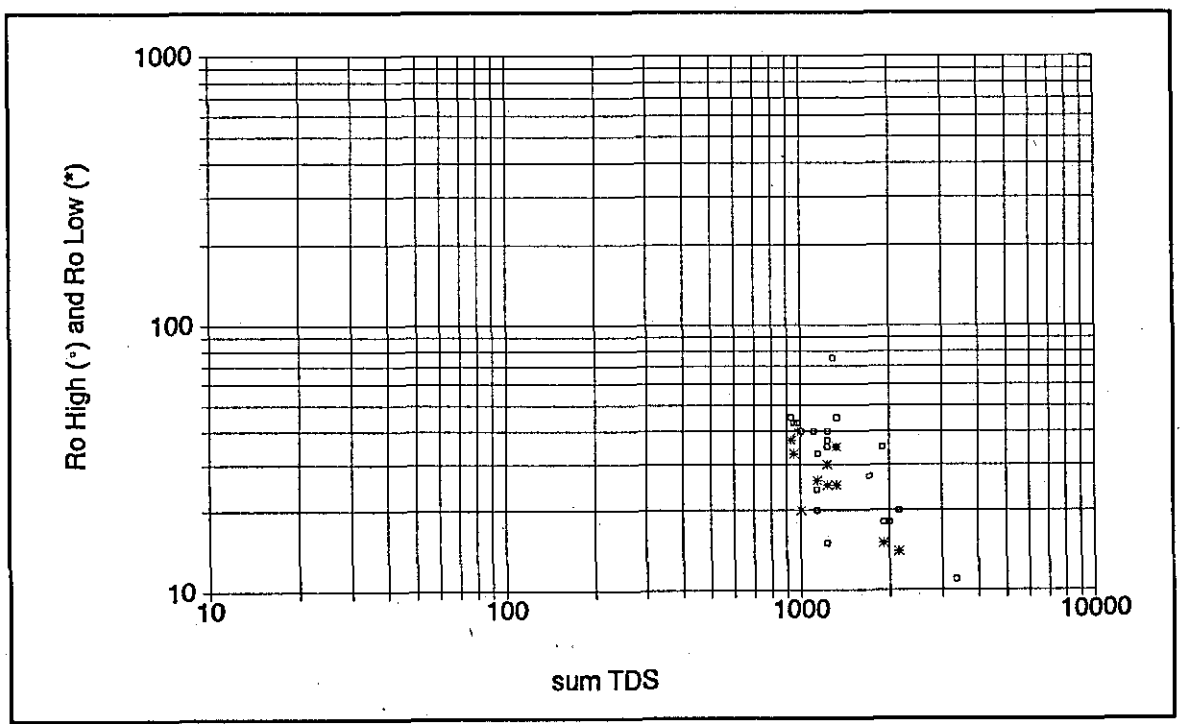

Figure 14-2. Ro-TDS graph that has a low correlation between Ro and TDS. Data are from Dallas County. Sum TDS includes 100 percent of the bicarbonate value.

b. If borehole conditions warrant, an environmental correction should be made to the resistivity value on the log (Ra) before it is used as Ro and plotted on the graph. (Chapters 8 and 9 discuss environmental corrections for each resistivity tool.)

4. TDS values should include 100 percent of the bicarbonate value.

5. A line-fitting routine can be applied to the data, but is not necessary. If there is much scatter, the equation of the line does not give an accurate TDS value. It is better to simply plot new Ro values on the graph and to look at the range of corresponding TDS values (Figure 14-2).

This technique has one serious limitation: it requires Ro values to be solely a function of water salinity (TDS). This condition exists only in shale-free sandstone aquifers that have approximately the same porosity. Such conditions normally are approximated only in sandstones that are consistent in lithology, unconsolidated to semi-consolidated, Tertiary or younger, and less than about 1000 feet deep (aquifers such as the Gulf Coast and Carrizo-Wilcox). Sandstones from the same depositional facies and a limited geographical area give the best correlation.

TDS-Ro graphs do not work as well for consolidated sandstones and carbonates such as the Trinity, North-Central Texas Paleozoic formations, Edwards, and Ellenburger. Several of the graphs in Section 5 of Volume II substantiate this fact. Figure 14-2 is an example of a poor correlation. In these types of aquifers porosity can vary considerably within a well and from well to well. In such cases, Ro is a function of both porosity and TDS, so there is no consistent correlation between Ro and TDS. The water quality calculation must account for the effect of porosity on Ro (Ro_c-TDS Graphs, Field Formation Factor, Water Saturation Equation, and Ro-Porosity Graphs) or factor it out (Rxo-Ro Ratio).

Few Ro-TDS graphs have been published. Guo (1986) and Fogg and Blanchard (1986) are the only examples this author found. Guo applied the technique to Quaternary alluvial sand aquifers in the North China Plain (Figure 14-3). The one graph that he published does have a high correlation between TDS and Ro values.

Fogg and Blanchard constructed a TDS-Ro graph for the Carrizo-Wilcox aquifer system in the Sabine Uplift area of Texas (Figure 14-4). The correlation is only fair (0.80) and the graph is a good example of the inaccuracy of this technique. An Ro of 30 ohm-meters could represent a TDS anywhere from 300 to 1400 mg/l and a TDS of 1400 mg/l could have an Ro ranging from 10 to 40 ohm-meters. The scatter is probably due, in large part, to variations in porosity. Grouping the data according to smaller geographical areas would probably improve the correlation. Also, the graph would be much easier to interpret if the data had been plotted as whole numbers.

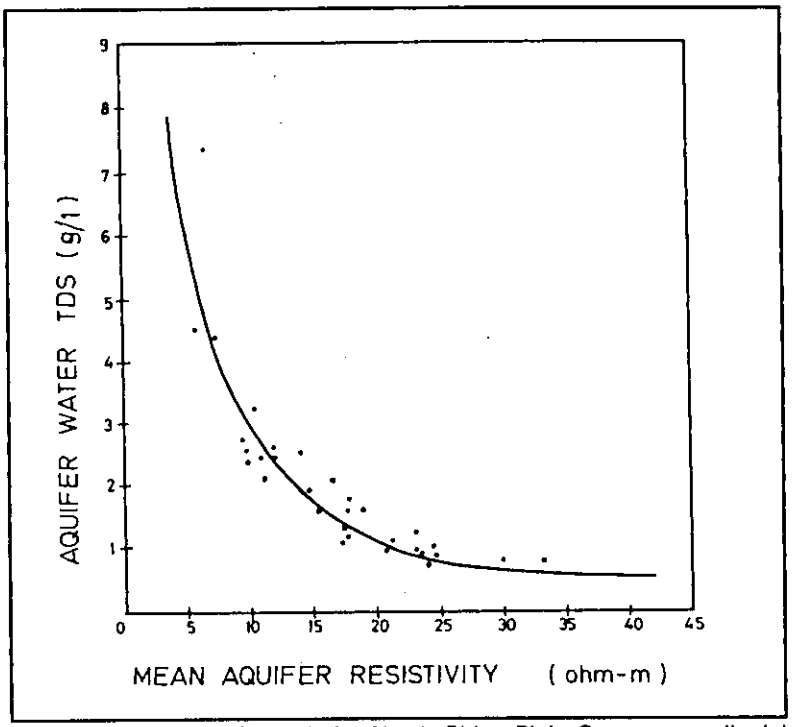

Figure 14-3. Ro-TDS graph for North China Plain Quaternary alluvial sands (Guo, 1986). g/l x 1000 = mg/l

Ro-TDS graphs were constructed from the data base assembled for this project. Ro values are from Section 3 and TDS values are from the Sum TDS column of Section 2 of Volume II. The data was plotted by counties. Forty-eight counties had enough data for a graph (Volume II, Section 5, Figures 5-1 to 5-48). Each graph contains 2 to 20 data sets.

Thirty-six graphs had sufficient data to judge the quality of the curve fit: 33 percent (Brazos, Cherokee, Denton, Ellis, Harris, Hidalgo, Hunt, McMullen, Milam, Rusk, Shelby, and Wood Counties) had a good fit, 47 percent (Anderson, Angelina, Collin, Dallas, Dimmit, El Paso, Fannin, Freestone, Gonzales, Grayson, Jefferson, Montgomery, Nacogdoches, Smith, Tarrant, Upshur, and Van Zandt) had a fair fit, and 20 percent (Erath, Karnes, Robertson, Limestone, McLennan, Red River, and Walker) had a poor fit. The graphs represent data from four major Texas aquifers: Carrizo-Wilcox, Trinity, Gulf Coast, and Bolson Deposits. The Trinity has the highest percentage of poor curve fits, but it does have three counties with good curve fits.

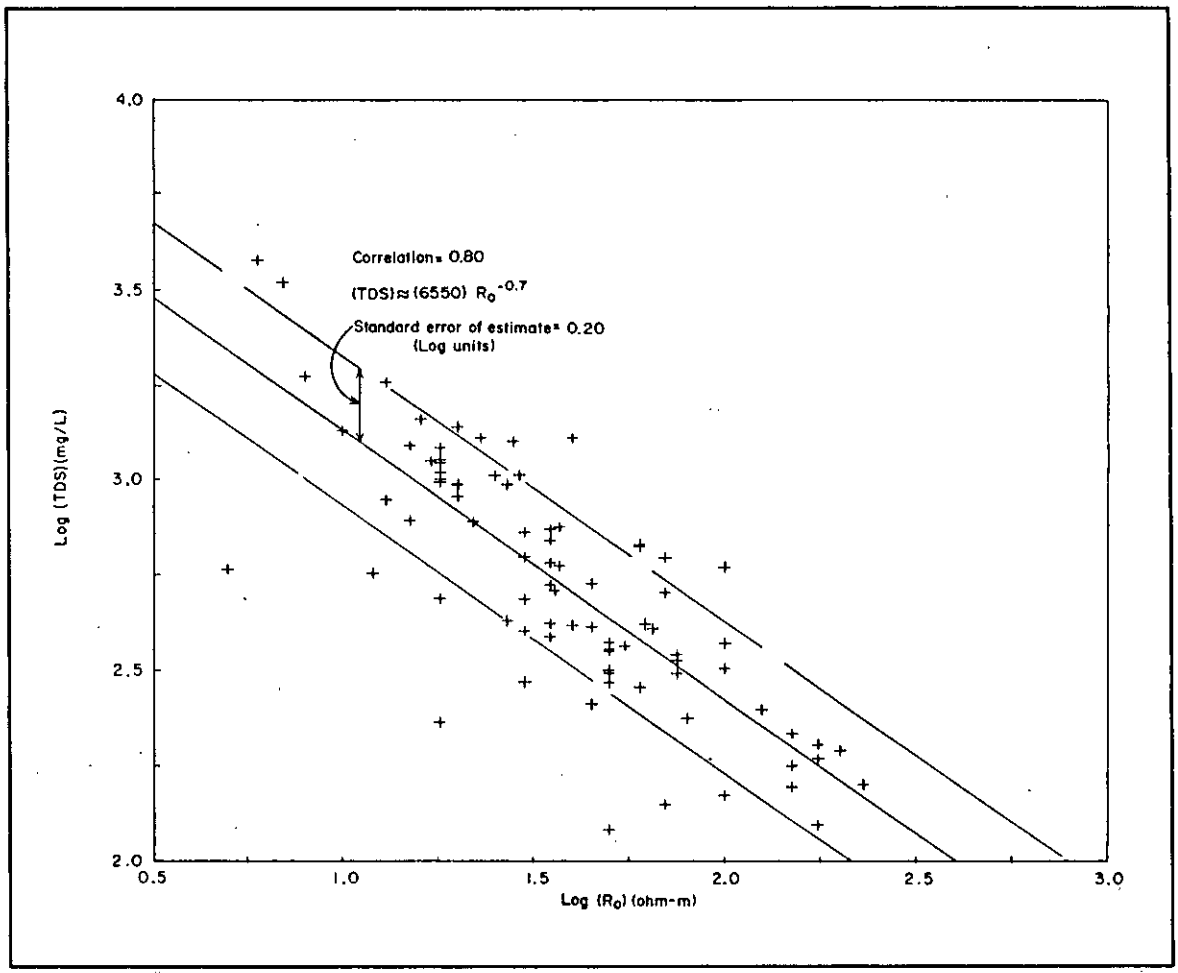

Figure 14-4. Ro-TDS graph for the Carrizo-Wilcox aquifer system, Sabine Uplift area. Ro values are from 64" normal and induction logs. Data are from water wells that are screened primarily in channel-fill sands at depths of 200 to 1,200 feet (Fogg and Blanchard, 1986). There is considerable scatter in the data. The graph would be much easier to interpret if the data had been plotted as whole numbers.

Of the twelve counties with good curve fits, nine have parallel curve fits (Figure 14-5). However, the variations in the curve fits underscore the fact that Ro-TDS graphs are site-specific and should be used with caution.

For thirty counties the data distribution was such that the Ro values corresponding to 1,000 mg/l TDS could be determined from the Ro-TDS graph. Five counties had sufficient data to determine the Ro value corresponding to 10,000 mg/l TDS. Table 14-1 is a compilation of the Ro values. The data distribution for some counties was such that it was necessary to include a range of Ro values, rather than a single Ro value, in the table.

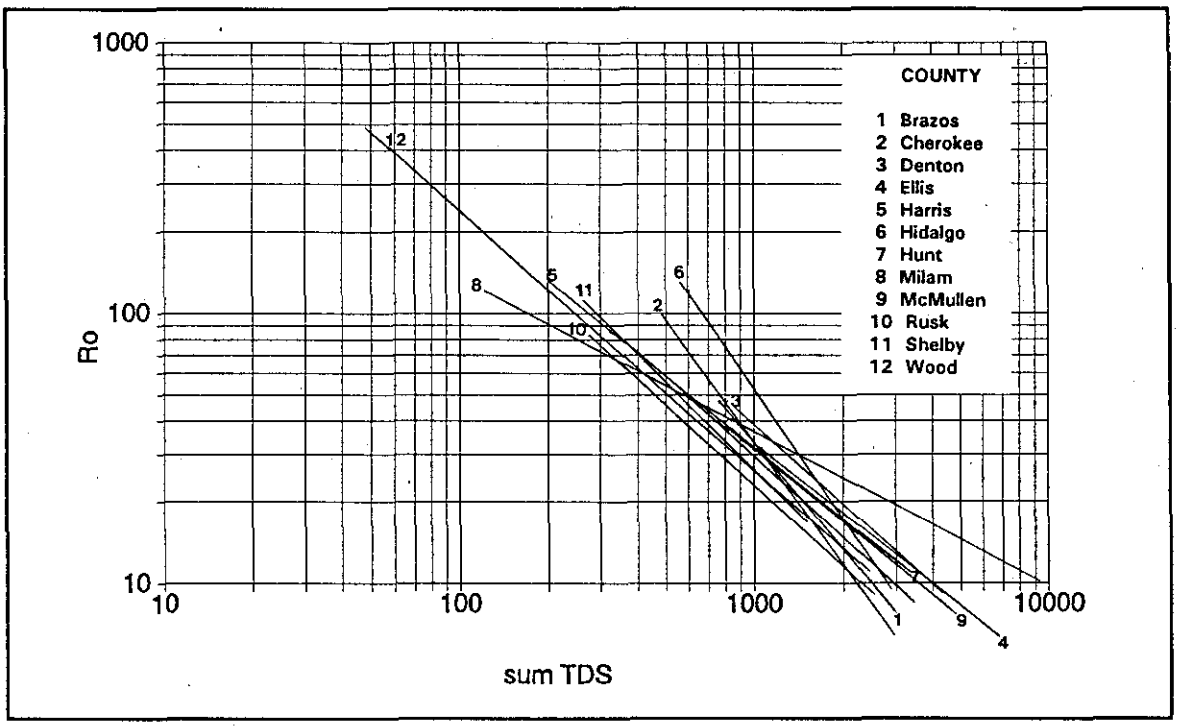

Figure 14-5. Curve fits for the Ro-TDS graphs of 12 counties. The graph of each county is in Volume II, Section 5. The correlation for each county was good, so the curve fits were "eyeballed".

Table 14-1 shows that for a TDS of 1,000 mg/l, Ro values vary considerably (15 to 45 ohm-meters). However, when grouped by aquifers, the Ro values show fairly consistent patterns. In the case of the Carrizo-Wilcox, an additional grouping by geographic area further enhanced the consistency. Ro values for 10,000 mg/l TDS, while ranging from 1 to 10 ohm-meters, are usually less than 2 ohm-meters. Table 14-1 further underscores the site-specific nature of this technique. It illustrates that using an Ro cutoff for determining a particular water salinity will usually be valid only in a limited geographic area.

When the aforementioned guidelines are followed, Ro-TDS graphs can be used with a limited amount of success to estimate TDS. The graphs are site-specific and should always be used cautiously.

Ro_e-TDS Graphs

When an aquifer extends to depths of several thousand feet, variations in Ro values at widely different depths will be, to some degree, due to the fact that formation temperature and porosity vary with depth. Alger (personal communication, 1988) proposed that the correlation

TABLE 14-1. Ro VALUES CORRESPONDING TO TDS OF 1000 AND 10,000 MG/L ON COUNTY Ro-TDS GRAPHS

Aquifer/County	Ro ohm-meters for 1000 mg/l TDS	Ro ohm-meters for 10,000 mg/l TDS
Huecho Bolson Aquifer		
El Paso	15	-
Carrizo-Wilcox Aquifer (North)		
Anderson	18 to 40	-
Angelina	15	1 to 2
Cherokee	20	-
Gregg	20	-
Nacogdoches	30	-
Rusk	18	-
Shelby	25	-
Smith	25	-
Wood	25	-
Carrizo-Wilcox Aquifer (Central)		
Brazos	30	-
Burleson	30	-
Freestone	40	-
Gonzales	35	-
Leon	25	-
Milam	30	10
Carrizo-Wilcox Aquifer (South)		
McMullen	30	-
Gulf Coast Aquifer		
Harris	20 to 40	5
Hidalgo	-	2 to 3
Jefferson	20	2
Kleburg	25	-
Trinity Aquifer		-
Collin	30	-
Dallas	40	-
Denton	25 to 45	-
Ellis	25 to 35	-
Fannin	45	-
Grayson	30 to 40	-
Hunt	28	-
McLennan	45	-
Tarrant	40 to 45	-

coefficient of the corresponding Ro-TDS graph could be improved by using Ro values normalized or corrected for variations in porosity and formation temperature. The corrected Ro value is designated Ro_c.

The temperature correction normalizes Ro values, which are at formation temperature, to equivalent Ro values at 77° F (designated as Ro_c). The procedure is as follows:

1. A geothermal gradient must be established. It can be calculated for each well or an area-wide value can be used. Most counties in Texas have geothermal gradients of 1.0 to 2.5° F/ 100 feet. Columns 3 and 4 of Section 3, Volume II, list geothermal gradients for counties studied during this project. The Explanation section of Section 3 documents the geothermal gradient calculation and explains the problems associated with calculating a geothermal gradient from the bottom hole data available for many water wells.

2. The geothermal gradient is used to calculate the temperature at the depth at which Ro was measured. The equation for this calculation is listed in the explanation for Column 7 in Section 3, Volume II.

3. Ro is normalized to Ro at 77° F (Ro_c) by substituting formation temperature into Equation 2-4.

4. Ro_c is plotted versus TDS.

Temperature corrections can be made to Ro values from any type of aquifer. Alger (personal commmunication, 1988) suggested that they would be helpful when an aquifer extends below 1000 feet.

This study found that normalizing Ro values to a common temperature (77° F) did nothing to improve the curve fit of Ro_c-TDS graphs over that of the corresponding Ro-TDS graphs. This was true even for Ro values from depths of up to 4,000 feet.

Temperature corrections using both site-specific and county-wide geothermal gradients were applied to all the wells in this study (Section 3 of Volume II). Many of these wells had Ro values from depths of 2,000 to 4,000 feet. Ro_c-TDS graphs utilizing county-wide geothermal gradients were prepared for all 48 Ro-TDS graphs (Figures 14-6 and 14-7 are examples).

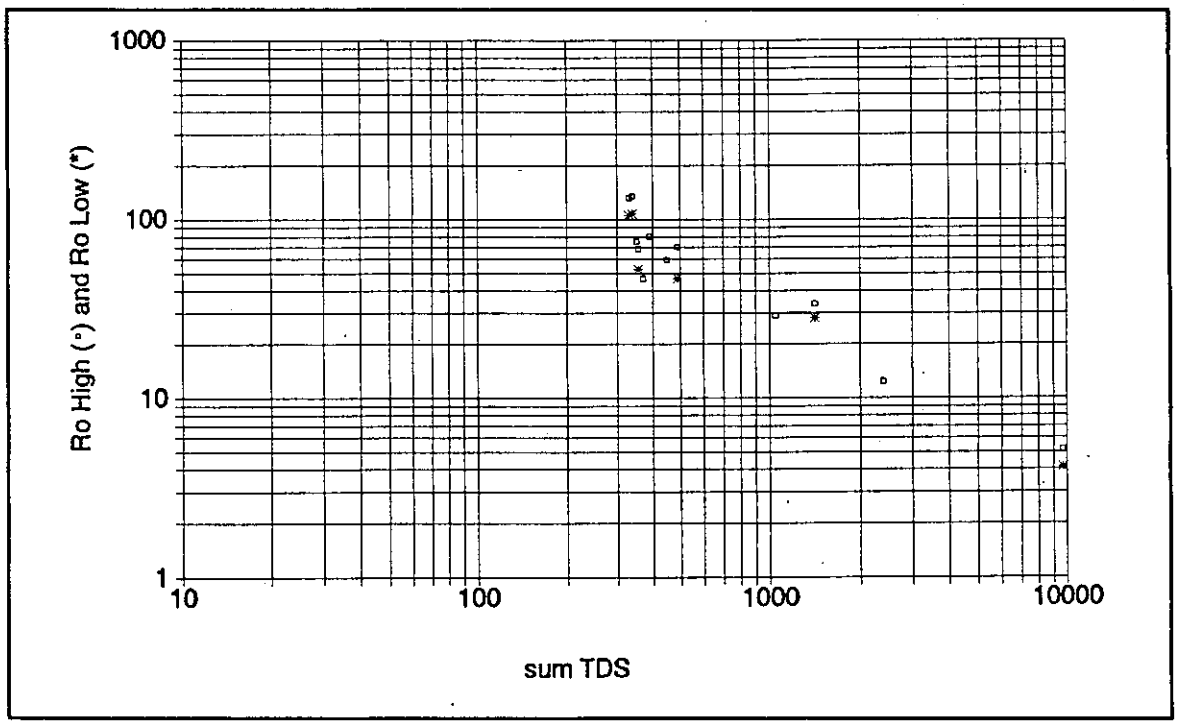

Figure 14-6. Ro_c-TDS graph for Harris County. Ro_c has been normalized to 77° F using a county-wide geothermal gradient. The curve fit is no better than that of the Ro-TDS graph (Figure 14-1).

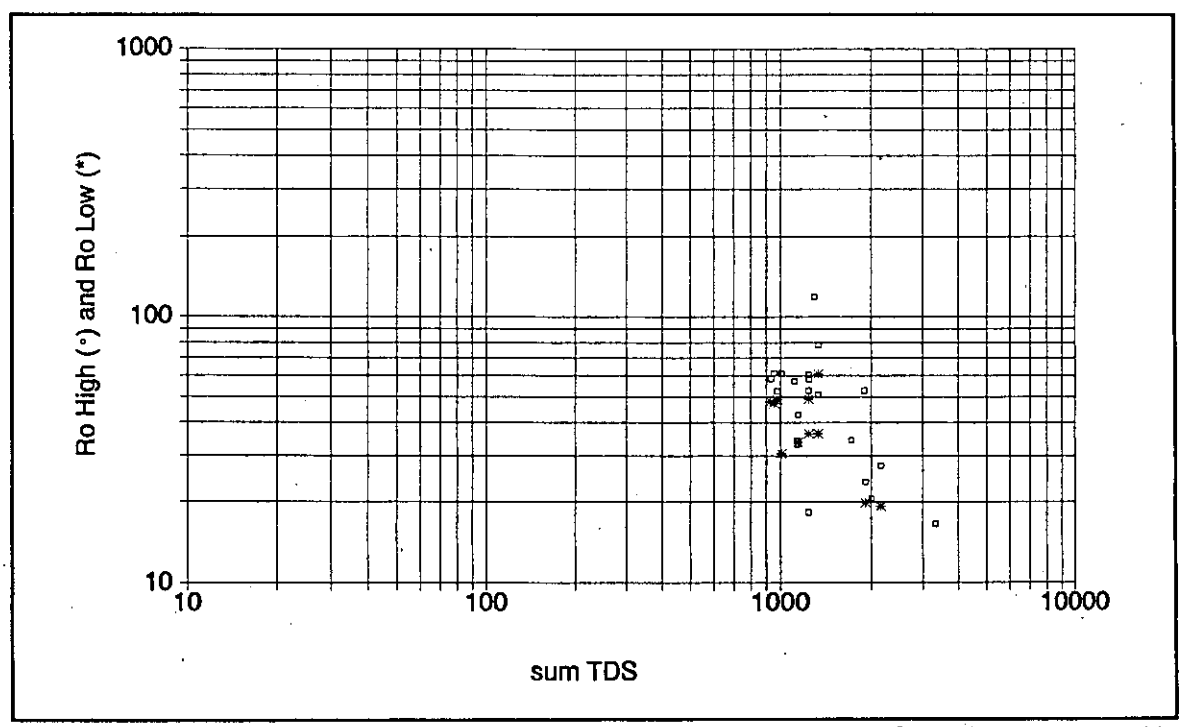

Figure 14-7. Ro_c-TDS graph for Dallas County. Ro_c was normalized to 77° F using a county-wide geothermal gradient. The curve fit is no better than that of the Ro-TDS graph (Figure 14-2).

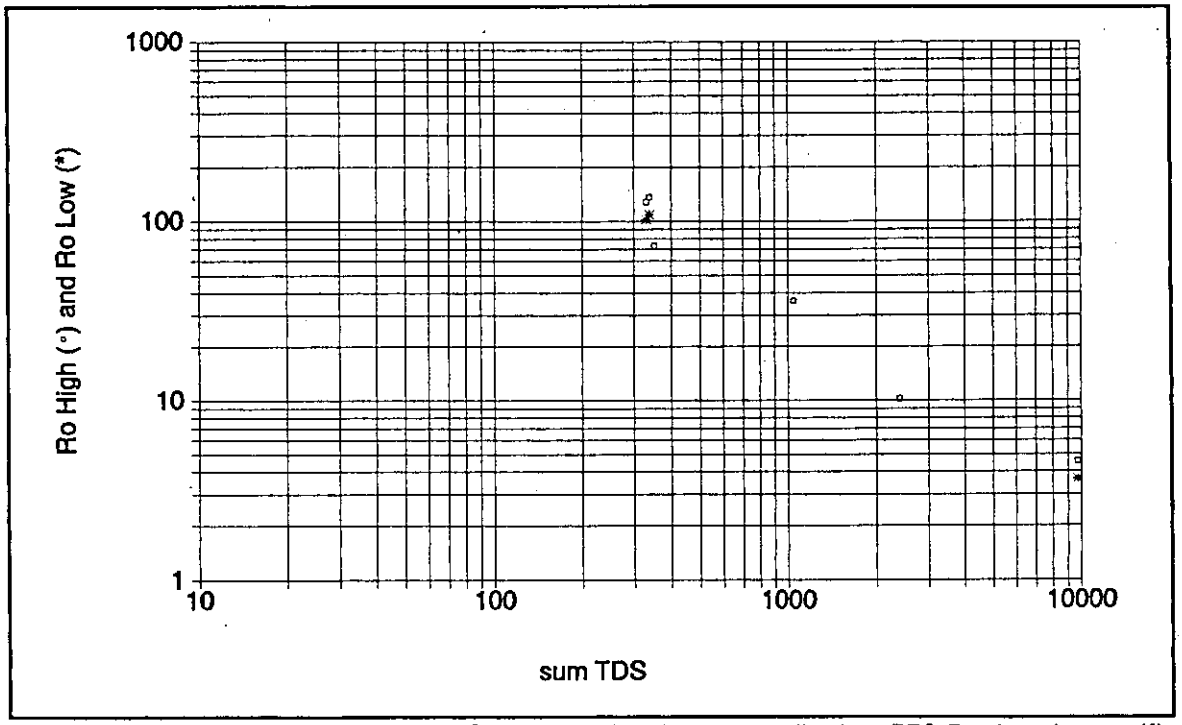

Figure 14-8. Ro_c-TDS graph for Harris County. Ro_c has been normalized to 77° F using site-specific geothermal gradients. The curve fit is no better than that of the Ro-TDS graph (Figure 14-1).

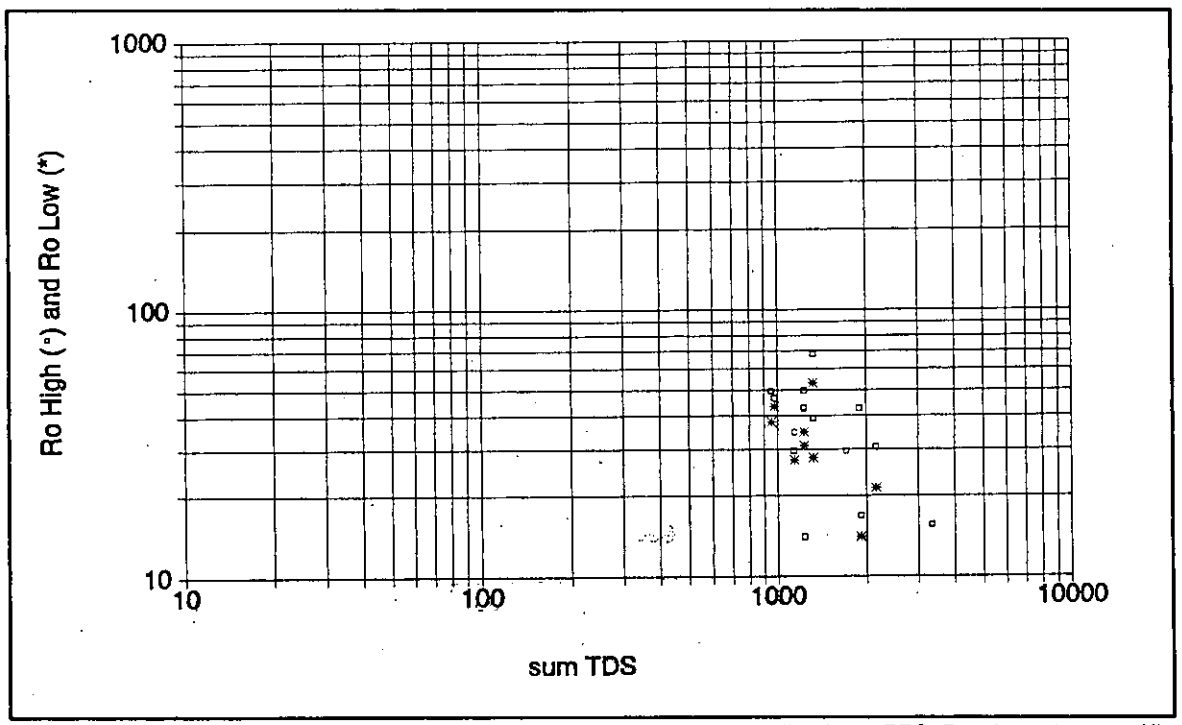

Figure 14-9. Ro_c-TDS graph for Dallas County. Ro_c was normalized to 77° F using site-specific geothermal gradients. The curve fit is no better than that of the Ro-TDS graph (Figure 14-2).

Ro_c-TDS graphs utilizing site-specific geothermal gradients were prepared for only 27 counties, since many wells lacked a bottom hole temperature (Figures 14-8 and 14-9 are examples). None of the 75 Ro_c-TDS graphs had a curve fit that was any better than the corresponding Ro-TDS graph, as illustrated by a comparison of Figures 14-1, 14-6, and 14-8, or 14-2, 14-7, and 14-9. (The rest of the Ro_c-TDS graphs were not included in this report.)

This lack of improvement in the curve fit, while due in part to inaccurate geothermal gradients, demonstrates that scatter in the curve fit is largely a function of factors other than temperature variations. Porosity variations are the most likely explanation.

Ro can also be normalized for variations in porosity due to compaction. The correction is valid only for unconsolidated sandstones in which porosity decreases with depth as a function of increasing compaction. Alger (*personal communication*, 1988) suggested that such Ro_c values would yield better curve fits for the portions of unconsolidated aquifers from 1,000 to 3,000 feet in depth. He considered the South Texas Carrizo-Wilcox and the Gulf Coast aquifers good candidates for the correction.

The procedure to normalize Ro for variations in porosity due to compaction is as follows:

1. A porosity value must be established for the depth that corresponds to each Ro value. This can be obtained from a porosity log, if available. Unfortunately, they seldom are available for water wells (see Chapter 13). The only alternative is to estimate porosity values by first establishing a porosity gradient from offsetting wells in the geographic area and depth range of the Ro values in question. As mentioned above, the porosity gradient will be valid only if porosity values are a function of compaction.

2. A formation factor (F) is calculated for each porosity value (i.e. each sample depth) using equation 14-7. Formation factor is discussed in the **Formation Factor Equation** section of this chapter.

3. A porosity value (depth) is chosen as the one to which all the rest of the data will be normalized.

4. Ro values are normalized to the common porosity (depth) value by the following equation:

$$Ro_c = Ro \times F_c / F \qquad \textbf{14-1}$$

Where:

Ro_c = Ro values corrected for variations in porosity due to compaction.
Ro = Resistivity of the uninvaded formation 100 percent saturated with water.
F_c = Formation factor of the common porosity (depth) value.
F = Formation factor corresponding to the Ro value being normalized.

5. Ro_c is plotted versus TDS.

Alger (personal communication, 1988) used density and sidewall core porosity values to calculate a porosity gradient for the Queen City and Carrizo-Wilcox in Atascosa, Karnes, LaSalle, and McMullen Counties. His equation is as follows:

$$\phi = 0.40 - .00003 \times \text{depth} \pm 0.01 \qquad \textbf{14-2}$$

Where:

ϕ = porosity
depth is in feet

Equation 14-2 was used to normalize Karnes County Ro values (Section 3, Volume II). Table 14-2 contains the calculations and Figure 14-10 is a graph of the results. Only the Ro_c value from 4,300 feet had an improved curve fit. All the rest of the Ro values were from a very small depth range (700 to 1,100 feet). The scatter in the data from this interval is most plausibly explained by porosity variations that are a function of geological factors other than compaction.

In theory, the curve fit of Ro-TDS graphs should be improved by normalizing Ro for the effects of temperature and porosity variations. In practice, such was not the case for temperature normalization and porosity normalization was only slightly successful. Ro_c-TDS graphs appear to offer an advantage over Ro-TDS graphs only for porosity normalization and only when porosity is a function of compaction.

TABLE 14-2. KARNES COUNTY Ro_c VALUES NORMALIZED FOR POROSITY

Depth (feet)	Porosity calculated from Equation 14-2	F	F_c	Ro_c High (ohm-meters) corrected to 77° F using a county-wide geothermal gradient	Ro_c High (ohm-meters) corrected to 77° F and 1000 feet
4300	0.27	10.4	5.3	29	15
1000	0.37	5.3	5.3	14	14
1000	0.37	5.3	5.3	15	15
1000	0.37	5.3	5.3	10	10
1100	0.37	5.3	5.3	6	6
700	0.38	5.0	5.3	5	5.3
800	0.38	5.0	5.3	7	7.4
800	0.38	5.0	5.3	7	7.4
700	0.38	5.0	5.3	8	8.5
800	0.38	5.0	5.3	8	8.5
700	0.38	5.0	5.3	9	9.5

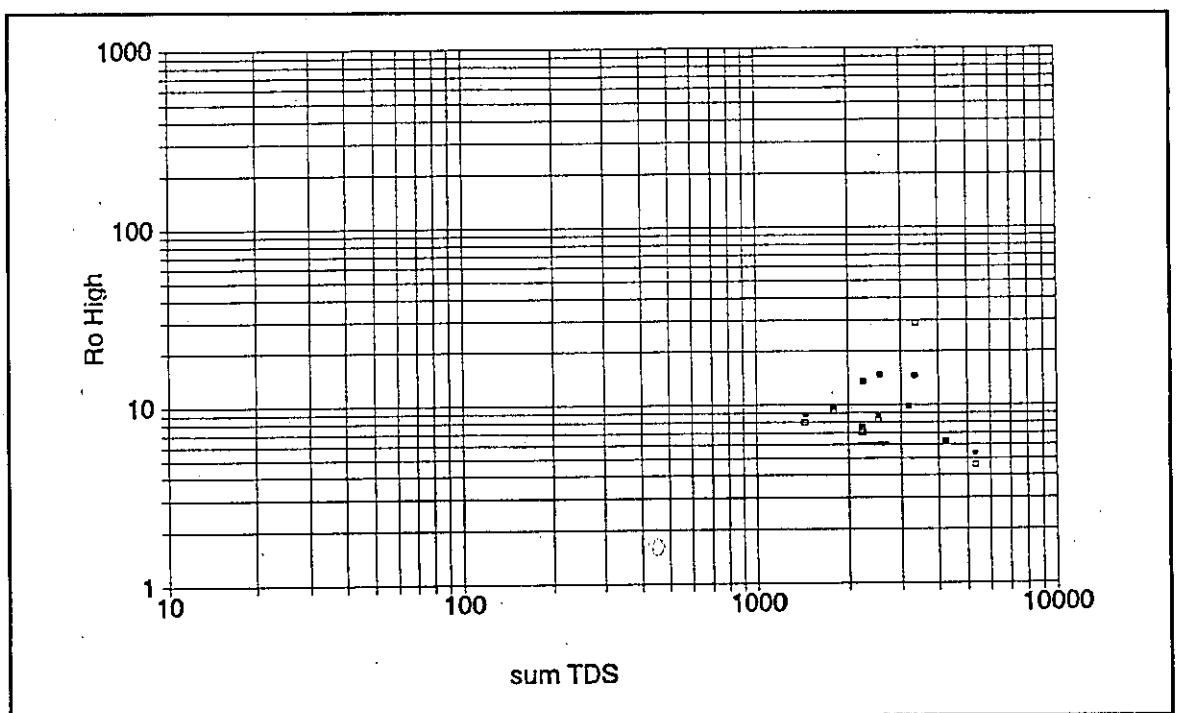

Figure 14-10. Ro_c-TDS graph for Karnes County. Ro_c High normalized to 77° F with a county-wide geothermal gradient (▫) was then normalized to 1,300 feet to compensate for porosity variations (°).

Field Formation Factor (FFF)

Turcan (1962) introduced the **Field Formation Factor (FFF)** technique as an empirical method of estimating Rw from resistivity logs. It is a slightly modified form of Archie's formation resistivity factor equation (14-5). In the FFF calculation Ro is first normalized to 77° F. This is done to negate the effects of variations in formation temperature on Ro and to calculate an Rw value at standard temperature (77° F).

There is one other significant difference between FFF and F. In fresh water (water with an Rw greater than 3 ohm-meters) FFF is less than F. In saltier water the two are equivalent. The difference between the two is due to surface conductance and is explained below. Surface conductance is explained in the **Formation Factor Equation** of this chapter.

FFF is the ratio of the Ro of a formation divided by the resistivity of the water in the formation (Rw):

$$FFF = Ro_{(@\ 77°\ F)} / Rw_{(@\ 77°\ F)} \qquad \textbf{14-3}$$

Where:

FFF = Field formation factor
$Ro_{(@\ 77°\ F)}$ = Resistivity of the uninvaded formation normalized to 77° F
$Rw_{(@\ 77°\ F)}$ = Resistivity of the formation water at 77° F

Having established the FFF of a formation, the Rw of a subsequent well can be estimated by substituting the Ro of the interval in question into a rearranged version of Equation 14-3.

$$Rw_{(@\ 77°\ F)} = Ro_{(@\ 77°\ F)} / FFF \qquad \textbf{14-4}$$

Rw is then converted to Cw (Equation 14-1). Finally, to determine TDS, Cw is plotted on the appropriate TDS-Cw graph or substituted into the equation of the graph (Chapter 4 and Section 4 of Volume II).

Equation 14-4 has one serious drawback for calculating Rw: FFF is porosity dependent. Therefore, an FFF constant is valid only as long as porosity remains fairly constant (i.e., shallow, unconsolidated sands in a limited geographic area). The method worked for Turcan because he was

analyzing shallow sands in a limited area (Eocene Wilcox Group in north Louisiana). His FFF values were fairly consistent, ranging from 1.7 to 3.0.

In deeper aquifers FFF increases with depth by as much as two orders of magnitude (MacCary, 1984). MacCary calculated F's for Catahoula, Frio, Yegua, and Wilcox sandstones of the Texas Gulf Coast. Figure 14-11, a graph of his Wilcox data, illustrates how F varies with depth, sometimes by as much as a factor of 10 within a few hundred feet. The overall trend of F increasing with depth is due to porosity decreasing due to compaction. Other diagenetic processes may be contributing to the trend. The wide variations in F over small vertical intervals are probably due to variations in porosity associated with varying depositional facies. Whatever the reasons for the variations in F, Figure 14-11 illustrates that calculating water quality from an FFF constant is unreliable in deeper aquifers.

Alger calculated FFF's for about 400 of the wells in the data base in Section 1 of Volume II. Values range from 0.1 to 28, with most of them between 2 and 7. Wilson County is the best example of a consistent county-wide FFF value. Five values range from 5.1 to 6.2, with one value of 3.9. There is considerable variation in the values for each of the other counties, even in the Carrizo-Wilcox and Gulf Coast aquifers. Dallas County is a good example of widely ranging values. FFF's range from 4.8 to 16, reflecting porosity variations within the Trinity aquifer.

The FFF's in this data base are smaller than values calculated using Archie's formation resistivity factor-porosity equation (Equation 14-6) and a known porosity value. The difference is due to surface conductance, which lowers Ro in fresh water aquifers. Consequently, in fresh water aquifers the FFF value

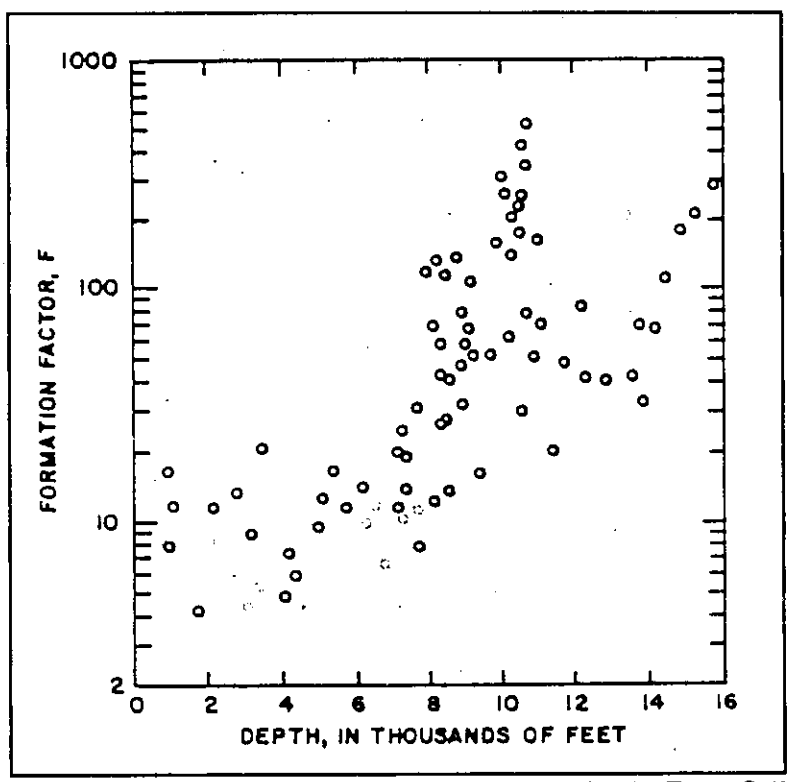

Figure 14-11. Graph of formation factor vs. depth for the Texas Gulf Coast Wilcox Group (MacCary, 1984).

calculated by Equation 14-3 is lower than an F value calculated with Equation 14-6, which is independent of Ro.

Examination of the data base in Section 1 of Volume II reveals that the FFF method of calculating water quality is not very accurate. In the absence of porosity data, an Ro-TDS graph is preferred over an FFF calculation. Indeed, a good linear fit to an Ro-TDS graph is really a plot of Equation 14-4 for varying Ro's and a constant FFF. The scatter about the linear fit demonstrates the degree to which porosity varies in the aquifer. Examination of the scatter allows one to visually take into account the effect of a change in porosity on Ro and consequently on the water quality estimation. This allows one to make a more intelligent estimation of the true water quality. An FFF calculation, on the other hand, offers no alternate interpretations and lends a false sense of accuracy to the water quality estimation.

STAND-ALONE TECHNIQUES FOR CALCULATING RW

Formation Factor Equation

Archie (1942) discovered that the resistivity of a water saturated rock (Ro) varies by a constant value as the resistivity of the formation water (Rw) changes. He quantified the relationship as:

$$Ro = F \times Rw \qquad R_w = \frac{R_o}{F} \qquad \textbf{14-5}$$

Where:

Ro = the resistivity in ohm-meters of the formation 100 percent saturated with water
F = the formation factor, a proportionality constant
Rw = the resistivity in ohm-meters of the water saturating the formation

The proportionality constant in Equation 14-5 is called the **formation resistivity factor (F_R)** or **formation factor (F)**. F ranges from 5 to several hundred in sandstones and from 10 to several thousands in carbonates (Helander, 1983).

Archie derived Equation 14-5 by saturating core samples of different porosities (10 to 40 percent) with waters of various salinities (20,000 to 100,00 mg/l of NaCl) and then measuring Ro. He found Equation 14-5 to be valid for his entire range of porosities and salinities.

Archie also observed that Ro, and consequently F, decrease as porosity increases. He inferred that F is a function of porosity and was able to derive an empirical relationship between the two:

$$F = 1 / \phi^m \qquad \textbf{14-6}$$

Subsequent investigation by Winsauer, et. al (1952) led to the addition of a variable a in the numerator of Equation 14-6:

$$F = a / \phi^m \qquad \textbf{14-7}$$

Where:

F = formation factor
a = tortuosity factor
ϕ = porosity in decimal form
m = cementation exponent

In the ideal case of pore spaces that are parallel cylindrical channels, F would be inversely proportional to porosity, a and m would both equal 1, and F would equal $1/\phi$. The pore system in almost all rocks, however, departs from the ideal case. Depositional and diagenetic processes result in pore diameters of varying cross-sectional areas and pore paths of varying lengths or tortuosities. a and m quantify the degree to which the pore system departs from the ideal case. The names tortuosity factor and cementation exponent are really misnomers for a and m, because the variables are the product of several factors. For instance, Helander (1983) lists eight factors that influence m:

1. Degree of cementation
2. Shape, sorting, and packing of the particulate system
3. Type of pore system (intergranular, intercrystalline, vuggy, etc.)
4. Tortuosity of the pore system

5. Constrictions existing in porous system
6. Presence of conductive solids (clays, pyrite, etc.)
7. Compaction due to overburden
8. Thermal expansion

The pore system of natural rocks is too complicated for a and m to be measured. Instead, they are empirically derived from the best line fit of a logarithmic plot of Ro/Rw (F) and porosity in decimal form (Figures 14-12, 14-13, and 14-14). The Ro and porosity values are obtained either from core (Figure 14-12) or log (Figures 14-13 and 14-14) measurements. Rw must be known independently.

The data is plotted on three-cycle log-log paper: F on the y axis with a scale of 1.0 to 1000 and porosity on the x axis with a scale of .001 to 1.0. m is the slope of the line that fits the data (Figure 14-13) and a is the value of F when $\phi = 1.0$. a can also be expressed in terms of a rearranged version of Equation 14-7 :

$$a = F \times \phi^m \qquad \textbf{14-8}$$

Theoretically, a should always equal 1, since a porosity of 1.0 (100 percent) has an Ro/Rw or F of 1 and these values substituted into Equation 14-8 calculate an a of 1. In reality, a sometimes varies from 1.0. Such cases may be an artifact of the curve fitting routine or compensation for consistent variations in pore geometry (Hilchie, 1987).

Over the years a and m have been calculated for thousands of rock samples. a's of 0.6 to 4 and m's of

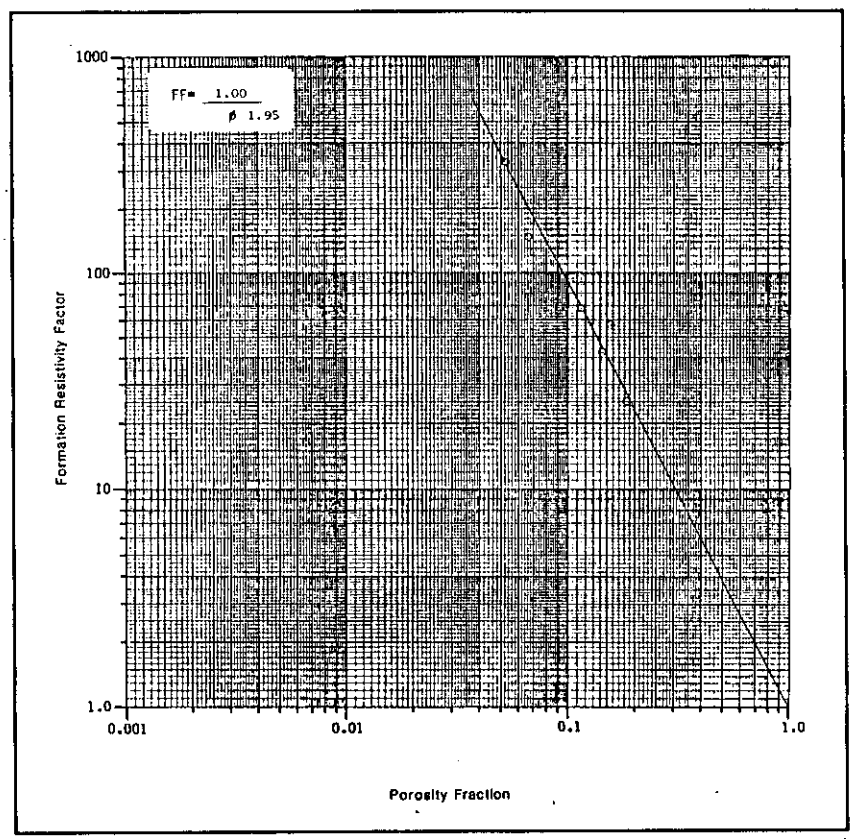

Figure 14-12. Example of a formation factor-porosity graph constructed from core data (Collier, 1988). For an a of 1, m is 1.95.

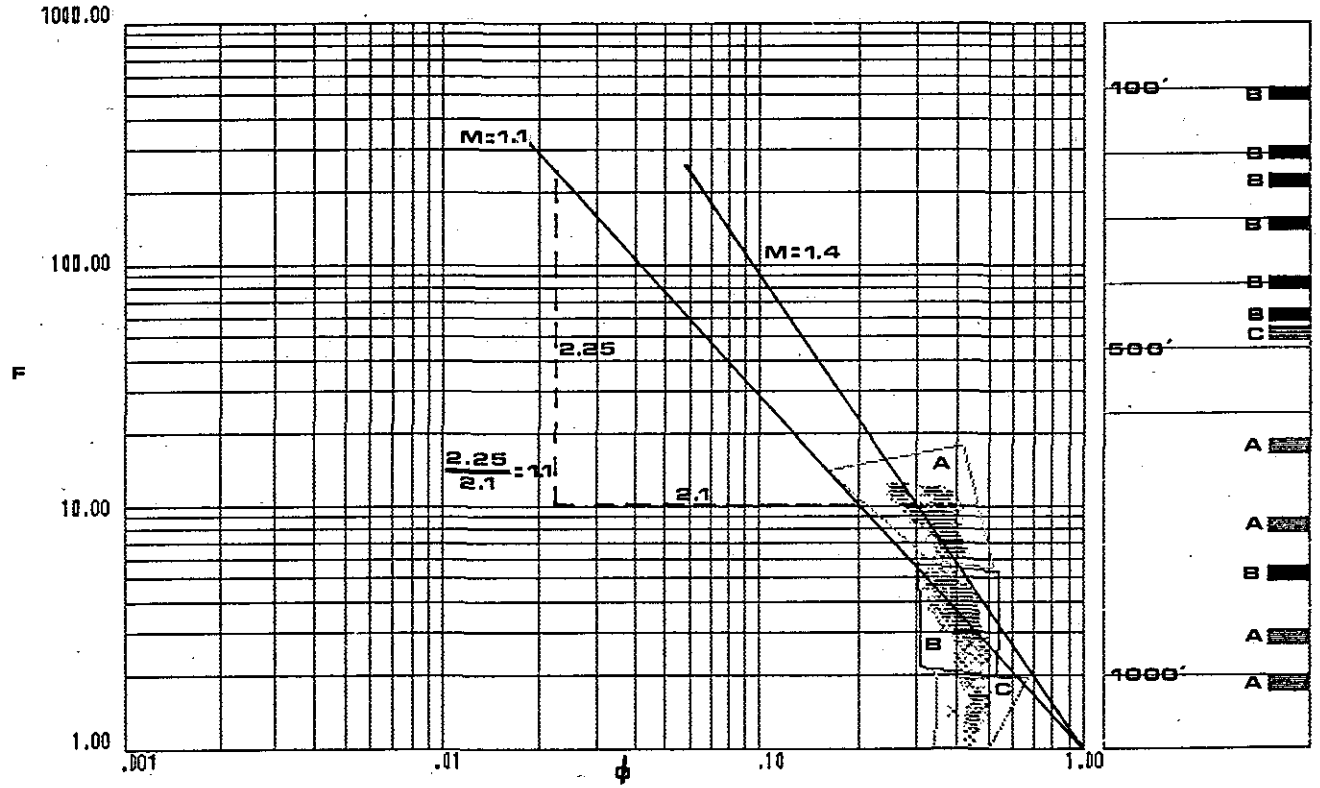

Figure 14-13. Formation Factor-Porosity graph constructed from log data. The porosity values are density-neutron crossplot porosity. The data clusters into three groups, with the two main clusters (A and B) correlating to the portion of the borehole above or below 500 feet. The column to the right of the graph is a diagram of the borehole with the intervals plotted on the graph noted by blocks. These intervals were chosen because water samples were available. The data clusters into distinct groups because of differences in the pore systems. m is 1.4 for group A and 1.1 for group B. Other differences such as water chemistry and SP behavior (refer to Plate 2) between the two intervals reinforce the conclusion of a significant difference in the petrophysical properties of the two intervals. The well was drilled in the Gulf Coast aquifer. The well is the TWDB PUB Test Well Site F, Cameron County, Texas (state well number 88-59-411). Plates 1 to 4 and Figures 13-12 and 14-20 are also from this well.

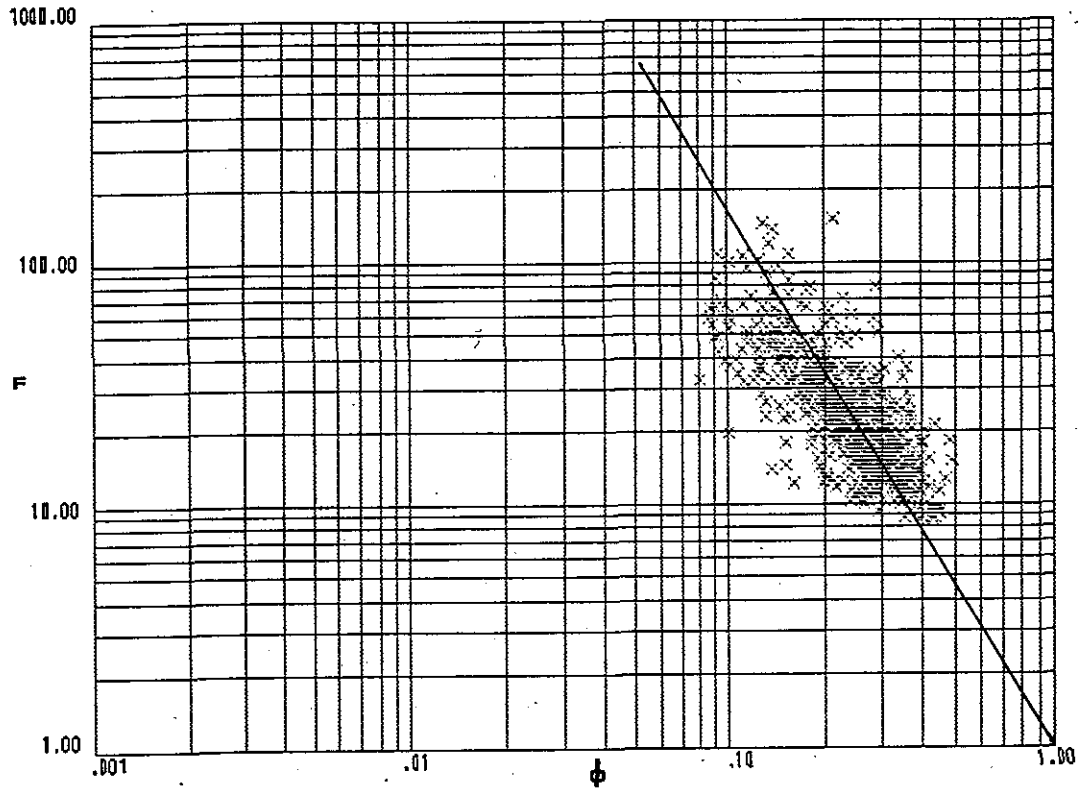

Figure 14-14. Formation Factor-Porosity graph constructed from log data. The porosity values are density-neutron crossplot porosity. The data shows a high correlation. Forcing the line fit through 1.0 on the x axis (a = 1.0) gives an m of 1.8. An m of 2 was used in the Rwa calculation for this well and yielded accurate Rw values (Poteet, Collier, and Maclay, 1992). The well is in the Edwards aquifer, San Marcos, Texas. The well is the Edwards Underground Water District, D, Hays County, Texas (state well number 67-01-814).

0.57 to 5.4 have been documented (Porter and Carothers, 1970 and Focke and Munn, 1987). Although specific a and m values have been calculated for some formations, most of the time log analysts use one of three versions of Equation 14-7:

$$F = .62 / \phi^{2.15} \qquad \textbf{14-9}$$

was developed by researchers at Humble Oil and Refining Company (Winsauer, et. al, 1952) and is known as the Humble equation. It is used for granular formations such as sandstones with porosities of 13 to 35 percent.

$$F = .81 / \phi^{2} \qquad \textbf{14-10}$$

is known as the Tixier equation. It also applies to granular formations. It is often substituted for the Humble equation when porosity is approximately 20 to 10 percent because it is easier to calculate and the two equations are equivalent for this porosity range (Figure 14-15).

$$F = 1 / \phi^{2} \qquad \textbf{14-11}$$

is called the Archie equation. It is used for carbonates and low porosity (i.e. cemented or compacted) sandstones.

Figure 14-15 is a graphical solution of the three equations. Plate 1 demonstrates that the Humble equation is more accurate than the other two in high porosity, uncompacted sandstones (the environment of most shallow clastic aquifers, as well as the Gulf Coast and Carrizo-Wilcox aquifers).

The most accurate approach, however, is to calculate formation-specific a and m values. Many log analysts set a equal to 1 and just deal with m (Figures 14-13 and 14-14). For an a of 1, certain patterns emerge regarding m:

1. For uncemented grains m increases as sphericity decreases. m ranges from 1.3 for uncemented spheres to 1.8 for uncemented plates (Hilchie, 1982).

2. m increases as the cementation of the rock increases. m ranges from 1.3 for completely unconsolidated sands to 2.2 for well cemented sandstones (Helander, 1983).

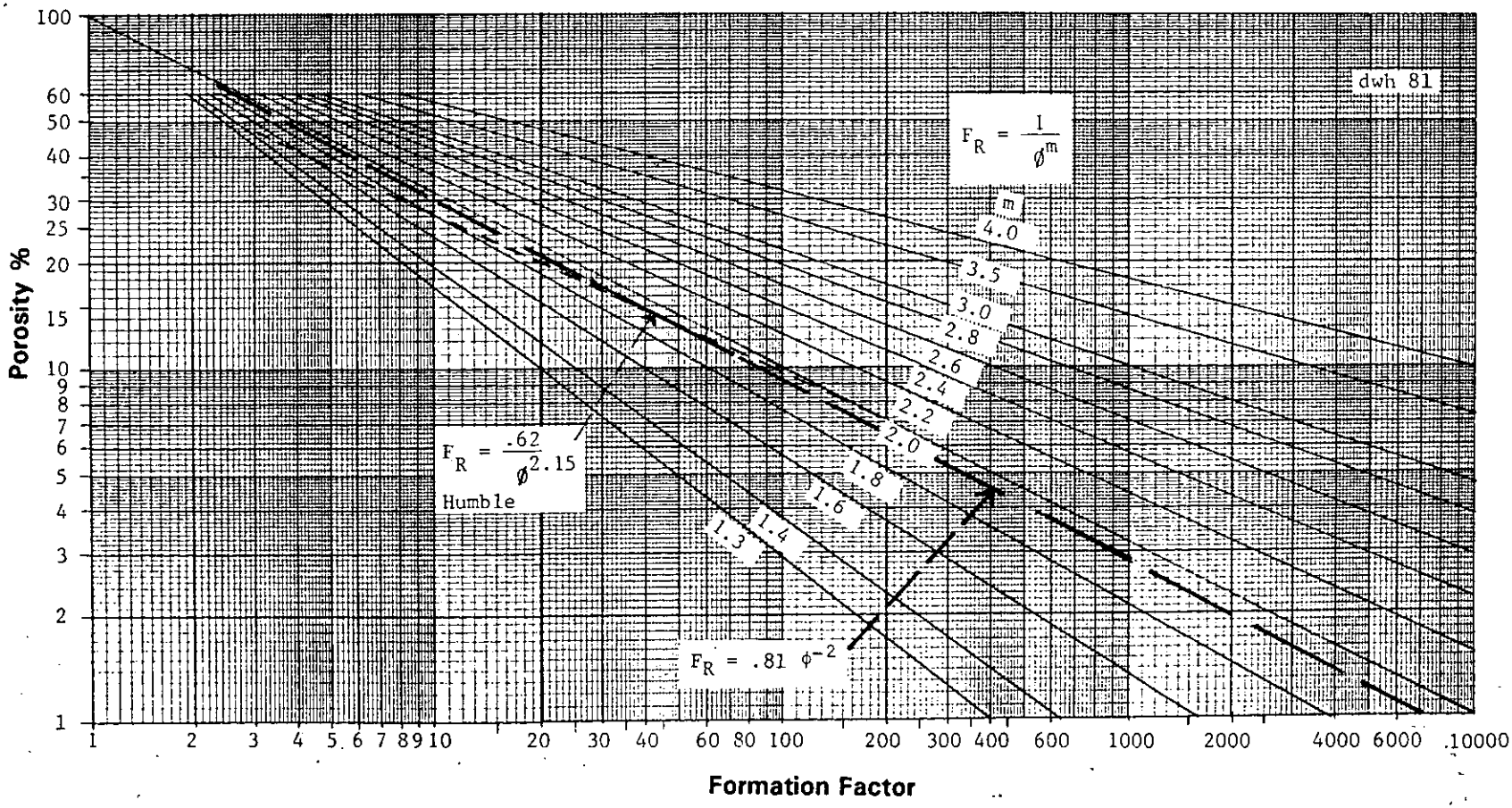

Figure 14-15. Formation Factor versus Porosity and m (modified from Hilchie, 1982). The graph is used to calculate F, given m and porosity.

3. m is 2 for carbonates with interparticle and intercrystalline porosity greater than 5 percent (Focke and Munn, 1987). Below 5 percent, m decreases as porosity decreases, down to 1.5 at 1 percent porosity.

4. For carbonates with vuggy and moldic porosity, m increases as the ratio of total porosity to vuggy/moldic porosity decreases (Towle, 1962). This is true when total porosity is greater than 5 percent. At less than 5 percent total porosity, m decreases as porosity decreases, down to about 1.3 at less than 1 percent porosity (Focke and Munn, 1987).

5. Fractures decrease m. Wide open fractures can have an m as low as 1.1 (Hilchie, 1982). This is because the pore geometry is approaching the ideal case of parallel cylindrical channels.

Rw calculated from Equation 14-5 using an F obtained from the Ro/Rw ratio in an offsetting well is the previously discussed Field Formation Factor technique. The previous discussion of F clarifies why the technique is so site specific. F will be the same in two wells only when porosity, m, and a are the same.

A much more accurate method, herein called the **Formation Factor Method**, is to substitute Equation 14-7 into 14-5 and rearrange the equation in terms of Rw:

$$Rw = Ro \times \phi^m / a \qquad \textbf{14-12}$$

This equation is called an **Rwa** calculation in petroleum logging literature. The term Rwa (apparent Rw) is used because when hydrocarbons are present in a formation Ro becomes Rt (the resistivity of the uninvaded formation with its naturally occurring fluids) and Equation 14-12 calculates an incorrect Rw value (Rwa) that is greater than Rw. The Rwa curve is an optional curve, so it is not found on many logs. It is usually placed in Track 1. The values are at formation temperature (Figure 14-16).

When the Formation Factor Equation is used to calculate water quality, Rw must be converted to 77° F. This is done by first establishing the geothermal gradient of the well (refer to the explanation for column 3 in Section 3, Volume II) and then calculating the temperature at the depth of interest (refer to the explanation for colume 6 in Section 3, Volume II). The

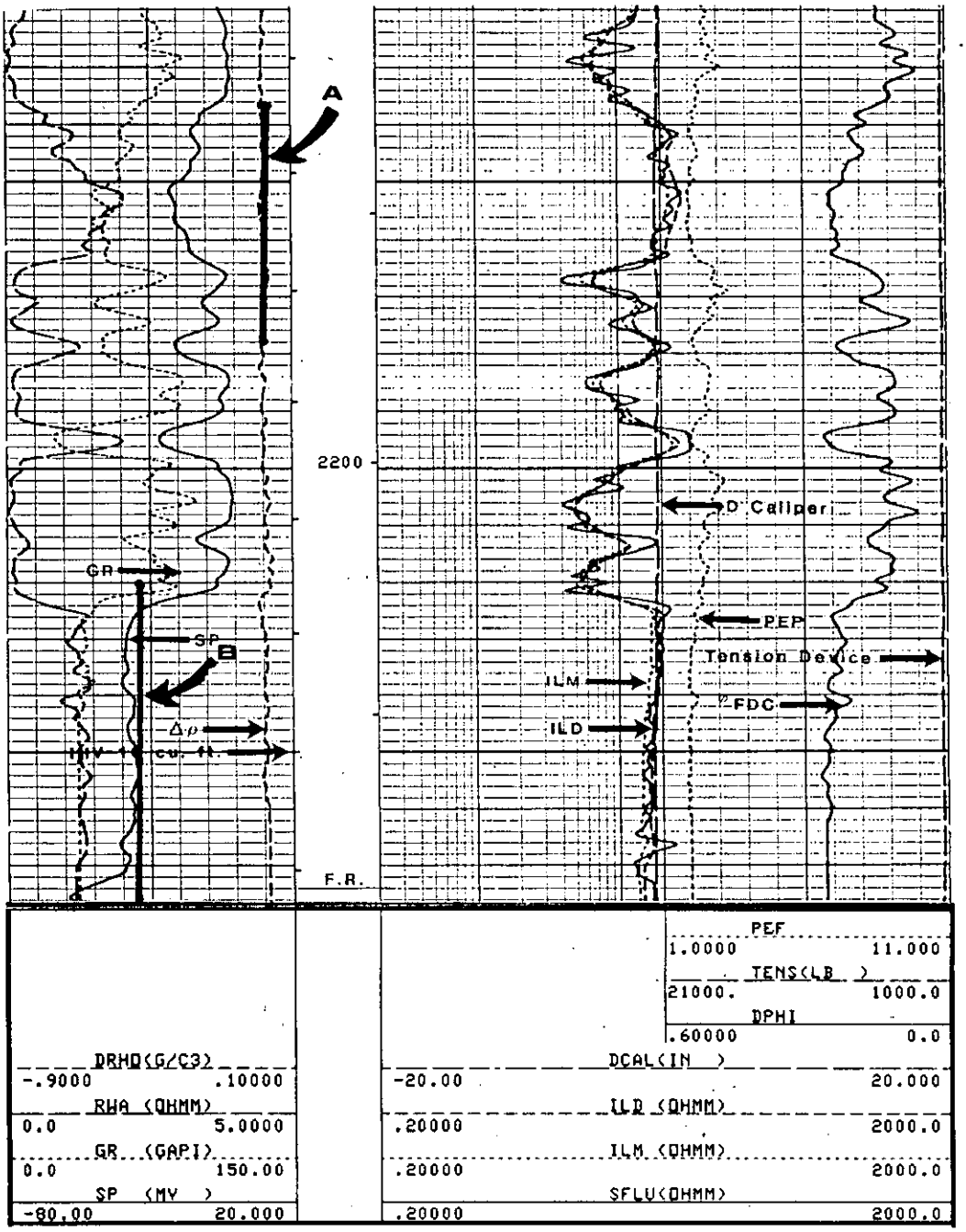

Figure 14-16. Example of a petroleum type Rwa curve. Track 1 contains an Rwa curve computed by the Formation Factor method using $1/\phi^2$ and density porosity (track 3). Rwa values are at formation temperature. The arrows point to Rw values obtained from water samples and adjusted to formation temperature. The Rwa value of zone A is 55 percent less than the measured Rw, while the Rwa value of zone B is 40 percent less than the measured Rw. The difference between Rw measured and Rwa is greater than the difference observed in laboratory tests by Evers and Iyer (Figure 14-18) for this Rw range. However, the differences may be due to factors other than surface conductance. The gamma ray curve shows shale in the sands, which would lower Rwa. The interval is part of the Carrizo-Wilcox. The well is the McKinley Drilling Company, George Strait #1, Webb County, Texas. Rm is 5.23 ohm-meters at 90° F and Rmf is 5.87 ohm-meters at 75° F. T.D. is 2,280 feet, bottom hole temperature is 105° F, and bit size is 9⅞ inches. Density porosity was computed using a matrix density of 2.65 g/cm^3.

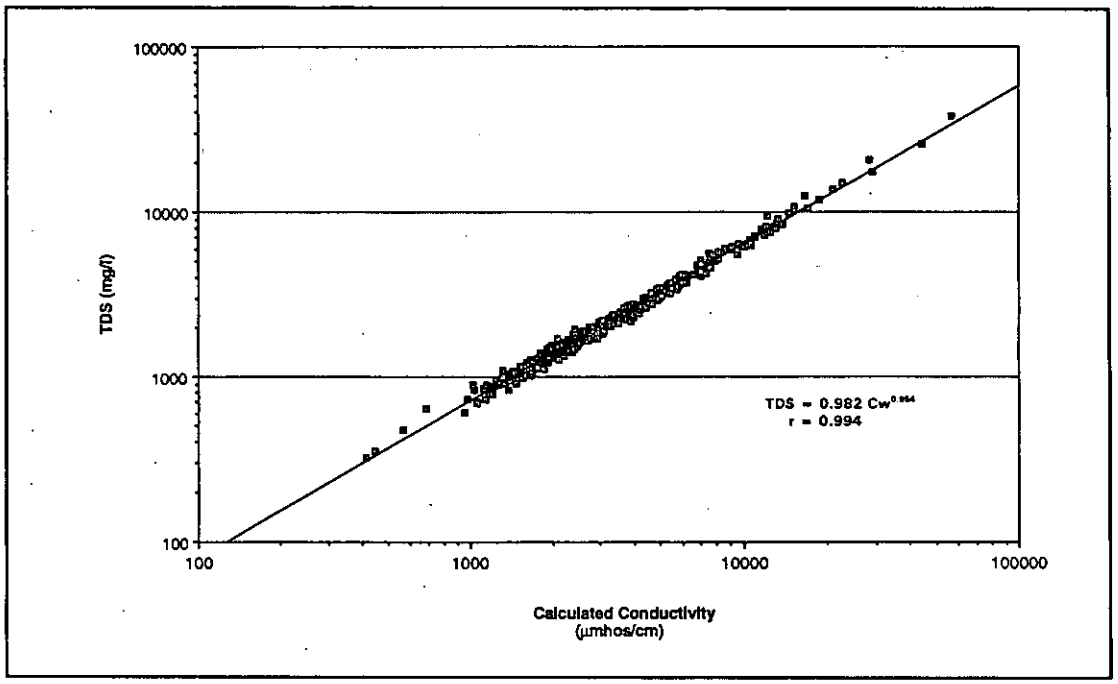

Figure 14-17. TDS-Cw graph for the Gulf Coast aquifer in Cameron, Hidalgo, Starr, and Willacy Counties. The equation is used to calculate TDS in Plate 3. TDS includes 100 percent bicarbonate.

calculated Rw value is then converted to Rw at 77° F by substituting the formation temperature into Equation 2-4. Rw at 77 ° F is converted to Cw using Equation 14-1. Finally, Cw is converted to TDS using the appropriate TDS-Cw graph (Section 5 of Volume II). Figure 14-17 is the TDS-Cw graph for Plate 3.

Equation 14-12 will calculate accurate Rw values when the following conditions are met:

1. The formation is shale-free. Shale lowers Ro, which means that the calculated Rw will be too low.

2. The porosity value is accurate. If a single porosity log is used, the lithology must be constant. If the lithology varies, a crossplot porosity should be used (Chapter 12). The porosity log(s) must be on depth with the resistivity curve. Porosity logs are run in very few water wells. However, they are often available for post-1960 hydrocarbon tests.

3. The proper a and m values are used. Ideally, they should be calculated for the formation being analyzed. However, as discussed above, they can only be calculated if Rw is known! The

only alternative is to estimate a and m based on available geological information about the formation (sample description, porosity log, regional geology, etc.). Most of the time a should be set at 1.0 and m considered a variable. It may be advantageous to establish a range for Rw, using high and low values of m (Plate 1).

4. Rw is less than 2 to 3 ohm-meters at 77° F. For higher Rw's surface conductance causes the logging tool to record an Ra value that is less than Ro. There is no way to accurately correct Ra to Ro using just log data, so Ra is used for Ro in Equation 14-12. This results in a calculated Rw that is too low and Cw and TDS values that are too high. (This is the problem in Figure 14-16).

The surface conductance effect is a major drawback to using the Formation Factor Equation to calculate the water quality of aquifers with fresh to slightly saline water. Surface conductance has such a profound effect on calculated Rw values that it deserves further explanation.

Surface conductance increases the conductivity (or reduces the resistivity) of an aquifer. Chemists (McBain, et al., 1929; Urban, et al., 1935) have shown that solid surfaces in contact with aqueous solutions attract a layer of ions which, in turn, attract a layer of oppositely charged ions which, in turn, attract... The result is double layer conductivity -- a more concentrated solution of predominantly positively charged ions near the surface of the solid, which has a higher conductivity than the rest of the solution. Electrical current preferentially travels through the more conductive double layer, thus making an aquifer appear to have a lower resistivity than is actually the case.

Surface conductance occurs in all aquifers, fresh or saline. Its magnitude is related to the ion concentration of the solution. In fact, surface conductance increases with increasing salinity. However, the increase in surface conductance always remains within the same order of magnitude, while the increase in water conductivity may be several orders of magnitude (McBain, et al., 1929). This means that only in fresh water aquifers will surface conductivity be a large enough percentage of the log-measured Ra value to noticeably affect Ro. For aquifers in Texas, this study found that Ro is significantly affected when Rw is greater than 2 ohm-meters (conductivity less than 5000 μmhos/cm). This agrees with the laboratory work of Evers and Iyer (1975b) which found a cutoff of 3 ohm-meters (3333 μmhos/cm).

Evers and Iyer (1975b) documented that the magnitude of surface conductance is also a function of grain size. The smaller the grain size the greater the surface conductance. Figure 14-18 is an example of two of their data sets. They also quantified the extent to which Ro is reduced as Rw increases: from a few percent at 3 ohm-meters to as much as 60 percent at 50 ohm-meters (Figure 14-18).

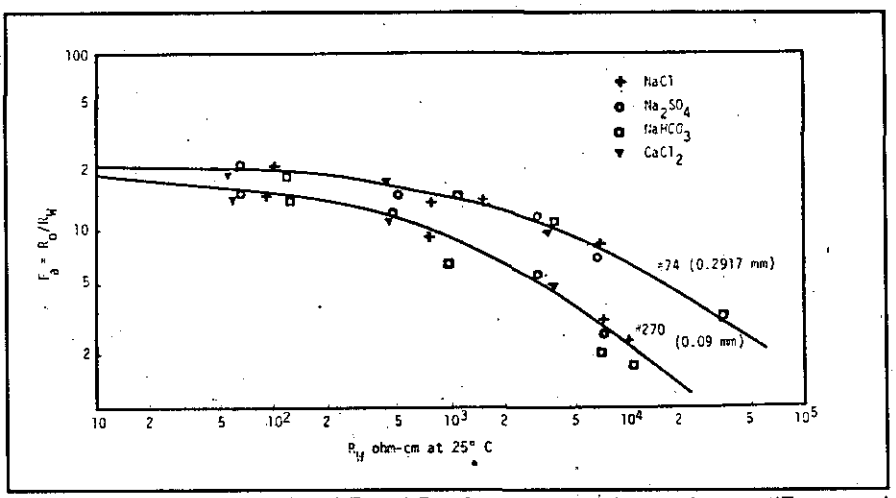

Figure 14-18. Relationship of F and Rw for two experimental cores (Evers and Iyer, 1975). Grain size is in parentheses. Note: divide the Rw values by 100 to get ohm-meters.

The amount of surface conductance is difficult to calculate from log data. There are so many factors that affect Ra (shale, borehole effects, etc.) that from log data it is very difficult to isolate and quantify the effect of surface conductance on Ra. This makes it is very difficult to establish any type of guidelines for correcting calculated Rw values. Calculations on a well in the Carrizo-Wilcox (Figure 14-16) show a much larger difference between Rwa and Rw measured than would be extrapolated from the lab data. However, other factors (e.g. shale) may be contributing to the difference.

Plates 1 to 5 are two examples of water quality calculations using the Formation Factor Equation. Plates 1 to 4 are from a well in an unconsolidated, high porosity sandstone (Gulf Coast aquifer). Plate 5 is from a well in a high porosity carbonate (Edwards aquifer).

Ro-Porosity Graphs

The Ro-Porosity graph, commonly known as the Pickett plot, is a graphical solution of Equation 14-12. It is a slightly modified version of a Formation Factor-Porosity graph (Figure 14-13). However, it is discussed separately in logging literature and is therefore discussed separately in this chapter.

The data is plotted on log-log paper. Ro is plotted on the x axis and porosity on the y axis. The data plots as a straight line as long as m and Rw remain constant and there is enough variation in porosity to establish a straight line. m is the negative slope of the line, the measured distance on Ro divided by the measured distance on ϕ (Figure 14-19). The point at which the line intersects the 100 percent porosity line is a × Rw at formation temperature. If a is 1 (as it usually is), the point of intersection is Rw at formation temperature.

The Ro-Porosity graph is subject to the same limitations as Equation 14-12. In many aquifers it is difficult to use the method to calculate Rw. In homogenous, high porosity aquifers there will not be enough variation in porosity to establish the slope of the line. In fresh to slightly saline aquifers the curve fit will estimate an Rw that is too low and an m that is too high due to surface conductance. An additional complication is the accuracy of the curve fit (refer to Appendix II). However, an Ro-TDS graph should always be constructed in conjunction with the Formation Factor Equation method. Under the right circumstances (refer to the **Formation Factor Equation** section) it can be used for several purposes:

1. Rw can be estimated if m is constant, Rw is constant, and a is known (Figure 14-19).

2. m can be estimated if Rw is known and is constant (Figure 14-19).

3. Variations in m can be discerned if Rw is constant.

4. Variations in Rw can be discerned if m is relatively constant (Figures 14-20 and 14-21).

Resistivity Ratio Method

Petroleum log analysts have been using the Resistivity Ratio method to determine Rw for a number of years. Alger and Harrison (1988) proposed that the technique should be utilized more often in ground-water logging.

The Resistivity Ratio method calculates Rw by comparing the resistivity of the flushed zone (Rxo) with the resistivity of the uninvaded zone (Ro). The technique is based on four assumptions, all of which are normally valid:

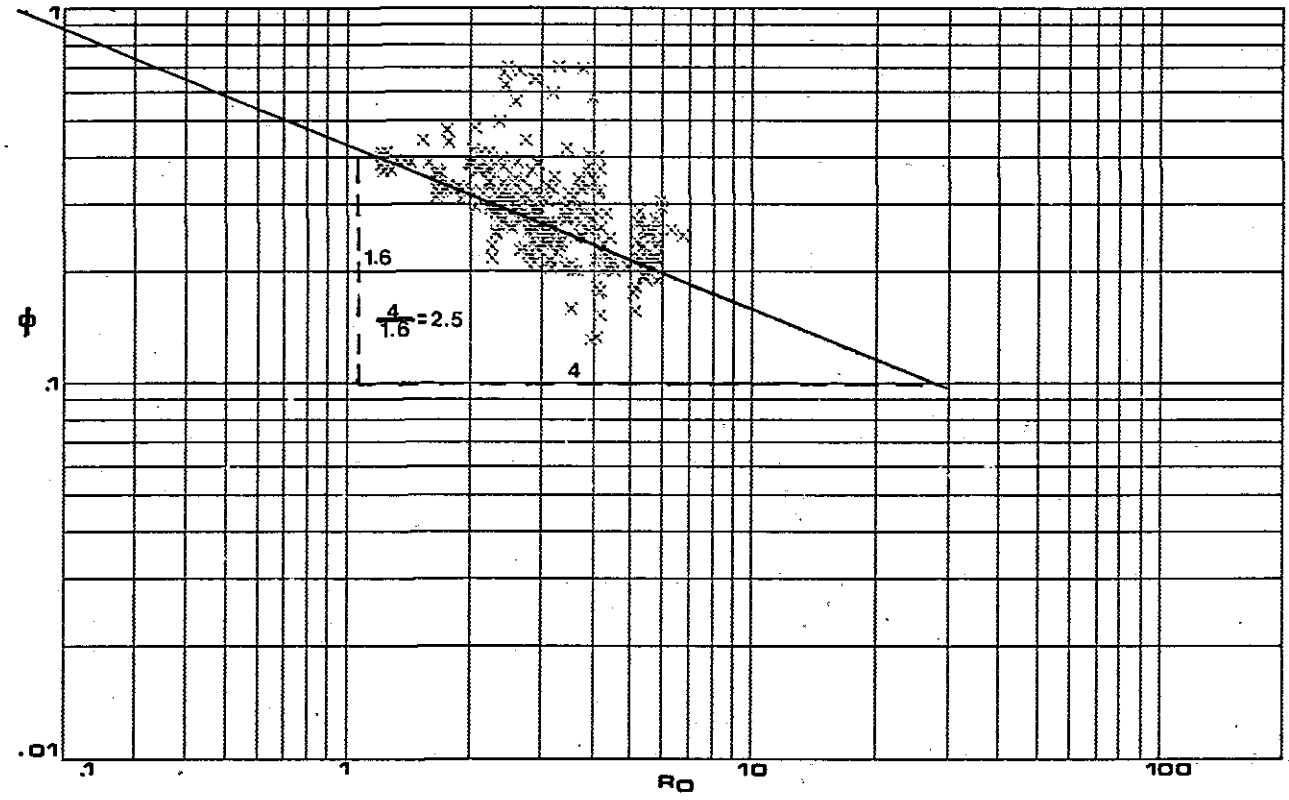

Figure 14-19. Using an Ro-Porosity plot to estimate Rw and m. Ro values are from the deep induction curve and porosity values are density-neutron crossplot porosity. The well is in the Edwards aquifer and the data is from part of the Kirschberg Evaporite and Dolomitic Members of the Kainer Formation. The data is from an interval that has a constant Rw (1.8 ohm-meters at formation temperature). Rw is from water samples obtained during pump tests. Although there is scatter in the data, a fairly consistent pattern is present. The data is consistent enough to estimate Rw and/or m from the graph. Assuming an a of 1, a line with an Rw of 1.8 ohm-meters was fitted to the data. This line yields an m of 2.5, not an unreasonable value in a vuggy-moldic carbonate. However, an m of 2 was used in the Formation Factor Equation method and it gave accurate Rw's (Plate 5). Not knowing Rw, a best fit line through the data would yield an Rw close to the actual value. The well is the Edwards Underground Water District, A-1. Figure 13-32 and Plate 5 contain additional information on this well.

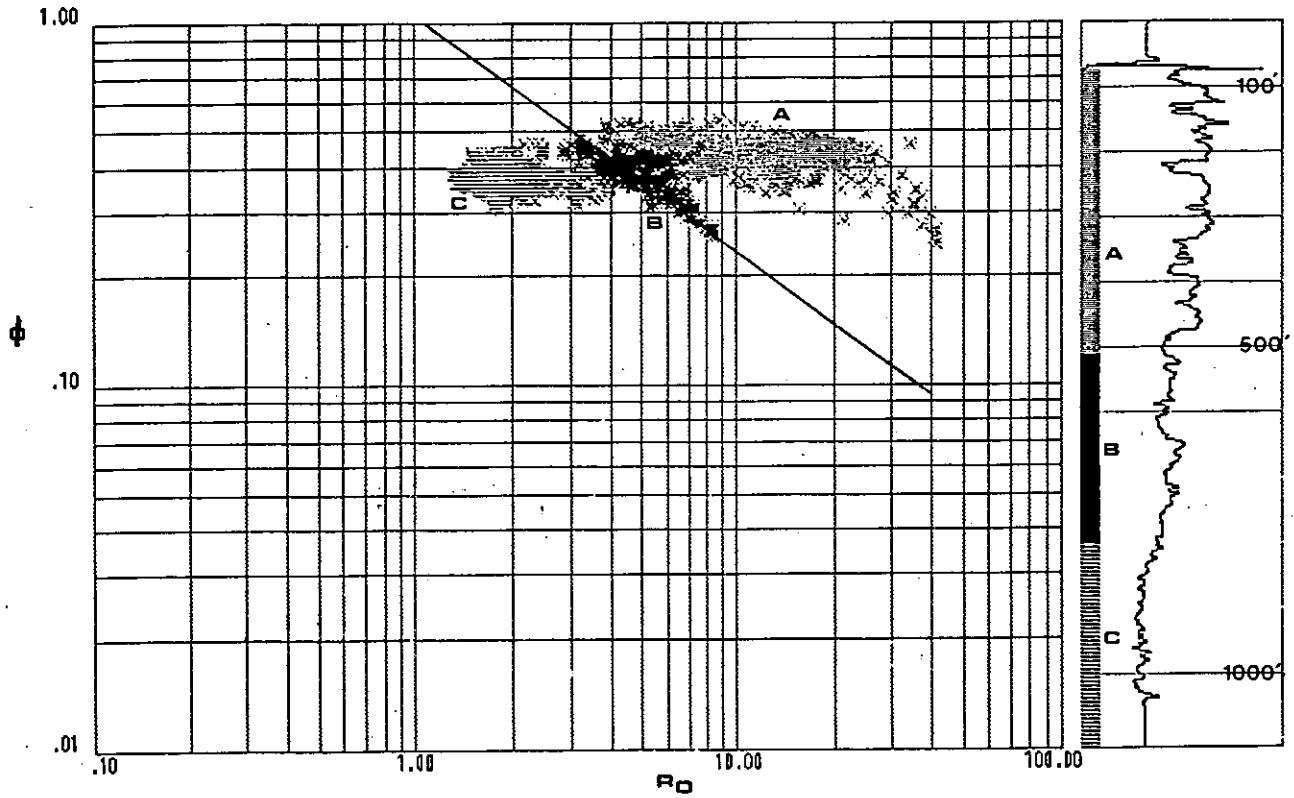

Figure 14-20. Using an Ro-Porosity graph to distinguish waters of different salinities. Ro values are from the deep induction curve and porosity values are from density-neutron crossplot porosity. The data is from the entire length of the borehole. The data cluster into three groups (A, B, and C), suggesting three different water salinities. Rw values from water samples taken during pump tests confirm three Rw ranges. The scatter in groups A and C is such that it is impossible to estimate either m or Rw. A good line fit can be drawn through group B, yielding an Rw that is too high (about 1.05 ohm-meters versus an actual Rw of about 0.54 ohm-meters at formation temperature) and an m of 1.3. This m is consistent with m's of 1.1 and 1.4 estimated from the Formation Factor-Porosity graph (Figure 14-13). The column to the right of the graph contains the deep induction curve and a few 100 foot depth markers. It also identifies the intervals in the well that correspond to the three clusters of data. The well is the TWDB PUB Test Site F, Cameron County, Texas. Refer to Figure 13-12 and Plates 1 to 4 for additional information on this welll.

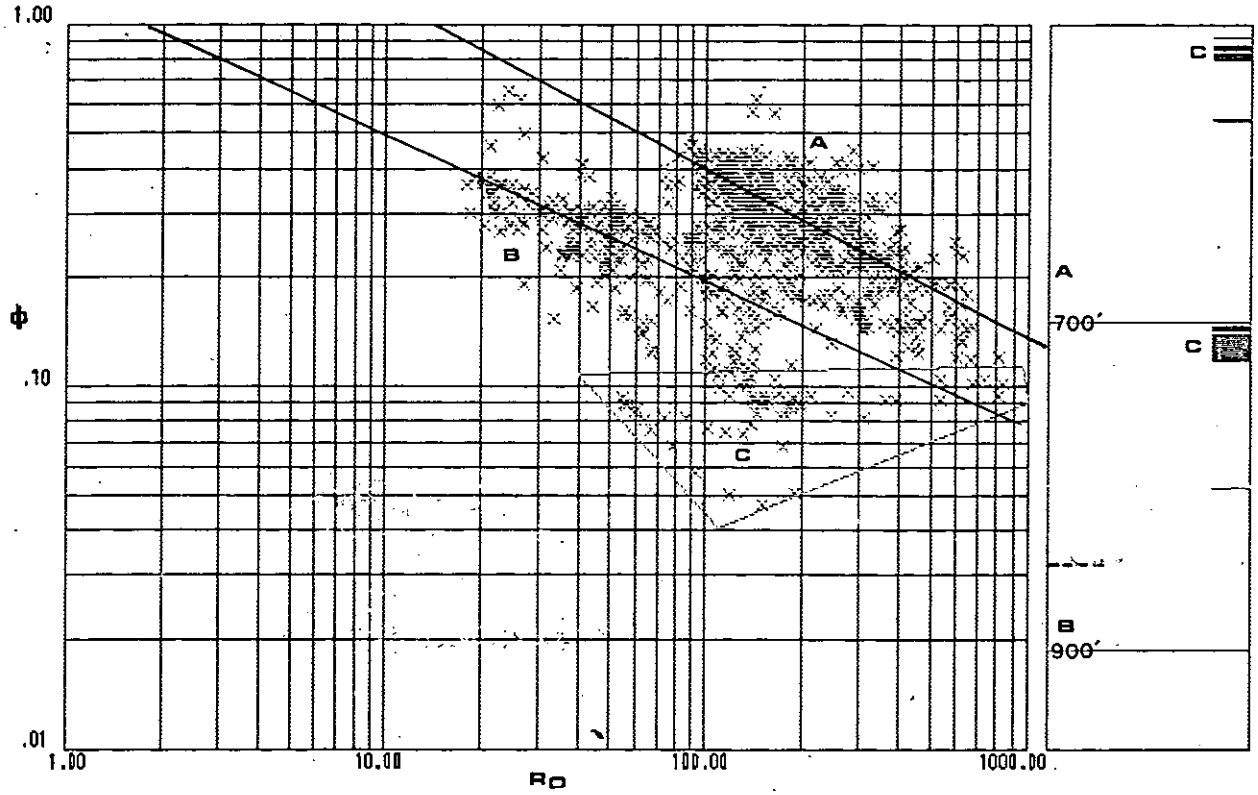

Figure 14-21. Using an Ro-Porosity graph to distinguish waters of different salinities. Ro values are from an averaged spherically focused curve and porosity values are from density-neutron crossplot porosity. The data is from the entire length of the borehole. The data cluster into three groups (A, B, and C), suggesting three different water salinities. Group C, however, is the Georgetown Formation and the Regional Dense Member of the Person Formation. Both are low porosity and very low permeability limestones. Therefore, in the case of group C the cluster represents a different pore structure, rather than a distinct water salinity. Rw values from water samples taken during pump tests confirm two Rw ranges: 16 to 17 ohm-meters for group A and 2 ohm-meters for group B. These Rw's agree closely with Rw's estimated from the graph. Group A has an m of 2.0 and B has an m of 2.2 (2 was used in the Formation Factor Equation). The column to the right of the graph identifies the intervals in the well that correspond to the groups. The well is in the Edwards aquifer. It is the Edwards Underground Water District, C-1, New Braunfels, Texas (state well number 68-23-619). Poteet, Collier, and Maclay (1992) contains detailed information on the well.

1. The pore geometry and lithology of the formation near the borehole is the same as it is laterally in the formation at the depth of investigation of the deep reading resistivity tool (normally a few feet).

2. The amount of surface conductance is the same in both the flushed and the uninvaded zones.

3. The difference between Ro and Rxo is solely a function of the difference in Rmf and Rw.

4. There is mud filtrate invasion. However, near the bottom of the hole there may not be enough invasion for a resistivity contrast between the two zones.

When the above assumptions are valid, the Formation Factor Equations for the flushed zone and the uninvaded zones (Equations 14-13 and 14-14) are equivalent (Equation 14-15). The Formation Factor Equation for the flushed zone is

$$F = Rxo / Rmf \qquad \textbf{14-13}$$

The Formation Factor Equation for the uninvaded zone is

$$F = Ro / Rw \qquad \textbf{14-14}$$

Equations 14-13 and 14-14 are equivalent, so they can be set equal to each other:

$$Rxo / Rmf = Ro / Rw \qquad \textbf{14-15}$$

The equation can then be rearranged to solve for Rw:

$$Rw = Rmf / Rxo / Ro \qquad \textbf{14-16}$$

Since F has been factored out of Equation 14-15, the Rw calculation (Equation 14-16) is independent of porosity, m, and a. Surface conductance effects are also factored out. If Rmf is adjusted to 77° F, Rw will be calculated at 77° F, thus eliminating any need to know formation temperature. The only data required for the calculation are accurate Ro, Rxo, and Rmf values.

Accurate Ro values are usually not a problem if the formation is thick and shale-free. (Chapters 8 and 9 explain how to correct resistivity curves for borehole effects.) If the formation is shaly, both Ro and Rxo must be corrected (Alger and Harrison, 1988):

$$(Rxo / Ro)^{1 / (1 - Vcl)} = (Rxo / Ro)_{clean} \qquad \textbf{14-17}$$

Where:

Rxo / Ro = log values uncorrected for shale
Vcl = clay volume
$(Rxo / Ro)_{clean}$ = log value corrected for shale

The clay volume can be calculated from either the gamma ray (Figure 10-7) or the SP curves (Equation 12-1).

Accurate Rxo values are essential. In wells with fresh-water muds and fresh-water aquifers, Rxo curves read much too high. Any subsequent Rw calculations will be too low. The appropriate borehole correction is not difficult to make, but it has usually not been applied to the Rxo curve on the log. It must be made before using the Resistivity Ratio method (refer to the **FOCUSED PAD MICROELECTRODE TOOLS** section in Chapter 9).

A greater problem with Rxo data is its availability. Rxo tools are virtually never run in water wells and they are normally utilized by the petroleum industry only in certain sections of the state, the Permian Basin being the chief area. In the absence of an Rxo curve, an Rxo value can be estimated from an Ri value obtained from a shallow reading resistivity curve (LL8, SFL, Short Guard, or Short Normal). As shown by Figure 8-3, the Short Normal reads deeper than the other three tools. Consequently, it will be the least accurate. Figure 14-22 is a nomograph correcting Ri / Ro to Rxo/ Ro for various curve combinations. The chart assumes an invasion

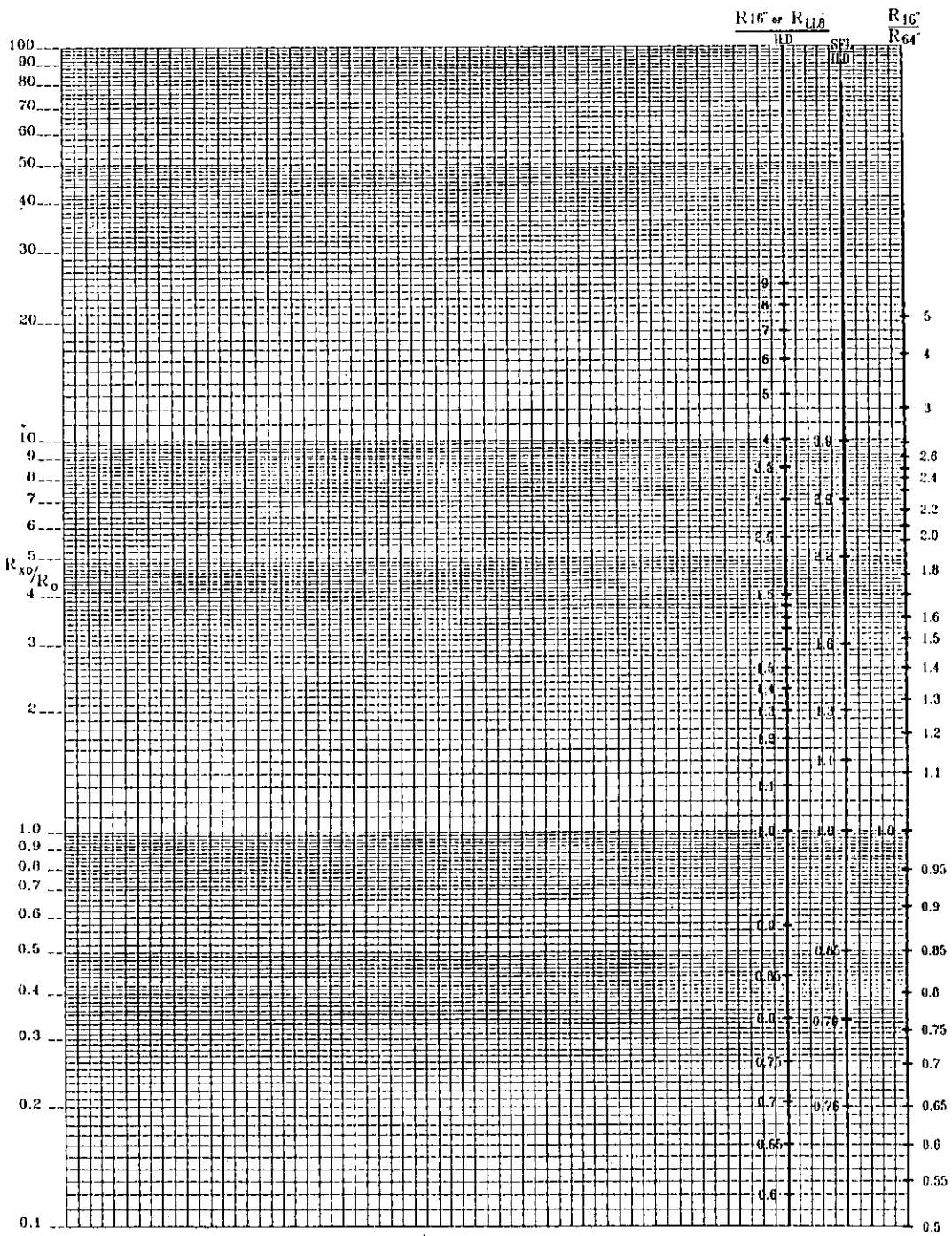

Figure 14-22. Nomograph for converting Ri / Ro to Rxo / Ro. The chart converts the most common log combinations: 16" normal / 64" normal, 16" normal / deep induction, LL8 / deep induction, and SFL / deep induction. An Ri / Ro value is entered on the appropriate line on the right side of the chart and a horizontal line is drawn to corresponding Rxo / Ro value on the left side. The chart was calculated for an invasion diameter of 20 inches, which is fairly typical for shallow, high porosity sandstones. Therefore, it contains generalized conversion factors. Bob Alger constructed the chart.

diameter of 20 inches, which is fairly typical for shallow, high porosity sandstones (Alger, personal communication). The chart, therefore, contains generalized conversion factors and the Rxo / Ro value obtained from the nomograph will usually be an estimate that has an unknown degree of accuracy. An Rw value calculated from data derived from Figure 14-22 is subject to a great deal of error.

An accurate Rmf measurement may or may not be a problem. Rm and Rmf are often measured on a sample of the drilling mud at the time of logging (refer to the **Drilling Fluid Invasion** section of Chapter 6). The values are usually included on the log header. If only Rm is measured, Rmf can be calculated from Rm. In fact, Alger (personal communication) believed that an Rmf value calculated from Rm is more accurate than a measured Rmf. This is because such a small volume of mud filtrate is available for the Rmf measurement. However, most log analysts prefer measured values (Schlumberger, 1988).

When calculating Rmf from Rm, some log analysts simply multiply Rm by 0.75. The most commonly used conversion factor is the one developed by Overton and Lipson (1958):

$$Rmf = K_m (Rm)^{1.07} \qquad \textbf{14-18}$$

The value of the constant K_m is a function of the mud weight (Table 14-3). The equation is for drilling muds with Rm in the range of 0.1 to 10 ohm-meters at 75° F. Most chart books contain a nomograph of Equation 14-18.

TABLE 14-3. K_m VALUES FOR VARIOUS MUD WEIGHTS

Mud Weight lb/gal	K_m
10	0.847
11	0.708
12	0.584
13	0.488
14	0.412
16	0.380
18	0.350

Lowe and Dunlap (1986), after reworking Overton and Lipson's data and making Rmf measurements on additional samples, developed their own conversion equation. The test data from both studies (Figure 14-23) shows that the Rmf / Rm value of muds lighter than 11 pounds per gallon is much more variable than it is for denser muds. In fact, for these lighter muds Rmf can be greater than Rm. In the wells analyzed for this study, a wide range was also observed in the ratio of Rmf to Rm, and in 14 percent of the wells Rmf was greater than Rm (Section 1, Volume II).

The best policy is to accurately measure the Rm and Rmf of a circulated sample of the drilling fluid. If possible, the measurements should be taken daily during drilling because mud properties can change during the course of drilling a well. In the absence of a measured value, Rmf can be estimated from Equation 14-18. However, the calculated Rmf may be too low for muds lighter than 11 pounds per gallon.

The Resistivity Ratio method will calculate an accurate Rw, if accurate Rmf and Rxo values are available and if there is some invasion. Accurate Rw values were calculated for approximately a dozen wells analyzed during

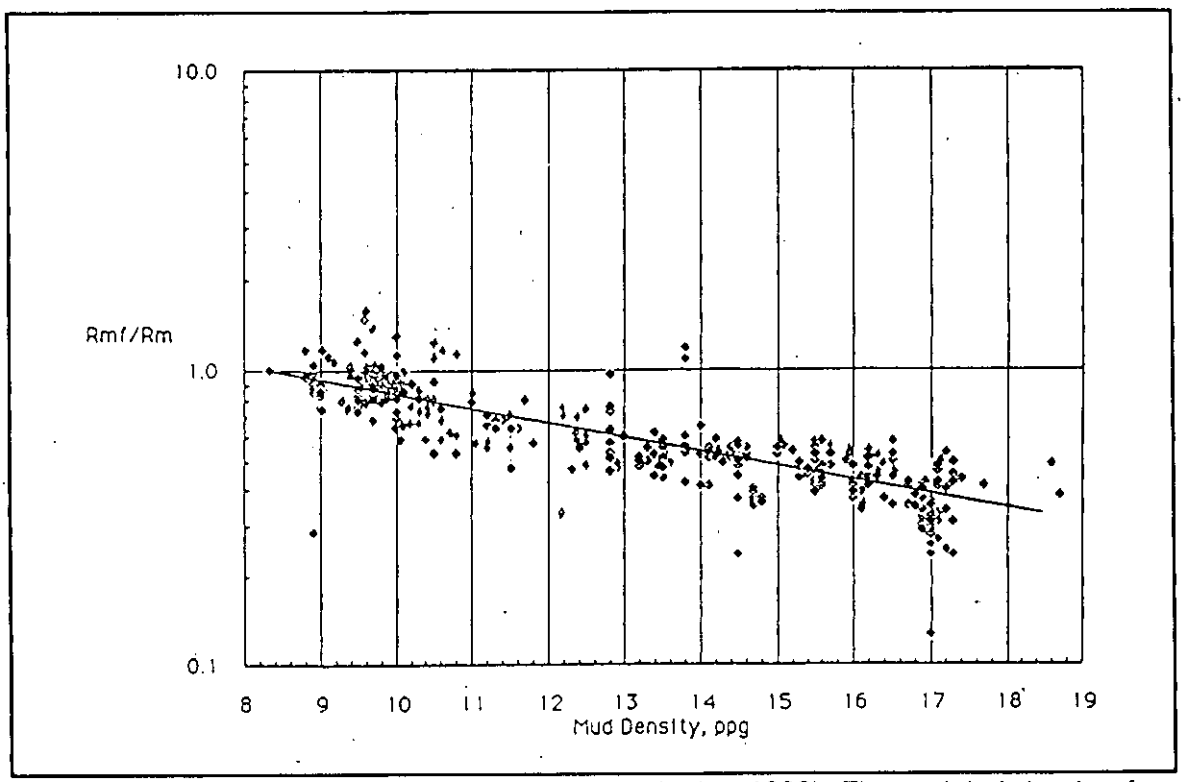

Figure 14-23. Rmf / Rm versus Mud Weight (Lowe and Dunlap, 1986). The graph includes data from Overton and Lipson (1958). The data for muds less than 11 pounds per gallon has considerable scatter.

this study (Figures 14-24 and 14-25 and Plates 2 and 3 are examples). The technique should be utilized more widely in ground-water studies, but Rxo tools must first start being run.

SP

Rw calculations from an SP curve date back to the earliest days of quantitative log analysis. Wyllie (1949) and Gondouin, et al. (1957) authored the technique. Alger (1966) elaborated on the difficulties of determining water quality with the SP curve. He also attempted to use the curve to estimate hardness (Alger and Harrison, 1988). McConnell (1983, 1985, 1988, and 1989) has been the latest to publish on the use of the SP curve in water quality calculations.

The technique requires a shale-free formation that is thick enough to have a static SP (SSP). It also assumes that static SP is solely a product of an electrochemical potential and that the shale adjacent to the formation of interest is an ideal ionic permeable membrane. (The various aspects of the SP curve are discussed in Chapter 12.) Under these conditions, SSP is related to the chemical activities of the cations in the formation water (a_w) and the mud filtrate (a_{mf}) by the formula:

$$SSP = -K \log a_w/a_{mf} \qquad \textbf{14-19}$$

For sodium chloride solutions and shales that are ideal ionic permeable membranes, K is solely a function of temperature:

$$K = 61 + 0.133\ T_{°F} \qquad \textbf{14-20}$$

For pure sodium chloride solutions that have an Rw or an Rmf of greater than 0.12 ohm-meters (83,333 μmhos/cm), resistivity is inversely proportional to the activity of the sodium ions (Figure 14-26). This means that Equation 14-19 can be rewritten as:

$$SSP = -K \log Rmf/Rw \qquad \textbf{14-21}$$

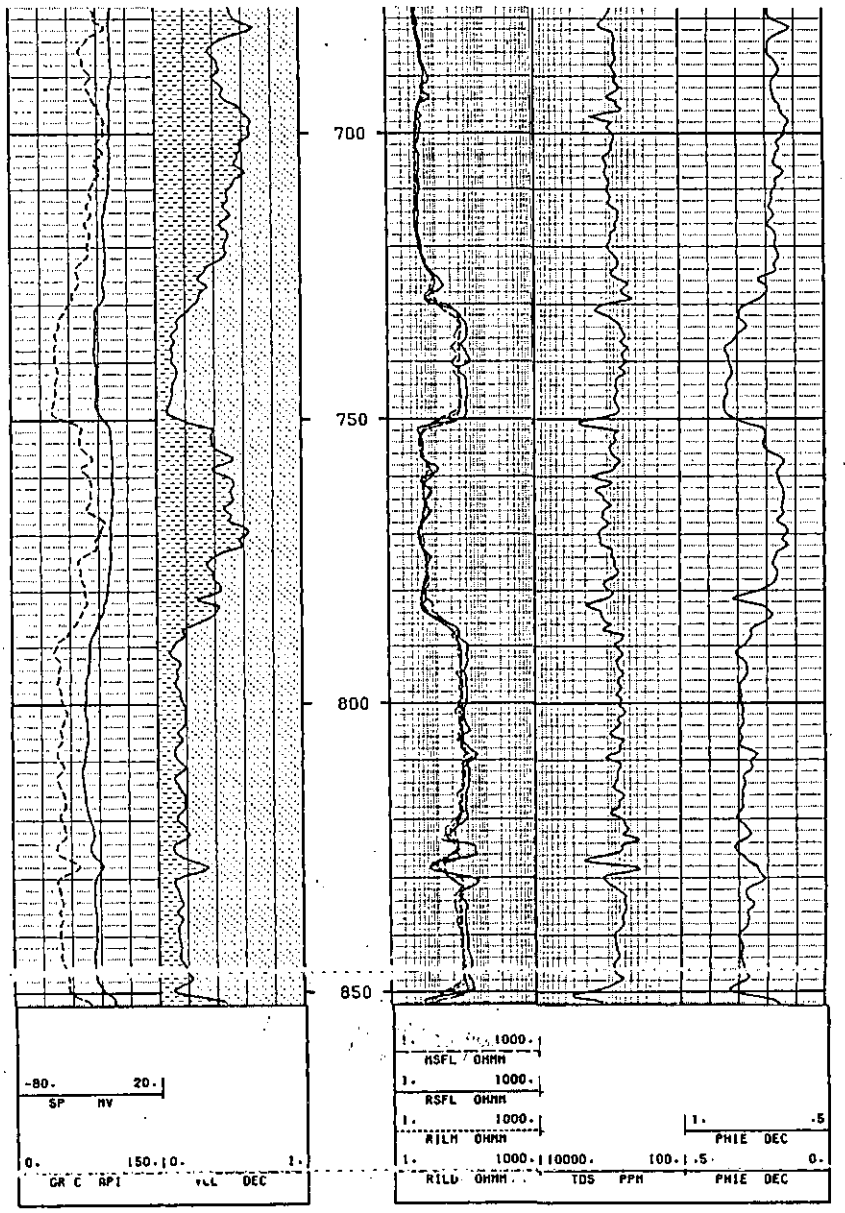

Figure 14-24. Water quality curve calculated by the Resistivity Ratio method using an Rxo curve. Track 4 contains a TDS curve calculated from Rw values obtained from the Resistivity Ratio method. Rw was converted to Cw and then TDS was calculated from Cw. The water analysis from a test hole drilled to 813 feet has a TDS of 590 mg/l. The calculated TDS of the two sands from 730 to 813 feet varies from 500 to 700 mg/l, very close to the TDS values that would give a composite TDS of 590 mg/l for the two sands. The resistivity curves nearly overlay, which indicates that Rmf and Rw are about the same. Rmf is 8.2 ohm-meters at formation temperature (82° F). Track 1 contains SP and borehole corrected gamma ray curves (GR C). Track 2 is a lithology column calculated from the gamma ray and porosity logs. The volume of clay (VCL) and the volume of quartz (dot pattern) are in decimal form (DEC). Track 3 contains microspherically focused (MSFL) and dual induction curves. Track 5 contains a density-neutron crossplot porosity curve (PHIE) in decimal form (DEC). The well is the Alsay, Cypress Creek U.D., #3, Harris County, Texas. The interval is part of the Gulf Coast aquifer. Figure 9-14 contains additional information on this well.

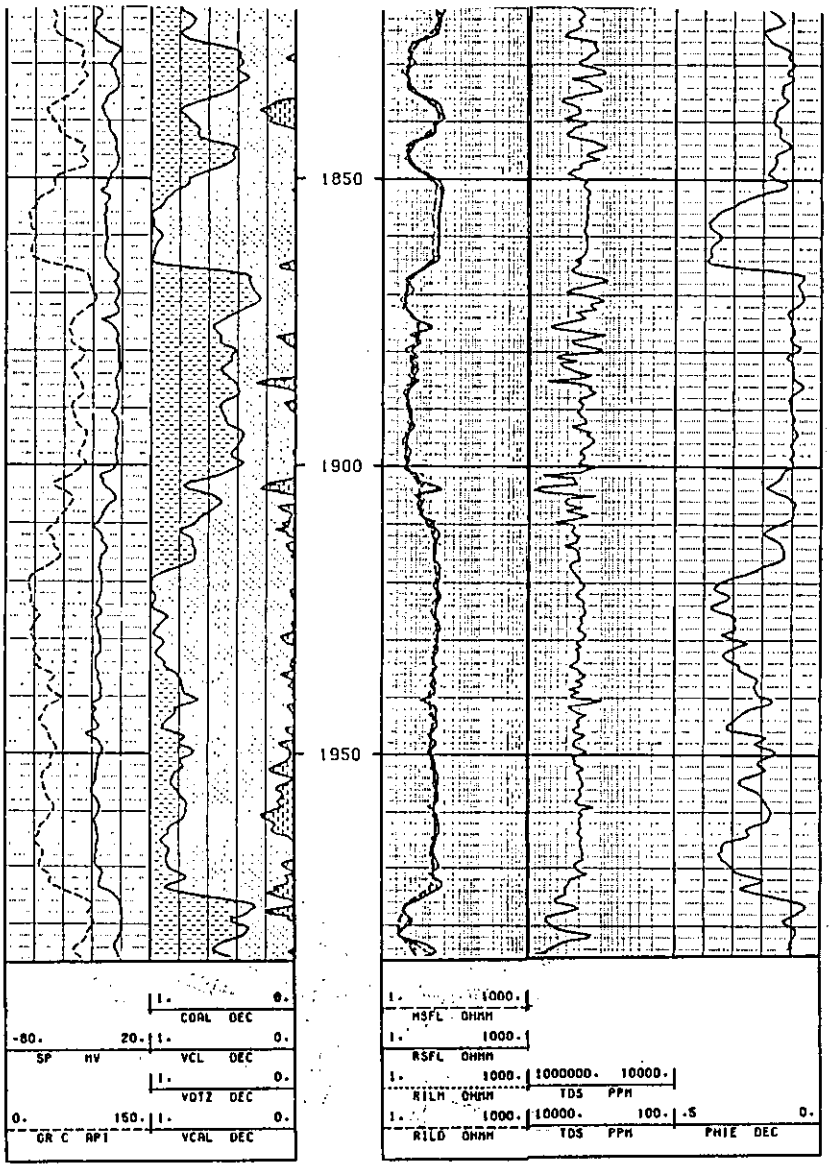

Figure 14-25. Water quality curve calculated by the Resistivity Ratio method using an Rxo curve. Track 4 contains a TDS curve calculated from Rw values obtained from the Resistivity Ratio method. Rw was converted to Cw and then TDS was calculated from Cw. The water analysis of the screened interval (1850 to 1866 and 1910 to 1974 feet) has a TDS of 2330 mg/l. The calculated TDS of the main sandstone (1910 to 1970 feet) varies from 1900 to 2100 mg/l, an error of about 10 percent. Some of the error may be due to the wrong exponent being used to convert Cw to TDS. The resistivity curves nearly overlay, which indicates that Rmf and Rw are about the same. Rmf is 3.38 ohm-meters at 81° F. Track 1 contains SP and borehole corrected gamma ray curves (GR C). Track 2 is a lithology column calculated from the gamma ray and porosity logs. The volume of clay (VCL), quartz (VQTZ), and calcite (VCAL) are in decimal form (DEC). Track 3 contains microspherically focused (MSFL) and dual induction curves. Track 5 contains a density-neutron crossplot porosity curve (PHIE) in decimal form (DEC). The well is the J.L. Myers, Bristol Water Supply #2, Ellis County, Texas. The aquifer is the Woodbine. Figure 9-11 contains additional information on this well.

By rearranging Equation 14-21, Rw can be calculated:

$$Rw = Rmf/10^{(-SSP/K)} \qquad 14\text{-}22$$

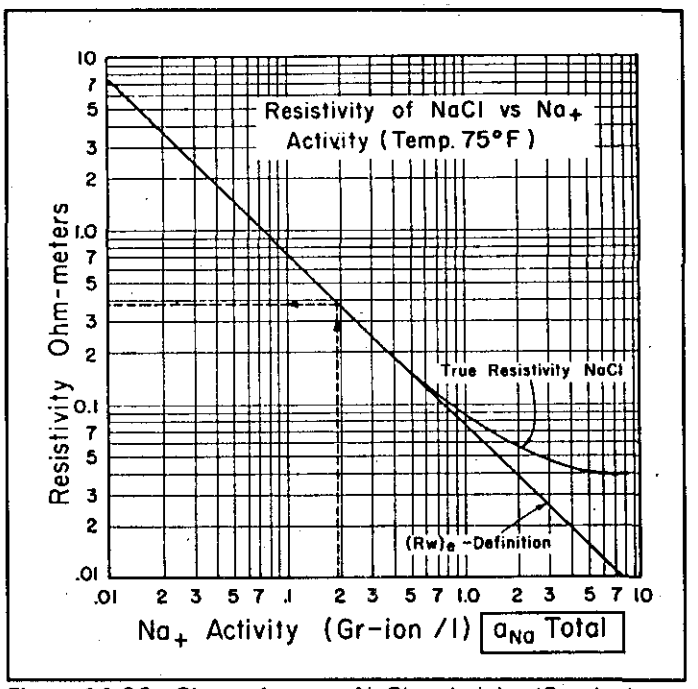

Figure 14-26. Chart of a_{Na} vs. NaCl resistivity (Gondouin, et al. 1957).

If Rw or Rmf is less than 0.12 ohm-meters (Figure 14-26), if the formation water is a type other than sodium chloride, or if polyvalent cations are present in either the formation water or the mud filtrate, Rw and Rmf are no longer inversely proportional to a_w and a_{mf}. Under any of these circumstances, Rw and Rmf in Equations 14-21 and 14-22 become **equivalent resistivities (Rmfe** and **Rwe)**. An equivalent resistivity is the resistivity value of the sodium chloride solution that will generate the same SSP as that generated by a non-sodium chloride solution. Any basic petroleum log analysis text has a discussion of equivalent resistivities for low resistivity waters. This research was limited to non-sodium chloride waters, including those with polyvalent cations.

Polyvalent cations were found to be common in fresh to moderately saline ground waters in Texas (Section I, Volume 2). Most commonly the polyvalent cations are divalent calcium and magnesium ions. These two ions have a chemical activity that is about an order of magnitude greater than that of sodium ions (Figure 14-27). Consequently, divalent ions generate a negative SP that is much larger than the SP generated by an equivalent concentration of sodium ions. Therefore, Rwe is much lower than Rw. Rwe must be converted to Rw by means of an empirically derived correction factor.

The relationship between Rw and Rwe for a particular water type can be established if a sample of the water in question is available. The conversion factor is the ratio of the Rw of the water sample to the Rwe calculated using Equation 14-22. Figure 14-28 is a graph of Rw-Rwe

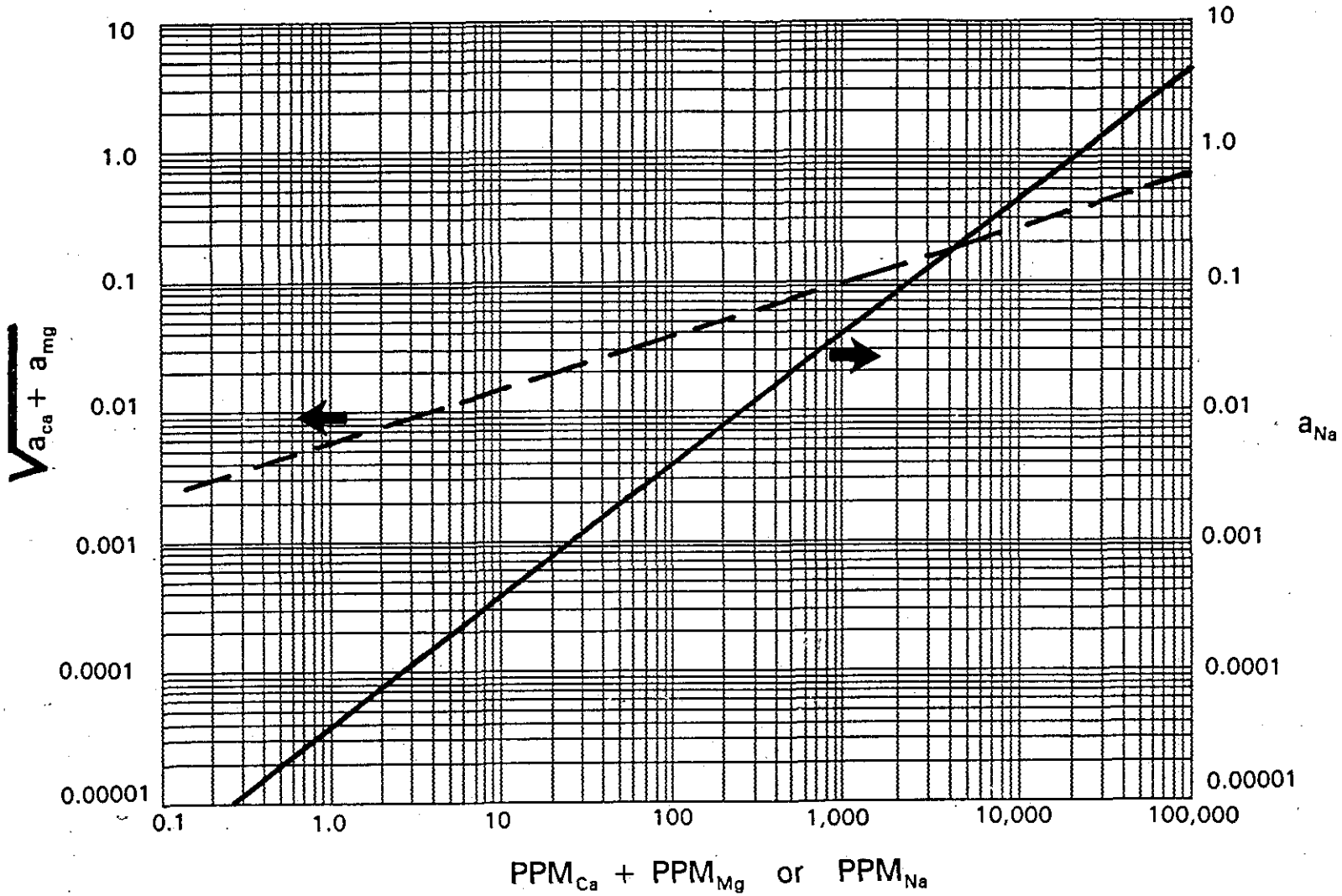

Figure 14-27. Cation concentrations vs. activities for sodium and calcium plus magnesium ions at 77° F (modified from Alger, 1966).

relationships for several pure end-member water types. Natural waters will fall somewhere in between the end members.

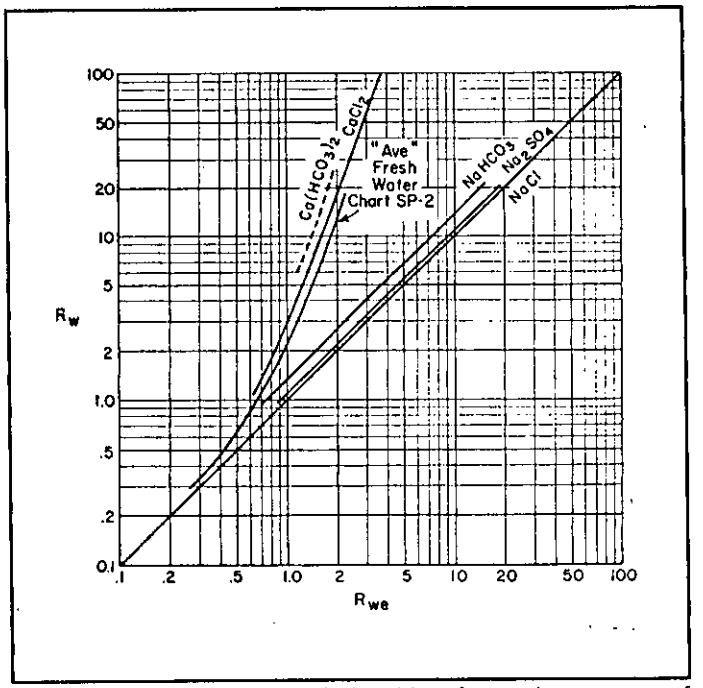

Figure 14-28. Rw-Rwe relationships for various types of waters (Schlumberger, 1972).

If a water sample is not available, the only option is to use an Rw-Rwe relationship from an offsetting well that has the same concentration of divalent ions. Unfortunately, the only way to be sure that the concentrations are the same is to have an analysis of both waters! An additional difficulty is that the water sample may not accurately reflect the chemical composition of the formation water. Mud filtrate invasion may alter the sodium/calcium/magnesium ratio of formation water passing through the invaded zone until several pore volumes of water have been produced (McConnell, 1985).

Calcium and magnesium ions can occur in mud filtrate, but the filtrate is usually a sodium chloride solution. This is because the divalent ions are preferentially adsorbed by clay platelets in the mud, while sodium ions are released into the drilling fluid (Gondouin, et al., 1957). If aquagel has been added to the drilling fluid or if long shale sections have been drilled, there is usually enough clay in the mud to adsorb any polyvalent ions (Alger and Harrison, 1988). At least, this is the assumption that has to be made, since a chemical analysis of the mud is seldom available (Alger, 1966).

There are several other conditions under which the SP curve will calculate an erroneous Rw value:

1. The presence of clay in an aquifer, or a thin-bedded aquifer. Both reduce the amount of negative SP deflection, so a calculated Rw value will be too high (Plate 2).

2. An SSP with an electrokinetic potential component. SSP will be larger than expected, so a calculated Rw value will be too low.

3. A formation water or a mud filtrate that is predominately sodium bicarbonate. K will be less than that calculated by Equation 14-20 (Schlumberger, 1989). This will result in a calculated Rw that is too high.

4. Shales that are non-ideal membranes. Since K is a function of the cation exchange capacity of the shale (Silva and Bassiouni, 1981), it will be different than the K calculated with Equation 14-20. Unfortunately, cation exchange capacities are very seldom measured. Silva and Bassiouni (1981) recommend determining K from a previously established empirical relationship between K and shale resistivity. Shales that behave as non-ideal membranes are usually Tertiary or younger and K is less than what Equation 14-20 calculates (Alger and Harrison, 1988).

A water analysis can also be used to predict SSP. A known Rmf is converted to a_{mf} (Figure 14-26). a_w is calculated from the sum of a_{Na} and $\sqrt{a_{Ca} + a_{Mg}}$ (Figure 14-27). Equation 14-19 is then used to calculate SSP. However, such an exercise is mainly of academic interest and has little practical application in ground-water studies.

Calculating Rw from the SP curve was very unsuccessful for the wells studied in this project. This was especially true in cemented sandstones with varying porosities, such as the Trinity aquifer. Plate 2 contains an Rw curve calculated from the SP of a well in Cameron County, Texas. The calculated Rw values are accurate down to 500 feet, but below this depth they are much too high. Possible explanations for the discrepancies are discussed in the explanation for Plate 2.

Calculating Rw from an SP curve works well for sodium chloride waters as long as the aforementioned conditions are met. If, however, the water has appreciable divalent ions, as is the case of many fresh to moderately saline ground waters, the technique is very difficult to use. It will work only if an Rw-Rwe relationship has been established. Unfortunately, the only way to establish the relationship is to first measure the Rw of a sample of the water; if a water sample is available, logging techniques are not needed! An Rw-Rwe relationship can be used from an adjacent well, as long as the calcium and magnesium concentrations are the same in both wells. But again, the only way to be sure of this is to have a water analysis from both wells. Thus Rw calculations from an SP curve in ground waters with divalent ions are only reliable after the fact.

SUMMARY AND CONCLUSIONS

Borehole geophysical techniques are a viable method of determining the water quality and hydrogeological parameters of aquifers. However, accurate answers require utilization of the correct logging suite, the appropriate interpretation techniques, and appropriately constructed TDS-Cw graphs.

This study found a wide variety in the accuracy with which labs in Texas measure specific conductance. Some labs need to improve their calibration procedures. It was found that the Texas Department of Health's method of calculating specific conductance from diluted conductance does not give accurate values. Diluted conductance should not be substituted for measured conductance. It was documented that in the absence of a measured conductivity value, specific conductance can be accurately calculated from ionic concentrations.

Temperature-conductivity relationships for slightly to moderately saline non-NaCl type waters have not been published in either petroleum or groundwater literature. One of three equations is normally used to adjust conductivity for temperature fluctuations: Arp's, simplified Arp's, and 2 percent per ° C. Analysis of published data and laboratory experiments conducted during this project revealed that no one equation consistently yielded more accurate values. All three equations give acceptable temperature-corrected conductivity measurements, but the 2 percent per ° C equation is less likely to yield extreme values.

This study found a difference in the way labs calculate TDS. Some labs include 100 percent of the bicarbonate value, while others use 49.2 percent. Since ionic concentration governs Cw, 100 percent of the bicarbonate value should be included. Also, some labs do not document and perform a check on the accuracy of their TDS measurements.

TDS can be accurately estimated if Cw is known by using a TDS-Cw graph. These graphs have not previously been constructed for Texas ground waters. TDS-Cw graphs were constructed in this study for the major aquifers in the state. Also, a data base consisting of water analyses and log values from over 700 wellls in the major Texas aquifers was compiled and analyzed.

This study researched and established the proper procedure for constructing TDS-Cw graphs: guidelines for where to obtain water analyses, how to correct Cw to standard temperature (25° C), how to compute the proper TDS value, how to critique the accuracy of water analyses, and how to construct the graphs. Important conclusions include:

1. TDS should include 100 percent of the bicarbonate value.

2. The best graph is a log-log scale plot with the equation of the line fitted by reduced major axis and the equation of the line transformed to a power law.

3. Because of interionic interference, the graphs need to be established for a local area in order to conform to local water chemistry.

4. When the data is extrapolated to a TDS greater than the range of the data, TDS will be too low due to the effects of interionic interference on specific conductance.

There are two important fundamental differences between petroleum and ground-water/environmental logging:

1. Surface conductance has a significant effect on resistivity curves in ground-water logging. It was discovered that for ground waters in Texas, surface conductance becomes a factor when Rw is greater than 2 ohm-meters.

2. SP interpretation in petroleum logging is based on sodium chloride formation water. Many of the ground waters in Texas have calcium and magnesium, which complicates SP interpretation.

There are also important practical differences between the two types of logging. In ground-water/environmental logging, it is usually true that:

1. Bit sizes vary more, from a few inches to a few feet.

2. Poor quality drilling mud is common.

3. Little attention is paid to selecting the proper logging suite and to quality control.

4. There is a dearth of knowledge about logging techniques.

5. Slimhole logging tools are often used.

All of these factors complicate ground-water log interpretation.

Borehole geophysical tools have been run in ground-water wells since the early days of the science. However, little attention was ever paid to the subject by petroleum logging companies. Consequently, ground-water logging technology is decades behind petroleum logging. The applicability of many logging tools to ground-water studies was not previously documented, and guidelines for utilizing these tools in ground-water environments were not established.

Existing and new openhole logging tools were run in this study in the main types of aquifers in the state (unconsolidated clastics, consolidated clastics, and carbonates). Each tool was evaluated for its applicability to ground-water/environmental studies. Guidelines were also written for using the tools in ground-water/environmental studies. The most important conclusions of this phase of the study are:

1. The single-point resistance tool, popular in environmental and mineral logging, should never be the primary resistivity tool. The tool has few strengths and several weaknesses.

2. Apart from the problem with bed definition, normal logging tools are ideally suited to openhole ground-water logging. The tools have been abandoned by the petroleum logging industry in favor of induction tools. However, in ground-water environments it is easier to get accurate resistivity values with normal curves than with induction curves.

3. Focused electrode (guard) tools are designed for the exact borehole environment of most water wells. The tools give accurate resistivity values and excellent vertical resolution. They should be utilized much more widely in ground-water/environmental studies.

4. The gamma ray and caliper logs are infrequently run in water wells, but should be a standard part of every logging suite. The gamma ray provides lithology information and the caliper provides a picture

of the hole diameter. Both curves are useful in interpreting other curves.

5. Porosity logs are very seldom run in water wells. They should be run routinely in carbonate aquifers such as the Edwards and in consolidated clastics such as the Trinity.

6. The Litho or Spectral Density tool is the porosity tool of choice. It is an excellent stand-alone porosity tool, with the ability to both identify lithology and calculate porosity.

7. Contrary to popular opinion, the sonic log will give accurate porosity values in shallow, unconsolidated formations if the correct transform is used. The Raymer-Hunt transform gives accurate porosity values in such circumstances.

8. Considerable improvement needs to be made in the quality of some slimhole logging tools. Specifically, gamma ray tools must be calibrated in API units; density and neutron tools must be calibrated in such a manner that porosity can be calculated with the tools.

Seven techniques for calculating Cw and TDS from logs were evaluated, three empirical relationships (TDS-Ro Graphs, Ro_c-TDS Graphs, and Field Formation Factor) and four stand-alone techniques (Formation Factor Equation, Ro-Porosity Graphs, Resistivity Ratio Method, and SP). The Field Formation Factor method produced the least accurate results. Theoretically, Ro_c-TDS Graphs should be more accurate than TDS-Ro Graphs, but in reality they were not. Both types of graphs are site-specific. Ro-TDS graphs were constructed for 48 counties.

The Formation Factor Equation calculates accurate Rw values, as long as surface conductance is negligable (Rw less than 2 ohm-meters). The drawback is that a porosity curve is required and the cementation exponent must be accurately estimated. The Ro-Porosity Graph is simply a graphical solution of the Formation Factor Equation. The advantage is that m can be estimated and trends in water quality and m can sometimes be discerned. The Resistivity Ratio Method has the advantage of canceling the effect of surface conductance. It can, therefore, accurately calculate Rw regardless of the salinity of the water. The drawbacks are that it requires an accurate Rmf measurement and an Rxo tool. Rmf measurements are sometimes not

recorded and sometimes not representative of the zone of interest. Rxo logs are scarce, except in the Permian Basin. Rxo tools were run in a number of wells to demonstrate the viability of the technique. The SP method works only in sodium chloride water, which ground waters in Texas usually are not. In addition, there are a number of other conditions that must be met in order for Rw calculations from an SP to be accurate. The SP method is the least reliable of the four stand-alone methods.

When calculating water quality from geophysical logs, it is best to use all of the techniques for which data is available. It is also essential to make sure that any necessary environmental corrections have been applied to the logging curves and that one is making the correct interpretation as to the relationship of a resistivity curve to the invasion profile.

This study has shown the need for research in several areas:

1. TDS-Cw graphs need to be constructed for all aquifers and counties in Texas.

2. Several areas of slimhole logging need to be researched. Accurate density and neutron tools, along with additional guard and induction tools, need to be developed.

3. Temperature-conductivity relationships for slightly to moderately saline non-NaCl type waters need to be documented.

4. The applicability of logging technology to ground-water and environmental studies needs to be better documented in the literature. Quality control guidelines also need to be better documented.

5. The applicability of cased hole logging technology to ground-water and environmental studies needs to be studied. Subjects of particular importance include:

    a. Techniques to evaluate the integrity of bentonite grout in PVC cased holes.
    b. A cased hole resistivity tool.
    c. Cased hole porosity tools.

BIBLIOGRAPHY

Alger, R.P., 1966, Interpretation of electric logs in fresh water wells in unconsolidated formations, paper CC, *in* 7th annual symposium transactions: Society of Professional Well Log Analysts, 25 p.

Alger, R.P., and Harrison, C.W., 1988, Improved fresh water assessment in sand aquifers utilizing geophysical well logs, paper I, *in* 2nd international symposium on borehole geophysics for minerals, geotechnical, and groundwater applications [Golden, Colorado, Oct. 6-8, 1987], proceedings: Society of Professional Well Log Analysts, Minerals and Geotechnical Logging Society Chapter-at-Large, p. 99-118. Also published in 1988, *in* FOCUS conference on southwestern ground water issues [Albuquerque, New Mexico, March 23-25] proceedings: National Water Well Association, Dublin, Ohio, p. 281-309. Also published in 1988, *in* 2nd national outdoor action conference on aquifer restoration, ground water monitoring, and geophysical methods [Las Vegas, May 23-26] proceedings, volume 2: Association of Ground Water Scientists and Engineers (AAAS), p. 939-968. Later published in 1989, The Log Analyst, v. 30 (1), January-February, p. 31-44.

Allaud, L.A., and Martin, M.H., 1977, Schlumberger, the history of a technique: John Wiley & Sons, New York City, 333 p.

American Public Health Association, American Water Works Association, Water Pollution Control Federation, 1985, Standard methods for the examination of water and wastewater, (16th ed.): American Public Health Association, Washington, D.C., 1268 p.

Archie, G.E., The electrical resistivity log as an aid in determining some reservoir characteristics: Transactions AIME, v. 146, p. 54-62.

Arps, J.J., 1953, The effect of temperature on the density and electrical resistivity of sodium chloride solutions: Transactions AIME, v. 198, p. 327-330.

Baroid, 1991, Drilling fluid products for water well, mineral exploration, and geotechnical drilling: NL Baroid Corp., Houston, variously paginated.

Bateman, R.M., 1985, Openhole log analysis and formation evaluation: IHRDC Press, Boston, 647 p.

Beeson, C.M., and Wright, C.C., 1952, Loss of mud solids to formation pores: Petroleum Engineering, p. 40-52.

Bevington, P.R., 1969, Data reduction and error analysis for the physical sciences: McGraw-Hill Book Company, New York, p. 93-103.

Brown, C.E., 1988, Determination of rock properties by borehole-geophysical and physical-testing techniques and ground-water quality and movement in the Durham Triassic Basin, North Carolina: U.S. Geological Survey Professional Paper 1432, 29 p.

Brown, D.L., 1971, Techniques for quality-of-water interpretations from calibrated geophysical logs, Atlantic Coastal area: Groundwater, v. 9 (4), p. 25-38.

Clenchy, D.R., 1985, Effect of borehole diameter on log quality and interpretation--Grand Banks area, east coast Canada, paper V, *in* 10th formation evaluation symposium transactions: Canadian Well Logging Society, Calgary, 26 p.

Coates, G., Collier, H., Milligan, B., Vasilache, M., and Carter, J., in press, MRIL* an environmentally safe measure of porosity and permeability: *in* 4th international symposium on borehole geophysics for minerals, geotechnical, and groundwater applications [Toronto, Ontario, August 18-22], proceedings: Society of Professional Well Log Analysts, Minerals and Geotechnical Logging Society Chapter-at-Large.

Cohen, S.C., 1981, Relationships among the slopes of lines derived from various data analysis techniques and the associated correlation coefficient: Geophysics, v. 46 (11), p. 1606.

Collier, H.A., 1988, The effect of isolated biomoldic porosity on the log analysis of a Pennsylvanian carbonate reservoir in north Texas, paper X, *in* 29th annual symposium transactions: Society of Professional Well Log Analysts, 16 p.

_____, 1989, Assessment of the dielectric tool as a porosity device, *in* 3rd national outdoor action conference on aquifer restoration, ground

water monitoring and geophysical methods [Orlando, Florida], proceedings: National Well Water Association, Dublin, Ohio, p. 151-165. Also published in 1989 as paper L, *in* 3rd international symposium on borehole geophysics for minerals, geotechnical, and groundwater applicatons, proceedings: Society of Professional Well Log Analysts, Minerals and Geotechnical Logging Society, Chapter-at-Large, p. 183-197.

Davis, J.C., and Doveton, J.H., 1990, Overview of statistical methods in log analysis: Society of Professional Well Log Analysts computer applications workshop [Lafayette, Louisiana, June 28] course notes: Society of Professional Well Log Analysts, Houston, 19 p.

Davis, S.N., 1988, Where are the analyses?: Groundwater, v. 26 (1), p. 2-5.

Desai, K.P., and Moore, E.J., 1969, Equivalent NaCl determination from ionic concentrations: The Log Analyst v. 10 (3), p. 12-21.

Dewan, J.T., 1983, Essentials of modern open-hole log interpretation: PennWell Books, Tulsa, 361 p.

Doll, H.G., 1949, SP log: theoretical analysis and principles of interpretation: Transactions AIME, v. 179, p. 146-185.

Dresser Atlas, 1982, Well logging and interpretation techniques : Dresser Industries, Inc., Houston, variously paginated.

_____, 1985, Log interpretation charts: Dresser Industries, Inc., Houston, 157 p.

Driscoll, F.G., 1986, Groundwater and wells, (2nd ed.): Johnson Division, St. Paul, Minnesota, 1089 p.

Dunlap, H.F., and Hawthorne, R.R., 1951, The calculation of water resistivities from chemical analyses: Transactions AIME, v. 192, p. 373-375.

Dyck, J.H., Keys, W.S., and Meneley, W.A., 1972, Application of geophysical logging to groundwater studies in southeastern Saskatchewan: Canadian Journal of Earth Sciences, v. 9, p. 78-94.

Ellis, A.J., 1976, The I.A.G.C. interlaboratory water analysis comparison programme, Geochimica et Cosmochimica Acta, v. 40: Pergamon Press, Great Britain, p. 1359-1374.

Emerson, D.W., and Haines, B.M., 1974, The interpretation of geophysical well logs in water bores in unconsolidated sediments: Bulletin of Australian Society of Exploration Geophysics, v. 5 (3), p. 89-118.

Etnyre, L.M., 1984a, Practical application of weighted least squares methods to formation evaluation, part I: The logarithmic transformation of non-linear data and selection of dependent variable: The Log Analyst, v. 25 (1), p. 11-21.

_____, 1984b, Practical application of weighted least squares methods to formation evaluation, part II: Evaluating the uncertainty in least squares results: The Log Analyst, v. 25 (3). p. 11-20.

_____, 1989, Finding oil and gas from well logs: Van Nostrand Reinhold, New York, 306 p.

Evers, J.F., and Iyer, B.G., 1975a, A statistical study of the SP log in fresh water formations of northern Wyoming, paper K, *in* 16th annual symposium transactions: Society of Professional Well Log Analysts logging symposium, 8 p.

_____, 1975b, Quantification of surface conductivity in clean sandstones, paper L, *in* 16th annual symposium transactions: Society of Professional Well Log Analysts, Houston, 11 p.

Focke, J.W., and Munn, D., 1987, Cementation exponents in Middle Eastern carbonate reservoirs: SPE Formation Evaluation, v. 2 (2), p. 155-167.

Fogg, G.E., and Blanchard, P.E., 1986, Empirical relations between Wilcox ground-water quality and electric log resistivity, Sabine uplift area, *in* Geology and ground-water hydrology of deep-basin lignite in the Wilcox Group of east Texas, W.R. Kaiser, Principal Investigator, Bureau of Economic Geology, University of Texas at Austin.

Frank, R.W., 1986, Prospecting with old E-logs: Schlumberger Educational Services, Houston, 161 p.

Freeze, R.A., and Cherry, J.A., 1979, Groundwater: Prentice-Hall, Inc., Englewood Cliffs, N.J., 604 p.

Gardner, J.S., and Dumanoir, J.L., 1980, Litho-density log interpretation, paper N, *in* 21st annual symposium transactions: Society of Professional Well Log Analysts, 23 p.

Gearhart, 1981, Basic open hole seminar: Gearhart Industries, Inc., Fort Worth, variously paginated.

Glenn, E.E., and Slusser, M.L., 1957, Factors affecting well productivity - II. Drilling fluid particle invasion into porous media: Transactions AIME, v. 210, also published *in* Journal of Petroleum Technology (May), p. 132-139.

Glenn, E.E., Slusser, M.L., and Huitt, J.L., 1957, Factors affecting well productivity- I. Drilling fluid filtration: Transactions AIME, v. 210, also published *in* Journal of Petroleum Technology (May), p. 126-131.

Goetz, J.F., Dupal, L., and Bowler, J., 1979, An investigation into discrepancies between sonic log and seismic check shot velocities: unpublished.

Gondouin, M., Tixier, M.P., and Simard, G.L., 1957, An experimental study on the influence of the chemical composition of electrolytes on the S.P. curve: Transactions AIME, v. 210, also published *in* Journal of Petroleum Technology (February 1958), p. 58-70.

Guo, Y.A., 1986, Estimation of TDS in sand aquifer water through resistivity log: Ground Water, v. 24 (5), p. 598-600.

Guyod, H., 1944, Electric well logging, part 3; The single-point resistance method: The Oil Weekly, August 21, p. 44-52.

_____, 1957, Resistivity determination from electric logs: privately published, variously paginated.

_____, 1966, Interpretation of electric and gamma ray logs in water wells: The Log Analyst, v. 6, (5), p. 29-44.

Guyod, H., and Pranglin, J.A., 1959, Analysis charts for the determination of true resistivity from electric logs: Houston, 202 p.

Hallenburg, J.K., 1980, A comparison of nonpetroleum and petroleum logging, chapter E, *in* 21st annual symposium transactions: Society of Professional Well Log Analysts, 7 p.

_____, 1984, Geophysical logging for mineral and engineering applications: PennWell Books, Tulsa, 254 p.

Hansen, H.J., and Wilson, J.M., 1984, Summary of hydrogeologic data from a deep (2,678 ft.) well at Lexington Park, St. Mary's County, Maryland: Maryland Department of Natural Resources, Maryland Geological Survey, open-file report 84-02-01, 61 p.

Hartline, no date, Logging course notes: privately published, variously paginated.

Hartmann, D.J., 1975, Effect of bed thickness and pore geometry on log response, paper Y, *in* 16th annual symposium transactions: Society of Professional Well Log Analysts, 14 p.

Hassan, M., Hossin, A. and Combaz, A., 1976, Fundamentals of the differential gamma ray log interpretation technique, paper H, *in* 17th annual symposium transactions: Society of Professional Well Log Analysts, 18 p.

Helander, D.P., 1983, Fundamentals of formation evaluation: Oil and Gas Consultants International, Tulsa, 332 p.

Hem, J.D., 1982, Conductance; a collective measure of dissolved ions, *in* R.A. Minear and L.H. Keith, editors, Water analysis, v.1, Inorganic species, pt. 1: Academic Press, New York, p. 137-161.

_____, 1985, Study and interpretation of the chemical characteristics of natural water: U.S. Geological Survey Water-Supply Paper 2254, p. 1-249.

Hertzog, R., Colsen, L., Seeman, B., O'Brien, M., Scott, H., McKeon, D., Grau, J., Ellis, D., Schweitzer, J., and Herron, M., 1987, Geochemical logging with spectrometry tools, SPE-16792, in SPE annual technical

conference and exhibition, proceedings, volume omega, Formation evaluation and reservoir geology: Society of Petroleum Engineers, p. 447-460. Later published in 1989, SPE Formation Evaluation, v. 4(2), p. 153-162.

Hilchie, D.W., 1968, Caliper logging--Theory and practice: The Log Analyst, v. 9, (1), p. 3-12.

_____, 1979, Old (pre-1958) electrical log interpretation: D.W. Hilchie, Inc., Golden, Co., 161 p.

_____, 1982, revised, Applied openhole log interpretation: D.W. Hilchie, Inc., Golden, Co., variously paginated.

_____, 1987, The geologic well log interpreter notes: D.W. Hilchie, Inc., Boulder, Co., variously paginated.

_____, 1990, Wireline: a history of the well logging and perforating business in the oil fields: D.W. Hilchie, Inc., Boulder, Co., 200 p.

Hill, D.G., 1986, Geophysical well log calibration and quality control, *in* P.G. Killeen, editor, Borehole geophysics for mining and geotechnical applications [international symposium and workshop, (Toronto, Ontario, August 29-31, 1983), proceedings]: Geological Survey of Canada Paper 85-27, p. 379-392.

Hodges, R.E., 1988, Calibration and standardization of geophysical well-logging equipment for hydrologic applications: U.S. Geological Survey Water Resource Investigations Report 88-4058, 25 p.

Hounslow, A.W., 1987, Practical interpretation of water quality data, course notes: Oklahoma State University, Stillwater, Oklahoma, variously paginated.

Hurst, A., Lovell, M.A., and Morton, A.C., editors, 1990, Geological applications of wireline logs: Geological Society of London Special Publication, No. 48, 357 p.

International Critical Tables, 1928, International critical tables of numerical data, physics, chemistry and technology, v. III, prepared under the auspices of the International Research Council and the National

Acadamy of Sciences by the National Research Council of the United States of America: E.W. Washburn, editor-in-chief, New York Publishers, McGraw-Hill Book Company, Inc., p. 444.

_____, 1929, International critical tables of numerical data, physics, chemistry and technology, v. III, prepared under the auspices of the International Research Council and the National Acadamy of Sciences by the National Research Council of the United States of America: E.W. Washburn, editor-in-chief, New York Publishers, McGraw-Hill Book Company, Inc., p. 481.

Itoh, T., Miyairi, M., and Kimura, K., 1980, The high temperature well logging system for geothermal well, paper G, *in* 21st annual logging symposium: Society of Professional Well Log Analysts, 21p.

Jacobson, L.A., and Fu, C.C., 1990, Computer simulation of cased-hole density logging: SPE Formation Evaluation, v. 5 (4), p. 465-468.

Jansson, M., 1985, A comparison of detransformed logarithmic regressions and power function regressions: Geografiska Annaler, v. 67 A(1-2), p. 61-70.

Johnson, H.M., 1962, A history of well logging: Geophysics, v. 27 (4), p. 507-527.

Jones, P.H., and Buford, T.B., 1951, Electric logging applied to ground water exploration: Geophysics, v. 16, (1), p. 115-139.

Jones, T.A., 1979, Fitting straight lines when both variables are subject to error, part I; Maximum likelihood and least-squares estimation: Mathematical Geology, v. 2 (1), 25 p.

Jorden, J.R., and Campbell, F.L., 1984, Well logging I--Rock properties, borehole environment, mud and temperature logging: Society of Petroleum Engineers, Dallas, Monograph series No. 9, 167 p.

_____, 1986, Well logging II--Electric and acoustic logging: Society of Petroleum Engineers, Dallas, Monograph series No. 10, 192 p.

Jorgensen, D.G., 1988, Using geophysical logs to estimate porosity, water resistivity, and intrinsic permeability: U.S. Geological Survey, Denver, Water Supply Paper 2321, 24 p.

Keys, W.S., 1988, Borehole geophysics applied to ground-water investigations: U.S. Geological Survey open-file report 87-539, 305 p. Also published in Techniques of Water-Resources Investigations, 1990, O2-E2, 150 p.

Keys, W.S., and MacCary, L.M., 1971, Application of borehole geophysics to water-resources investigations: U.S. Geological Survey, Techniques of Water-Resources Investigations, book 2, chapter E1, 126 p.

Kienitz, C., Flaum, C., Olesen, J-R., and Barber, T., 1986, Accurate logging in large boreholes, *in* 27th annual logging symposium: Society of Professional Well Log Analysts, 21p.

Kwader, T., 1982, Interpretation of borehole geophysical logs in shallow carbonate environments and their application to ground-water resources investigations: Florida State University, unpublished dissertation, 335 p.

_____, 1984, The use of geophysical logs for determining formation water quality, *in* D.M. Neilsen and M. Curl, editors, 1984 NWWA/EPA conference on surface and borehole geophysical methods in ground water investigations, proceedings: National Water Well Association, Worthington, Ohio, p. 833-841. Later published in 1986, Ground Water, v. 24 (1), p. 11-15.

_____, 1985, Resistivity-porosity cross plots for determining in situ formation water quality--Case examples, *in* 1985 NWWA conference on surface and borehole geophysical methods in ground water investigations [Fort Worth, Texas, February 12-14], proceedings: National Water Well Association, Worthington, Ohio, p. 415-424.

_____, 1986, The use of geophysical logs for determining formation water quality: Ground Water, v. 24, (1), p. 11-15.

Labo, J., 1987, A practical introduction to borehole geophysics--An overview of wireline well logging principles for geophysicists: Society

of Exploration Geophysicists, Tulsa, Geophysical References Series, v. 2, 330 p.

Lancaster, J.R., and Atkinson, A., 1987, Computer processing of selected drilling, lithologic, and geophysical log data produces accurate permeability values and comprehensive aquifer analysis, including specific yield: COGS [Computer Oriented Geological Society] Computer Contributions, v. 3, (1), February, p. 13-36.

Logan, J., 1961, Estimation of electrical conductivity from chemical analyses of natural waters: Journal of Geophysical Research, v. 66 (8), p. 2479-2483.

Lowe, T.A., and Dunlap, H.F., 1986, Estimation of mud filtrate resistivity in fresh water drilling muds: The Log Analyst, v. 27 (2), p. 77-84.

MacCary, L.M., 1978, Interpretation of well logs in a carbonate aquifer: U.S. Geological Survey Water-Resources Investigations No. 78-88, 30 p. Later published in 1983 as, Geophysical logging in carbonate aquifers: Ground Water, v. 21 (3), p. 324-342.

_____, 1980, Use of geophysical logs to estimate water-quality trends in carbonate aquifers: U.S. Geological Survey Water-Resources Investigations, No. 80-57, 23 p.

_____, 1984, Relation of formation factor to depth of burial in aquifers along the Texas Gulf coast, *in* D.M. Nielsen and M. Curl, editors, 1984 NWWA/EPA conference on surface and borehole geophysics methods in ground water investigations, proceedings: National Water Well Association, Worthington, Ohio, p. 722-742.

Mann, C.J., 1987, Misuses of linear regression in earth sciences, *in* W.B. Size, editor, Use and abuse of statistical methods in the earth sciences: Oxford University Press, New York, p. 74-106.

Mark, D.M., and Church, M., 1977, On the misuse of regression in earth science: Mathematical Geology, v. 9 (1), p. 63-75.

McBain, J.W., Peaker, C.R., and King, A.M., 1929, Absolute measurements of the surface conductivity near the boundary of optically polished

glass and solutions of potassium chloride: Journal of American Chemical Society, v. 51, p. 3294-3312.

McConnell, C.L., 1983, Spontaneous potential corrections for ground-water salinity calculations; Carter County, Oklahoma, U.S.A.: Journal of Hydrology, v. 65, p. 363-372.

_____, 1985, Time dependence of the equivalent water resistivity in fresh water wells: The Log Analyst, v. 26 (3), p. 12-17.

_____, 1988, A general correction for spontaneous potential well logs in fresh water: Journal of Hydrology, v. 101 (1-4), p. 1-13.

_____, 1989, Characterization of wellhead protection areas using spontaneous potential well log analysis, paper II, *in* 3rd international symposium on borehole geophysics for minerals, geotechnical, and groundwater applications, proceedings: Society of Professional Well Log Analysts, Minerals and Geotechnical Logging Society, Chapter-at-Large, p. 671-697.

McCoy, R.L., Kumar, R.M., and Pease, R.W., 1980, Identifying fractures with conventional well logs: World Oil, v. 191 (7), Dec., p. 91-98.

Merkel, R.H., and Snyder, D.D., 1977 Application of calibrated slim hole logging tools to quantitative formation evaluation, chapter X, *in* 18th annual symposium transactions: Society of Professional Well Log Analysts, 21 p.

Miller, R.L., Bradford, W.L., and Peters, N.E., 1988, Specific conductance: theoretical considerations and application to analytical quality control: U.S. Geological Survey Water-Supply Paper 2311, p. 1-16.

Moelwyn-Hughes, E.A., 1961, Physical chemistry, (2nd ed.): Pergamon Press, New York, 1333 p.

Moore, C.V., and Kaufman, R.L, 1981, Your unsuspected problems--Fluid resistivity and water analysis, paper C, *in* 22nd annual symposium transactions: Society of Professional Well Log Analysts, Houston, 15 p.

_____, 1983, Resistivity techniques can cause unsuspected problems: World Oil, p. 49-53, 62.

Moore, E.J., 1966, A graphical description of new methods for determining equivalent NaCl concentration of chemical analysis, paper M, *in* 7th annual symposium transactions: Society of Professional Well Log Analysts, Houston, 34 p.

Moses, P.L., 1961, Geothermal gradients, drilling, and production practice: American Petroleum Institute.

National Research Council, 1928, International critical tables of numerical data, physics, chemistry and technology: McGraw-Hill Book Company, Inc., New York, v. 3, 444 p.

National Research Council, 1928, International critical tables of numerical data, physics, chemistry and technology: McGraw-Hill Book Company, Inc., New York, v. 4, 480 p.

Overton, H.L., and Lipson, L.B., 1958, Correlation of electrical properties of drilling fluids with solids content: Transactions AIME, v. 213, p. 333-336.

Peterson, B.R., 1991, Borehole geophysical logging methods for dissolved solids; a case study, *in* Ground water management: no. 5, [Las Vegas, Nevada, May 13-16], proceedings of the 5th national outdoor action conference on aquifer restoration, ground water monitoring, and geophysical methods, p. 1047-1072.

Pirson, S.J., 1963, Handbook of well log analysis for oil and gas formation evaluation: Prentice-Hall, Enlglewood Cliffs, N.J., 325 p.

Poteet, D., Collier, H., and Maclay, R., 1992, Investigation of the fresh/saline water interface in the Edwards Aquifer in New Braunfels and San Marcos, Texas: Edwards Underground Water District Report 92-02, San Antonio, Texas, 171 p.

Prensky, S.E., 1987, Geological applications of well logs--An introductory bibliography and survey of the well logging literature through September, 1986, arranged by subject and first author: The Log Analyst, parts A and B, v. 28, (1), January-February, p. 71-107, part

C, v. 28, (2), March-April, p. 219-248, (previous editions published as U.S. Geological Survey Open-File Reports 85-441, 86-170, 87-16).

Raymer, L.L., Hunt E.R., and Gardner J.S., 1980, An improved sonic transit time-to-porosity transform, paper P, *in* 21st annual symposium transactions: Society of Professional Well Log Analysts, Houston, 13 p.

Repsold, H., 1989, Well logging in groundwater development: International Association of Hydrogeologists, International Contributions to Hydrogeology, v. 9, 136 p.

Rider, M.H., 1986, The geological interpretation of well logs: John Wiley & Sons, Inc., New York, 175 p.

Rink, M., and Schopper, J.R., 1974, Interface conductivity and its implications to electric logging, paper J, *in* 15th annual symposium transactions: Society of Professional Well Log Analysts, Houston, 15 p.

Sanyal, S.K., and Jusbasche, J.M., 1979, Calculation of geothermal water salinity from well logs--A statistical approach: Geothermal Resources Council Transactions, v. 3, September, p. 613-616.

Sarma, V.V.J., and Rao, V.B., 1962, Variation of electrical resistivity of river sands, calcite, and quartz powders with water content: Geophysics, v. 27 (4), p. 470-479.

Schlumberger, 1958, Introduction to Schlumberger well logging: Schlumberger Well Surveying Corp., Houston, 176 p.

_____, 1972, Log interpretation: Volume I - principles: Schlumberger Limited, New York, New York, 112 p.

_____, 1979, Log interpretation charts: Schlumberger Well Surveying Corp., Ridgefield, Conn., 97 p.

_____, 1987, Log interpretation principles/applications: Schlumberger Educational Services, Houston, 198 p.

_____, 1988, Log interpretation charts: Schlumberger Educational Services, Houston, Document No. SMP-7006, 150p.

_____, 1989, Log interpretation principles/applications: Schlumberger Educational Services, Houston, Document No. SMP-7017, 223 p.

Sciacca, J., 1989, Operational and quality assurance considerations for borehole geophysical logging in hydrogeologic investigations, *in* 3rd national outdoor action conference on aquifer restoration, ground water monitoring and geophysical methods [Orlando, Florida], proceedings: National Water Well Association, Dublin, Ohio, p. 891-907.

Scott, J.H., 1978, A FORTRAN algorithm for correcting normal resistivity logs for borehole diameter and mud resistivity: U.S. Geological Survey, Open-File Report 78-779, 12 p.

Segesman, F., and Tixier, M.P., 1959, Some effects of invasion on the SP curve: Transactions AIME 216. Also published in 1959 *in* Journal of Petroleum Technology, p. 138-146.

Serra, O., 1984, Fundamentals of well-log interpretation, volume 1--The acquisition of logging data: Elsevier, New York, Developments in Petroleum Science, No. 15A, 423 p.

_____, 1985, Sedimentary environments from wireline logs: Schlumberger Technical Services, Paris, Document No. M-081030/SMP-7008, 211 p.

Sherman, H., and Locke, S., 1975, Depth of investigation of neutron and density sondes for 35 percent-porosity sand, paper Q, *in* 16th annual symposium transactions: Society of Professional Well Log Analysts, 14 p.

Shuter, E., and Teasdale, W.E., 1989, Application of drilling, coring, and sampling techniques to test holes and wells, chapter F1 in Collection of environmental data: U.S. Geological Survey Techniques of Water-Resources Investigations, Book 2, 97 p.

Silva, P., and Bassiouni, Z., 1981, A new approach to the determination of formation water resistivity from the SP log, paper G, *in* 22nd annual symposium transactions: Society of Professional Well Log Analysts, 14 p.

Snyder, D.D., and Fleming D.B., 1985, Well logging -- a 25-year perspective: Geophysics, v. 50 (12), p. 2504-2529.

Society of Professional Well Log Analysts, Houston Chapter, 1979, The art of ancient log analysis: Society of Professional Well Log Analysts, Houston, 131 p. plus reprints of 22 classic papers.

Society of Professional Well Log Analysts, 1982, Geothermal log interpretation handbook: Society of Professional Well Log Analysts, Houston, Reprint Volume, variously paginated.

Summers, W.K., 1972, Factors affecting the validity of chemical analyses of natural water: Groundwater, v. 10 (2), p. 12-17.

Taylor, K.C., Hess, J.W., and Mazzela, A., 1989, Field evaluation of a slim-hole borehole induction tool: Ground Water Monitoring Review, v. 9 (1) p. 100-104.

Taylor, K., Molz, F., and Hayworth, J., 1988, A single well electrical tracer test for the determination of hydraulic conductivity and porosity as a function of depth, *in* 2nd national outdoor action conference on aquifer restoration, ground water monitoring and geophysical methods [Las Vegas, May 23-26], proceedings, volume 2: Association of Ground Water Scientists and Engineers (AAAS), p. 925-938.

Taylor, T.A., and Dey, J.A., 1985, Bibliography of borehole geophysics as applied to ground-water hydrology: U.S. Geological Survey Circular No. 926, 62 p.

Tittman, J., and Wahl, J.S., 1965, The physical foundations of formation density logging (gamma-gamma): Geophysics, vol. 30 (2) p. 284-294.

Towle, G., 1962, An analysis of the formation resistivity factor-porosity relationship of some assumed pore geometries, paper 3, *in* 3rd annual symposium transactions: Society of Professional Well Log Analysts.

Troutman, B.M., and Williams, G.P., 1987, Fitting straight lines in the earth sciences, *in* W.B. Size, editor, Use and abuse of statistical methods in the earth sciences: Oxford University Press, New York, p. 107-128.

Truman, R.B., Alger, R.P., Connell, J.G. and Smith, R.L., 1972, Progress report on interpretation of the dual-spacing neutron log (CNL) in the United States, paper U, *in* 13th annual symposium transactions: Society of Professional Well Log Analysts, 34 p.

Turcan, A.N. Jr., 1962, Estimating water quality from electrical logs, *in* Geological Survey Research 1962: U.S. Geological Survey Professional Paper 450-C, p. C135-C136.

_____, 1966, Calculation of water quality from electrical logs--Theory and practice: Louisiana Geological Survey, and Louisiana Department of Public Works Resources Pamphlet 19, 23 p.

Urban, F., White, H.L., and Strassner, E.A., 1935, Contribution to the theory of surface conductivity at solid-liquid interfaces: The Journal of Physical Chemistry, v. 39 (3), p. 311-330.

Veneruso, A.F., and Coquat, J.A., 1979, Technology development for high temperature logging tools, paper KK, *in* 20th annual symposium transactions: Society of Professional Well Log Analysts, 13 p.

Vonhof, J.A., 1966, Water quality determination from spontaneous-potential electric log curves: Journal of Hydrology, v. 4, p. 341-347.

Wahl, J.S., Tittman, J., Johnstone, C.W. and Alger, R.P., 1964, The dual spacing formation density log: Journal of Petroleum Technology, p. 1411-1416.

Weiss, J.S., 1987, Determining dissolved solids concentrations in mineralized ground water of the gulf coast aquifer systems using electric logs, *in* Aquifers of the Atlantic and Gulf Coastal Plain, American Water Resources Association, Monograph No. 9, J. Vecchioli and A.I. Johnson, editors, p. 139-150.

Welex, 1985, Log interpretation charts: Welex, Houston, variously paginated.

Williams, G.P., and Troutman, B.M., 1987, Algebraic manipulation of equations of best-fit straight lines, *in* W.B. Size, editor, Use and abuse of statistical methods in the earth sciences: Oxford University Press, New York, p. 129-141.

Winsauer, W.O., Shearin, H.M. Jr., Masson, P.H., and Williams, M, 1952, Resistivity of brine-saturated sands in relation to pore geometry: Bulletin of the American Association of Petroleum Geologists, v. 36 (2), p. 253-277.

Winsauer, W.O., and McCardell, W.M., 1953, Ionic double-layer conductivity in reservoir rock: Transactions AIME, v. 198, p. 129-134.

Worthington, A.E., Hedges, J.H., and Pallatt, N., 1990, SCA guidelines for sample preparation and porosity measurement of electrical resistivity samples, part I, Guidelines for preparation of brine and determination of brine resistivity for use in electrical resistivity measurements: The Log Analyst, v. 31, (1) p. 20-28.

Wyllie, M.R.J., 1949, A quantitative analysis of the electrochemical component of the SP curve: Transactions AIME, v. 186, p. 17-26.

Wyllie, M.R.J., Gregory A.R. and Gardener, L.W., 1956, Elastic wave velocities in heterogeneous and porous media: Geophysics, v. 21, (1) p. 41-70.

Yearsley, E.N., Crowder, R.E., and Irons, L.A., 1991, Monitoring well completion evaluation with borehole geophysical density logging: Ground Water Monitoring Review, v. 11 (1), p. 103-111.

GUIDELINES FOR VERIFYING THE ACCURACY OF WATER ANALYSES

Appendix I

Examination of hundreds of water analyses from several laboratories in Texas revealed significant differences in analytical techniques and in the accuracy of TDS and specific conductance measurements (Chapters 2 and 3). Therefore, it was deemed necessary to include a section on guidelines for determining the accuracy of water analyses. Hem (1985) is the source of most of the guidelines. Hounslow (1987) is also a useful reference.

Virtually all of the analyses examined during this study were from six laboratories: the Texas Department of Health (TDH), Pope Testing, Edna Wood (formerly Microbiology Service Laboratories), Curtis (out of business), Texas Testing (out of business), and United States Geological Survey (USGS). Other laboratories exist in Texas, but these six laboratories have analyzed the vast majority of ground-water samples taken in the state. The petroleum industry has an entirely different group of laboratories.

The procedures listed below apply to water analyses from all of the laboratories named above and are for establishing the accuracy of TDS and specific conductance values. If a water analysis is run for another purpose (e.g. to measure the concentrations of minor ions), these guidelines, while of some help, will not be sufficient to verify the accuracy of the analysis.

The following guidelines apply to complete, routine analyses of normal waters. A complete, routine water analysis measures the following normal major constituents: silica (SiO_2), calcium (Ca), magnesium (Mg), sodium (Na), chloride (Cl), bicarbonate (HCO_3), sulfate (SO_4), and carbonate (CO_3). Normal waters are those which do not have excessive concentrations of organics, nitrate, sulfate, or suspended matter. TDS for such water analyses should be within $\pm$5 percent of the actual TDS and conductivity within $\pm$2 to $\pm$5 percent of the actual value (Hem, 1985, pp. 163 and 69).

METHODS FOR ASSESSING THE ACCURACY OF TOTAL DISSOLVED SOLIDS MEASUREMENTS

Three methods exist for determining the accuracy of TDS measurements: anion-cation balance, comparison of $TDS_{calculated}$ versus residue on evaporation, and the TDS-Cw relationship. Either of the first two methods is an excellent check of TDS. All water analyses should consist of the constituents mentioned above to allow one of the two checks to be done. The TDS-Cw relationship should be used only as a last resort, unless the relationship has been firmly established from other water analyses in the vicinity of the sample in question.

Anion-Cation Balance

An anion-cation balance is an efficient method of checking TDS measurements. The Texas Department of Health, the United States Geological Survey, and some petroleum laboratories routinely run this calculation. A laboratory may run the calculation, but not display it on its water analysis report (e.g. United States Geological Survey). PC programs are available to perform the calculation (contact Arthur Hounslow at Oklahoma State University). The procedure is as follows:

1. The concentration of each ion in the analysis is converted from mg/l, ppm or kg/m^3 to meq/l.

$$meq/l = mg/l \times \frac{valence\ number}{formula\ weight} \qquad \text{(I-1)}$$

This equation can be simplified to a series of conversion factors (see Table I-1):

$$meq/l = mg/l \times F \qquad \text{(I-2)}$$

Where:

F is a conversion factor.

For a particular ion F is $\frac{valence\ number}{formula\ weight}$.

2. The anions are summed and the cations are summed. Silica, which is electrically neutral, is excluded.

3. The two sums are compared. The closer the two values are, the more accurate the TDS calculation is. In theory, since all waters

TABLE I-1. MULTIPLIERS FOR CONVERTING MG/L TO MEQ/L FOR THE MOST COMMON IONS

Ion	Symbol	Valence Number	F
Bicarbonate	HCO_3	-1	0.01639
Calcium	Ca	+2	0.04990
Carbonate	CO_3	-2	0.03333
Chloride	Cl	-1	0.02821
Fluoride	F	-1	0.05264
Iron	Fe	+2	0.03581
Iron	Fe	+3	0.05372
Magnesium	Mg	+2	0.08229
Manganese	Mn	+2	0.03640
Nitrate	NO_3	-1	0.01613
Potassium	K	+1	0.02558
Sodium	Na	+1	0.04350
Sulfate	SO_4	-2	0.02082

Modified from Hem (1985).

are electrochemically neutral, the sums should be equal. In practice, however, the sums will not be exactly equal. Usually the cation sum is less than the anion sum. This is because most waters have far more cation than anion species and a number of the minor cation species are not analyzed in a routine water analysis. The difference is usually expressed as a percentage:

$$Anion\text{-}Cation\ balance = \frac{|\ sum\ of\ cations - sum\ of\ anions\ |}{sum\ of\ cations + sum\ of\ anions} \times 100 \qquad \text{(I-3)}$$

Having expressed the anion-cation balance as a percentage, the value should be interpreted according to the following guidelines:

1. If the sodium concentration is reported as either "Na by difference", "Na (diff.)", or "Na and K (diff.)", an anion-cation balance should not be performed. It is worthless as a quality control check. The ions will balance perfectly because of the procedure used to determine sodium.

Prior to about 1960 sodium and potassium were difficult to analyze accurately (Hem, 1985, p. 164). Consequently, all the common ions except sodium and potassium were measured, converted to meq/l, and then the difference between the anions and cations (calcium and magnesium) was attributed to the presence of sodium and potassium. This value was converted to mg/l and placed on water analyses as Na (diff.). Potassium concentrations are normally so small in relation to sodium that potassium was lumped under sodium. This means that analytical errors and/or undetermined ions are automatically included in the sodium value. The anion-cation balance is always perfect, yet worthless as a quality control check.

Two laboratories in Texas, Edna Wood and Pope Testing, still determine sodium by difference. If requested, they will measure sodium and potassium for a fee of $12 to $15 per ionic species. For internal quality control they measure the two ions when the results of a water analysis do not look right (Edna Wood Laboratories and Pope Testing Laboratories, personal communication, 1990). Measured sodium and potassium values are more accurate than calculated values but, for the purpose of this study, calculated values are fine as long as another quality control check of TDS is available.

2. If sodium is not listed as Na (diff.) and the ionic concentrations are in perfect agreement, the anion-cation balance still should not be used to judge the validity of the TDS value. A perfect balance more than likely indicates that sodium was determined by difference, whether or not it is identified as such on the water analysis. (Pope Testing is an example of this practice.) As discussed in previous paragraphs, determining sodium by difference invalidates an anion-cation balance.

3. If sodium was measured rather than calculated and the anion-cation balance is less than 5 percent, the analysis is probably accurate and the TDS value is reasonably correct (Hounslow, 1987).

4. If the balance is much greater than 5 percent to 10 percent, the TDS value is incorrect. The analysis may have one of several problems:

a. The analysis is complete but inaccurate due to analytical errors.
b. The analysis is incomplete.

   i. Other ions (such as heavy metals) are present but were not analyzed.
   ii. The water is very acidic (pH is less than 4) and the hydrogen (H^+) ions were not analyzed.
   iii. Organic ions are present in significant quantities (often indicated by colored water), but were not analyzed (Hounslow, 1987).

$TDS_{Calculated}$ vs. Residue on Evaporation

Two methods are used to determine TDS: $TDS_{calculated}$, also known as $TDS_{computed}$, and residue on evaporation, commonly labeled dissolved residue at a specified temperature. Comparing the two answers provides a good check of TDS.

For many years TDS was determined by evaporating a known amount of water and then weighing the residue. Normally this gives an accurate TDS. Errors can be introduced if the drying time or temperature is incorrect. Water will be retained by the residue or solutes other than bicarbonate (HCO_3^-) will be volatized. One unavoidable result of the procedure is that during evaporation HCO_3^- is converted to $CO_3^=$, CO_2, and H_2O with 50.8 percent of the HCO_3^- driven off as CO_2 and H_2O vapor while 49.2 percent remains as $CO_3^=$.

Laboratories today report $TDS_{calculated}$. The value is obtained by summing the measured dissolved constituents. The sodium value may be measured or calculated, depending on the laboratory (see the previous section). The bicarbonate value is either 100 percent (Edna Wood, Pope Testing, and Curtis) or 49.2 percent (Texas Department of Health, United States Geological Survey, and Texas Testing) of the measured value (see the **Measurement Techniques** section in Chapter 3).

Edna Wood is the only currently operating laboratory to still report dissolved residue. (Many Curtis water analyses reported it.) This is done as a quality control check on $TDS_{calculated}$. $TDS_{calculated}$ is considered accurate if it is within ± 3 percent of TDS_{actual} (Alice Perry, personal communication,

1990). TDS_{actual} is determined by summing the dissolved residue and the amount of bicarbonate ions volatized during the drying process:

$$TDS_{actual} = Dissolved\ Residue + (0.508 \times bicarbonate) \quad \text{(I-4)}$$

Either an anion-cation balance or a $TDS_{calculated}$-residue on evaporation check should be performed on every water sample. Both methods provide stand-alone verification of the accuracy of a water analysis. Of the existing laboratories surveyed in this study, Pope Testing is the only one that did not use one of these two methods. Therefore, they cannot use anion-cation balance, because sodium is determined by difference. They can measure residue by evaporation, but it must be requested by the customer and an additional fee of about $5 is charged.

TDS-Specific Conductance Relationship

The third method for checking a water analysis is to examine the relationship between specific conductance and TDS in mg/l. This is the least reliable of the three methods. The relationship is too variable and conductivity values are sometimes not measured accurately. Hem (1985, p. 168) provides several guidelines for using this relationship as an approximate accuracy check:

1. For normal waters up to a few thousand mg/l TDS:

$$\frac{TDS}{Specific\ Conductance} = 0.55\ to\ 0.75 \quad \text{(I-5)}$$

   a. These values are for TDS's calculated by using 49.2 percent of the bicarbonate ions.
   b. Silica has been excluded from the TDS value.
   c. Bicarbonate and chloride waters will be at the low end of the value.
   d. Waters high in both divalent cations (Ca^{++} and Mg^{++}) and divalent anions (SO_4^{-}) may reach a value as high as 1.0. The ions form uncharged pairs and thus do not contribute to conductivity. This allows TDS to increase at a faster rate than specific conductance (Hem, personal communication, 1990). These waters are often saturated with gypsum (Ca_2SO_4).

e. Waters containing large concentrations of silica may reach a value as high as 1.0.
f. Saline waters with more than 100,000 ppm TDS will have much higher values than nonsaline waters.
g. Acidic (low pH) waters may have much lower values than neutral waters.
h. This ratio is so variable that it is only good for determining gross errors in TDS. Confidence can be placed in the value only when it has been firmly established by utilizing water analyses in the vicinity of the sample in question.

2. The TDS values used in equation I-5 must be consistent in the treatment of the HCO_3^- value, either 100 percent or 49.2 percent of the measured bicarbonate value (see Chapter 3).

3. The relationship becomes more poorly defined for waters exceeding 50,000 mg/l TDS and for very fresh waters (such as rainwater), if the nature of the principal solutes is unknown.

Assorted Other Checks

If concentrations are converted to meq/l, a number of other checks can be used to determine whether the reported values of certain ions are reasonable (Hounslow, 1987). As long as one remembers that many accurate analyses have exceptions, the following general checks can be used:

1. Sodium in meq/l will be much greater than potassium in meq/l, unless both are less than about 5 mg/l.

2. Calcium in meq/l will be greater or equal to magnesium in meq/l unless the calcium has been removed by precipitation.

3. Calcium in meq/l will equal sulfate in meq/l unless calcium has been removed by precipitation. Note: in some oilfield waters the sulfate concentration may be decreased by sulfate reduction and can be unrelated to calcium concentration (Hem, personal communication, 1990).

4. Sodium in meq/l will equal chloride in meq/l unless sodium has been added by ion exchange.

5. If carbonate is absent, pH should be less than 8.

METHODS FOR ASSESSING SPECIFIC CONDUCTANCE ACCURACY

Specific conductance measurements should always be scrutinized closely. Some laboratories do not measure conductivity accurately. Unfortunately, verifying the accuracy of specific conductance measurements is not as straightforward as it is for TDS.

Three methods are available to determine the accuracy of specific conductance measurements: TDS-Cw relationship, ionic concentrations, and anion concentration in meq/l. All the available methods utilize TDS. Because TDS values are usually more accurate than specific conductance measurements, it is best to use the relationships to calculate specific conductance from TDS and not vice versa.

General Guidelines

1. The measurement must be recorded in μmhos/cm at 25° C (77° F). Field conductivity measurements and oilfield water resistivities (R_w) may require conversion to this temperature and/or this unit of measurement. Note: many conductivity meters have a built-in conversion factor to convert the conductivity value from the measured temperature to 25° C. Temperature-conductivity conversion factors vary according to the chemical composition (Hem, 1982). Little research has been done on how much this relationship varies, so this is a possible source of error. (Refer to the discussion of temperature under **Factors Controlling Water Conductivity** in Chapter 2.)

2. In order to assess the accuracy of a specific conductance measurement, determine whether a laboratory uses standard methods to routinely calibrate its conductivity meter and if the meter is calibrated for the conductivity range of a particular water sample. Such is not the case with Pope Testing and Texas Department of Health (Pope Testing Laboratories and Texas Department of Health, personal communication, 1990).

3. Diluted conductance is not valid as a substitute for specific conductance. The Texas Department of Health uses dilluted conductance, and most of the conductivities in the Texas Water

Development Board Ground-Water Data Base are diluted conductances. See item 4. in the section **Preparing the Data** in Chapter 4 for further details on the types of conductivities in the Ground-Water Data Base.

TDS-Specific Conductance Relationship

Normally only gross errors in specific conductance can be detected with the TDS-specific conductance relationship (see the previous **TDS-Specific Conductance Relationship** section). For a particular geographic area or water bearing unit where a number of water analyses exist, a precise relationship can be established between TDS and specific conductance. In such cases the relationship is a valid check of the accuracy of a specific conductance value. All the TDS values must be calculated the same way, using either 100 percent or 49.2 percent of the measured bicarbonate value.

Specific Conductance from Ionic Concentrations

It is possible to calculate water conductivity (C_w) from a chemical analysis. The ionic concentration of a water is converted to the equivalent NaCl concentration (Figure AI-1), which is then converted to C_w (Figure AI-2). Calculated C_w is accurate to within ± 5 percent of measured C_w (Desai and Moore, 1969).

Figure AI-1 lists the ionic charge of common ionic species relative to Na and Cl. The chart shows the relative contribution of each ion to water conductivity and how the contribution varies with TDS. A NaCl type water was chosen as the standard because most oilfield waters are NaCl type waters. The chart, compiled by Schlumberger, is constructed from data in Desai and Moore (1969) for TDS greater than 1000 ppm and from the Variable Dunlap Method for TDS less than 1000 ppm. Some curve smoothing was done (Schlumberger, 1972).

Figure AI-2 is a modified, quick and simple version of a Resistivity-TDS-Temperature chart found in logging chart books. It converts equivalent NaCl concentration directly to C_w in μmhos/cm at 25° C. The graph is constructed from data that Arps (1953) obtained from the **International Critical Tables** (1928, 1929). The equation for the graph, which was modified from the Dresser Atlas log interpretation chart book (1985), is as follows:

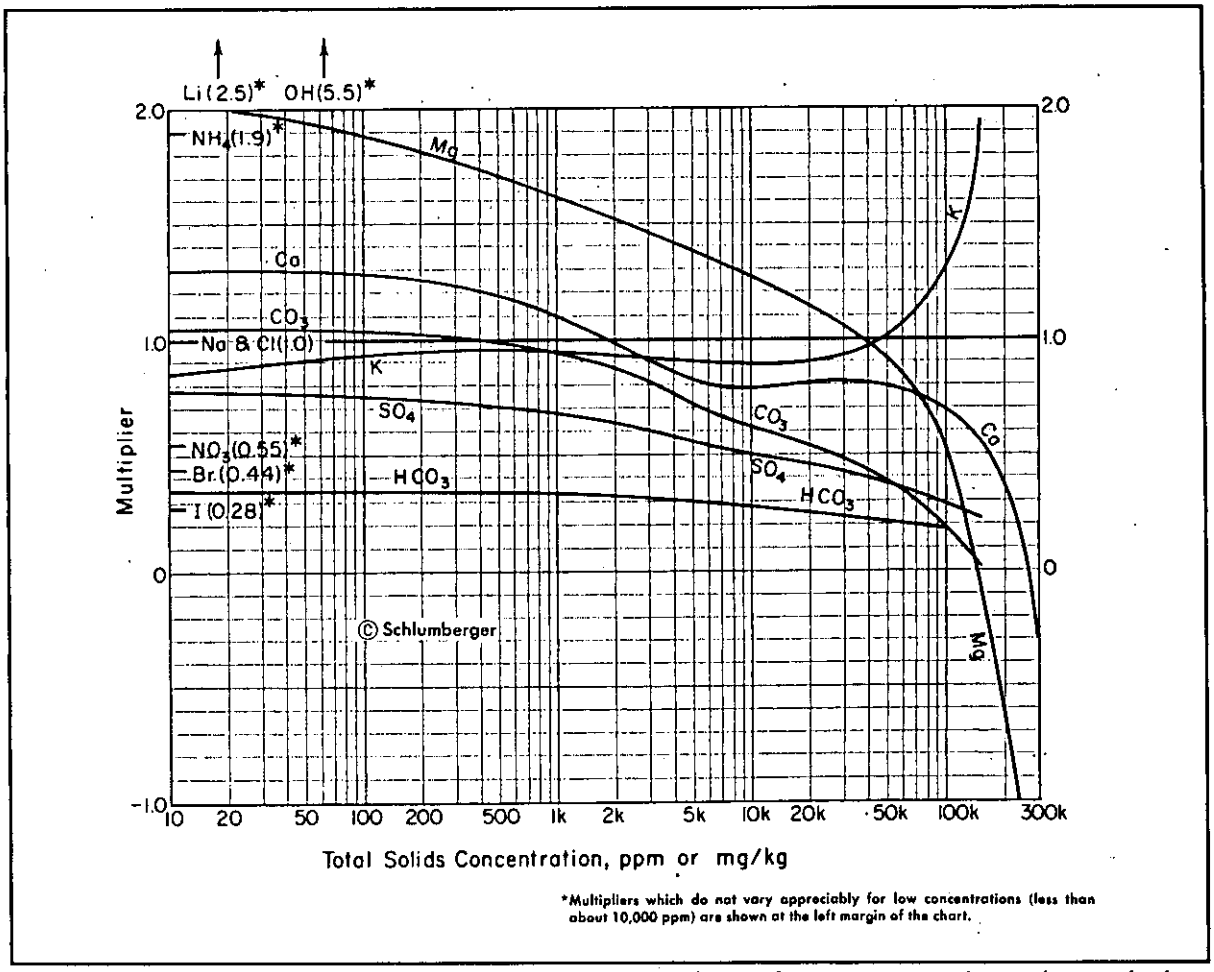

Figure AI-1. Chart for converting the ionic concentrations of a water sample to the equivalent NaCl concentration (Modified from Gen-8 Chart, Schlumberger, 1979).

$$Rw \text{ @ } 25°C = 0.012 + \frac{3552.7}{(equivalent\ NaCl)^{0.955}} \qquad \text{(I-6)}$$

The procedure for using Figures AI-1 and AI-2 to calculate Cw from ionic concentrations is:

1. The appropriate TDS value is entered into Figure AI-1. The TDS value should include 100 percent of the bicarbonate value and exclude the silica value. The TDS value can be in ppm or mg/l.

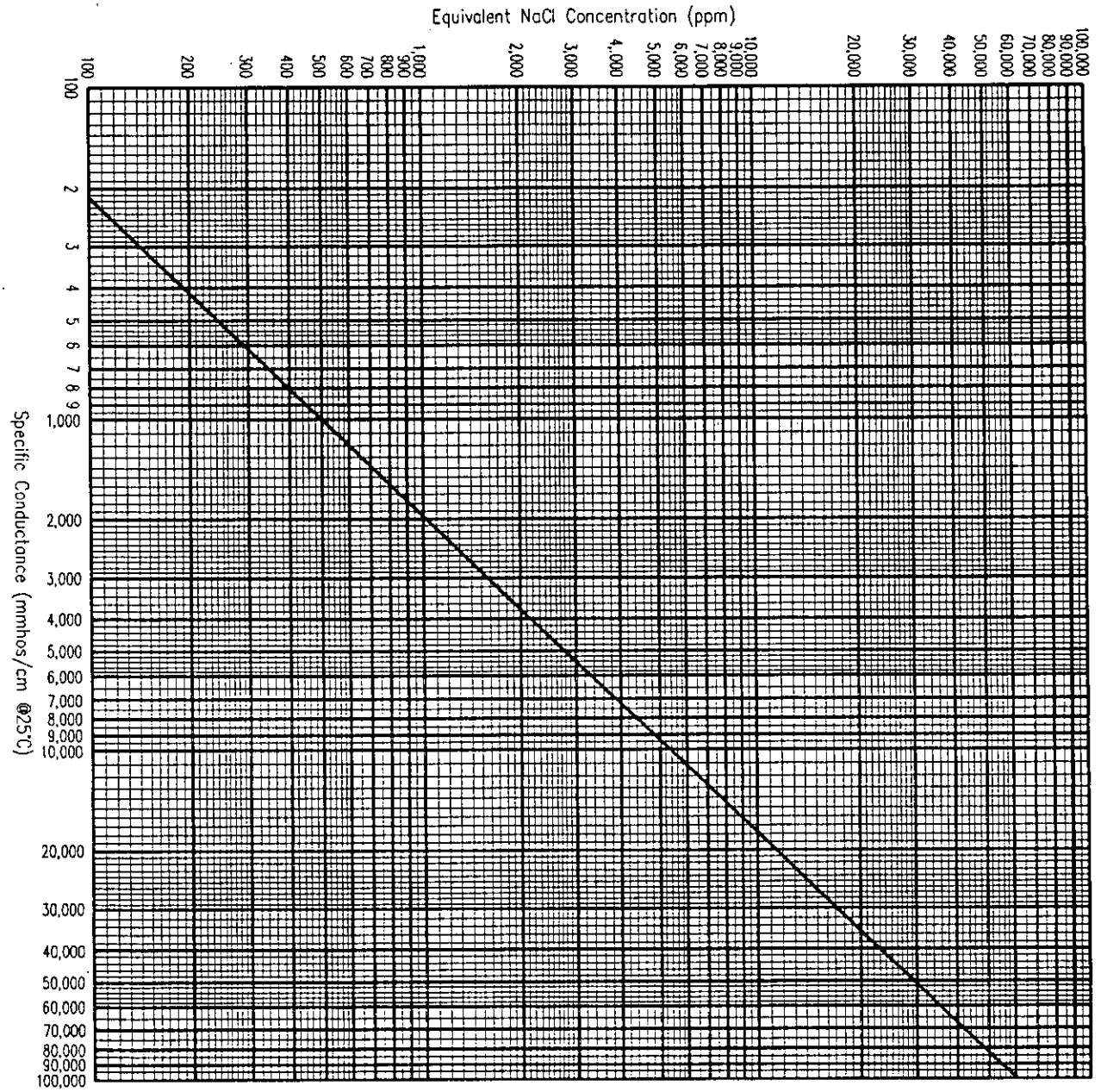

Figure AI-2. Graph for converting NaCl concentration to specific conductance. The data used to construct the graph is from Aarps (1953). The graph agrees with Chart Gen-9 (Schlumberger, 1988).

2. The appropriate multiplier for each ionic species in the water analysis is established by moving vertically to the intersection of the TDS value and the particular ion. For most water only Ca, Mg, Na, Cl, HCO_3, CO_3, and SO_4 occur in concentrations which are significant enough to be included in the calculation.

3. The concentration of each ionic species is multiplied by the appropriate multiplier. For the bicarbonate concentration 100 percent of the value is used.

4. The products calculated in step 3 are summed to yield the equivalent NaCl concentration.

5. The equivalent NaCl concentration is entered into Figure AI-2 and the corresponding Cw value is read. This is Cw μmhos/cm at 25° C for the water sample in question.

Specific Conductance from meq/l

The total of either anions or cations in meq/l multiplied by 100 usually approximates specific conductance. While not exact, this relationship is less variable than a general TDS-Cw relationship in mg/l. It is not as accurate as specific conductance calculated from ionic concentrations.

Two guidelines must be used with this method:

1. The anion-cation balance should be within acceptable limits (less than 5 to 10 percent).

2. If an acceptable difference exists, the anion value is used. Usually it will be more accurate than the cation value. This is because most waters have far more cation than anion species and a number of the minor cation species are not analyzed in a routine water analysis.

SUMMARY

1. Laboratories in Texas have significant differences in analytical techniques and in the accuracy of TDS and specific conductance measurements.

2. A water analysis should not be assumed to be correct until a quality control check is performed.

3. The TDS values should be verified by either an anion-cation balance (within less than 5 to 10 percent), or a $TDS_{calculated}$-residue on evaporation comparison (within less than 3 percent).

4. When comparing different TDS values, the method used to calculate TDS must be consistent, using either 100 percent or 49.2 percent of the measured bicarbonate value.

5. The TDS-Cw relationship should be used to verify TDS or specific conductance only when the relationship has been firmly established from other water analyses in the vicinity of the sample in question.

6. Specific conductances to within ± 5 percent of the actual value can be calculated from ionic concentrations.

7. Diluted conductance is an acceptable measurement only of fresh waters.

8. A laboratory should use standard methods to routinely calibrate its conductivity meters.

GUIDELINES FOR SELECTING AND UTILIZING LINE-FITTING ROUTINES

Appendix II

X-Y plots are the basis of many log analysis techniques. Plots such as TDS-Cw, Ro-TDS, Ro-Porosity, and Ro-Field Formation Factor are used to determine water quality. X-Y plots also are used to calibrate logging equipment and to calculate various rock properties.

X-Y plots are constructed in order to analyze the relationship between two variables. Scatter usually exists in the data, which makes the relationship less than perfect and difficult to quantify. In such cases, curve-fitting routines are utilized to establish the relationship that best fits the distribution of the data.

This section provides guidelines for selecting the proper straight-line fitting routine and correctly utilizing it. The discussion is limited to procedures for fitting straight lines to either untransformed data or data that have been transformed to their natural logarithms. Curvilinear-fitting routines are not discussed because most wireline log data sets fit a straight line.

Straight-line fitting routines warrant a review in this study because:

1. They are critical to many log analysis techniques.

2. There are many fitting routines from which to choose and the most appropriate one is frequently not used.

3. They are often misinterpreted.

4. Such a discussion provides the fundamentals for understanding the rationale behind the treatment of TDS-Cw graphs in this study.

Two excellent articles on straight-line fitting routines are Mann (1987) and Troutman and Williams (1987). The following discussion is a distillation of these two articles and verbal communications with Lee Etnyre, ARCO Oil and Gas; John Davis, University of Kansas; and Joe Booth, Abilene Christian University.

Step 1. Choose Between a Linear and a Curvilinear Fit.

The first step is to decide if a straight-line fit is appropriate for the data set:

1. The data should be plotted on a linear (arithmetic) scale. If the data appear to have a linear trend, a line-fitting routine can be applied.

2. If the trend is curvilinear, the data should be plotted on a logarithmic scale. If the trend is now linear, a straight-line fitting routine can be used.

3. If the trend is curvilinear on a logarithmic scale, a nonlinear fitting routine has to be used.

4. The data may have so much scatter that it is difficult to tell whether or not a linear relationship exists. In such cases one should apply the line-fitting routines, use a technique to analyze the quality of the lines, and then decide. Residual analysis is the best technique to determine linearity, but several other methods also can be used (e.g. Mann, 1987, pp. 94-100).

Step 2. Fit the Best Line to the Data.

The second step is to fit a straight line to the data set. No single, all-purpose, correct fitting technique exists. Each method usually gives a different line. The best line to use is dictated by the quality of the data, the amount of scatter in the data, and the intended use of the line. Personal biases also enter into the selection process. Straight-line fitting is not an exact science. Researchers sometimes differ as to which technique is best and what is the proper way to handle a data set.

This section reviews eight straight-line fitting routines common in scientific studies: eyeballing, averages, ordinary least squares, inverse least squares, weighted least squares, robust methods, least normal squares, and reduced major axis. Recommendations on when to use each method are also included. This section is, for the most part, a summary of Troutman and Williams (1987).

Quick-look Methods

The first two methods, eyeballing and averages, are simple, somewhat subjective, quick-look methods.

Eyeballing. Simply draw a straight line through what looks to be the best fit and calculate the equation of the line. Note: if the graph has logarithmic scales, the logs of X and Y must be used to calculate the equation.

While the method is quick and easy, it is subjective and there is no way to quantify the precision of the fit. At times, however, eyeballing may be all that is needed.

Averages. This method is also called semiaverages or groups averaged by residue summation. First, divide the data into two or more groups, usually according to increasing values of X. Calculate the average X (identified as $\overline{X}$) and average Y ($\overline{Y}$) for each group. Plot each ($\overline{X}$,$\overline{Y}$) on the graph, connect the points, and calculate the equation.

This technique is more precise than eyeballing, yet it is still relatively uncomplicated and easy to use. Unfortunately, the line may vary according to how the data are grouped. The equation cannot be reversed and the method is not as statistically sound as the following six mathematical methods.

Mathematical Methods

The following six procedures employ rigorous mathematical methods to fit the line. Each method varies as to how to minimize the deviation of points from the line (Figure AII-1). Consequently, each method usually draws a different line.

Ordinary least squares (Y on X). This method is the most commonly used straight-line fitting method. It is the method normally used for prediction. Ordinary least squares draws the line that has the minimum sum of the squared deviations (distances) of Y from the fitted line. It minimizes line AB in Figure AII-1A. This means, as shown in Figure AII-2, that the fitted line minimizes high values and maximizes low values.

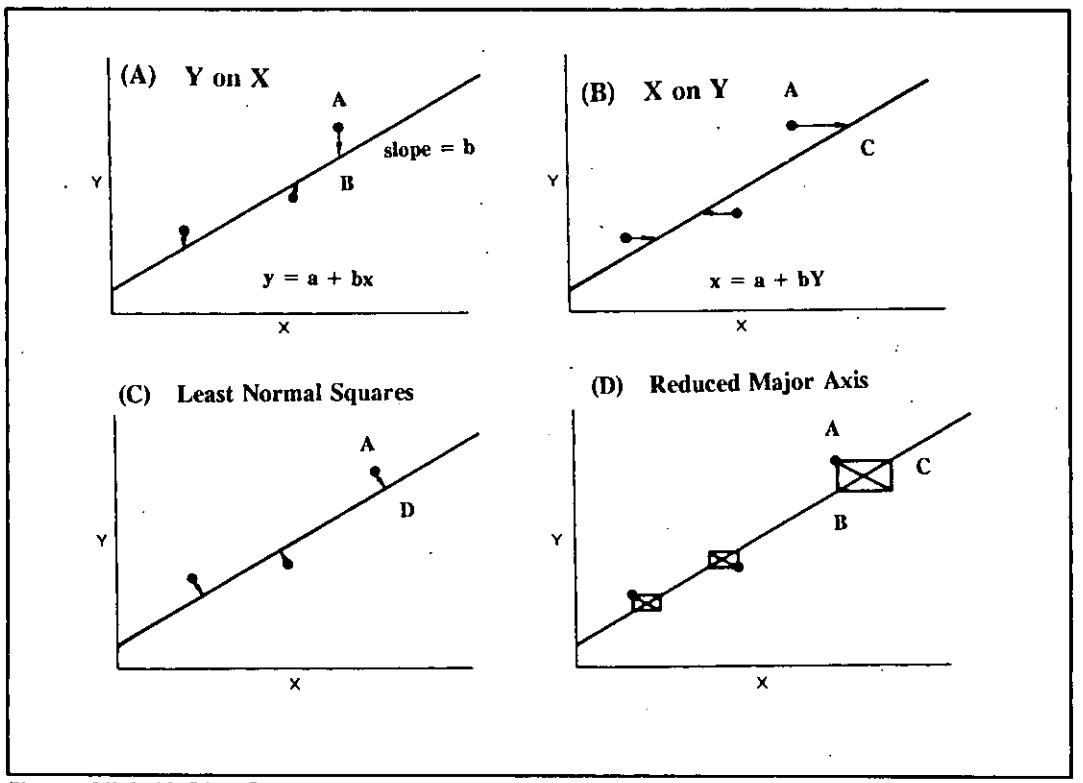

Figure AII-1 (A-D). Graphs showing the differences in line-fitting criteria for the four most common straight-line fitting routines (Modified from Jones, 1979).

An advantage of ordinary least squares is that the equation does not vary if one or both of the scales are changed (invariant to scale changes). One disadvantage is that unless the scatter of the data points about the line is very low (i.e. a very high correlation coefficient) the equation can only be used to predict Y; it cannot be reversed. In other words, the only valid form of the equation is $Y = a + bX$. It cannot be rearranged to $X = -a/b + Y/b$. Another disadvantage is that outliers, points having a large deviation from the line, have a disproportionate influence on the location of the fitted line.

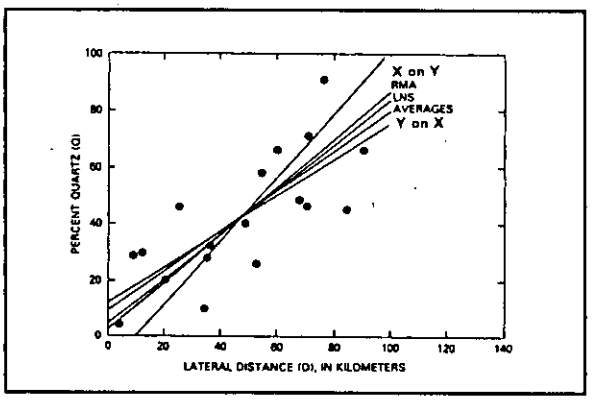

Figure AII-2. Hypothetical data set showing the line fits determined by five straight-line fitting methods (Modified from Troutman and Williams, 1987).

Ordinary least squares gives the best fit when errors in the data points are normally distributed with equal variances (Etnyre, 1984a). When this

condition is satisfied, the line has the minimum variance from the data points in the Y direction and the method gives the best possible prediction of Y. If the errors are not normally distributed, the method still can be used but the line may not be any better than lines obtained with other line-fitting routines. When the errors are not normally distributed, robust weighted least squares gives a better fit (Etnyre, 1984a). When the errors are normally distributed with unequal variances, weighted least squares provides the best fit when the weights are assigned as the reciprocal of the error variance for each data point (Etnyre, personal communication, 1990). Troutman and Williams (1987, p. 123) and Mann (1987, pp. 76-79) give details on other assumptions that underlie ordinary least squares.

Inverse least squares (X on Y). This method is a variation of ordinary least squares and is usually discussed under ordinary least squares. Inverse least squares draws the line that has the minimum sum of the squared deviations of X from the line. This is line AC in Figure AII-1B. This means, as shown in Figure AII-2, that the fitted line maximizes high values and minimizes low values. The resulting equation is $X = a + bY$. The equation cannot be rearranged. Inverse least squares has the same advantages and limitations as ordinary least squares.

Weighted least squares (WLS). This method applies a weighting factor to the squared deviation of each data point before fitting the line. It can be applied to both ordinary and inverse least squares. The weighting factors are used to decrease the effect of less reliable points on the line fit, thereby equalizing the errors in the data. It is also used to remove the weighting effect of a logarithmic transformation. The key to the method is assigning the proper weighting factors. Aside from being more complicated, weighted least squares has about the same advantages and disadvantages as ordinary and inverse least squares.

Robust methods. Robust methods are similar to weighted least squares. These methods are used to minimize the effect of outliers (points having large deviations from the line), which can adversely affect ordinary and inverse least squares lines. Robust methods should be used only after it has been determined that the outliers are erroneous.

These methods are more complicated than most other straight-line fitting routines. Please refer to Troutman and Williams (1987, pp. 116, 124, and 125) for further details.

Least normal squares (LNS). This method, also known as major axis, principal axis, and Pearson's 1901, draws the line that minimizes the sum of the squared perpendicular deviations of the data points from the line (line AD in Figure AII-1C). Line AD is therefore the shortest distance that can be obtained between a straight line and each point in the data set (see Figure AII-2).

The equation is reversible. Scale changes, however, require the slope to be recalculated. Even though this line gives the closest fit to the data, it is the best line to use only if the magnitudes of the errors in both variables are nearly the same.

Reduced major axis (RMA). This method minimizes the sum of the areas of right triangles formed between the data points and the fitted line. This is area ABC in Figure AII-1D. RMA assumes that on a percentage basis the measurement accuracy between the two variables is nearly equal.

The equation is reversible and scale changes do not alter it. However, unless the correlation coefficient is very high, the equation is not statistically as good as a least squares equation for predictive purposes.

Selecting the Proper Line-Fitting Routine

Remember that the selection of a line-fitting routine is dictated by the intended use of the line, the quality of the data, the amount of scatter in the data, and personal preference. Selection of the fitting routine also involves a decision as to which axis each variable is to be plotted on.

Linear regression. One objective of fitting a straight line to a data set is to provide an equation for predicting values of one variable, given values of the other variable (linear regression). Use the following guidelines to select the best line-fitting routine for linear regression:

1. If a data set has perfect correlation, it makes no difference which straight-line fitting routine is used and which variable is Y. Each of the eight methods will draw the same line and calculate the same rearrangeable equation.

2. If a data set has very high correlation, it makes little difference for the main body of the data set which fitting routine is used and which variable is Y. In the tails of the data set and beyond,

however, small variations from perfect correlation can mean considerable differences in the position of the various lines. If the tails are the important part of the data set, use guideline 3. below to choose the proper line.

3. If scatter exists in the data, each routine will draw a different line. Ordinary least squares and inverse least squares are the extremes of the fits, with all other lines falling between these two (Figure AII-2). All lines agree at the centroid (X,Y) and disagreement increases away from this point. As the scatter in the data decreases, the lines converge on the RMA line. When one variable has no error and the other variable has all the error (as is the case in some laboratory experiments), or when one variable has most of the error, the best equations for predictive purposes are ordinary least squares, inverse least squares, weighted least squares, and robust methods. The variable with the least amount of error is designated the independent variable. The variable with the greatest amount of error is the dependent variable and is usually assigned to the Y-axis.

   a. Ordinary least squares (Y on X) is used to predict values of Y, given values of X, when Y is the dependent variable. The equation solves for the mean value of Y given a particular value of X. The same answer will be obtained by assigning the variable with the most error to X and using inverse least squares (X on Y) to solve for X. Y on X, however, is the conventional arrangement.
   b. When the variable to be predicted (Y) has less error than X, there are two ways to regress the data. Some workers use (X on Y). X is treated as the dependent variable, although in truth it is not. Most statisticians, however, advocate calibration: regress Y on X and then invert the equation to solve for X. For values near the centroid, both methods give similar answers, while calibration gives better answers at and beyond the tails (Davis and Doveton, 1990). This is the only time that Y on X should be inverted.
   c. In order to minimize the effect of less reliable data points on either ordinary or inverse least squares, weighted least squares should be used. It can also be used to remove the weighting effect of a logarithmic transformation of the data.
   d. For data sets with spurious outliers, one can either use robust methods or discard any known or suspected outliers from the

data set. However, one should avoid rejecting any data without investigating the reasons for the outliers (Etnyre, personal communication, 1990).

4. Least normal squares and reduced major axis are the best routines for linear regression when the magnitudes of the errors in the two variables are nearly the same. Since both methods have reversible equations, it makes no difference which variable is Y.

Structural and functional analysis. Another reason for fitting a straight line to a data set is to estimate the true underlying linear relationship between two variables (structural and functional analysis).[1] Least normal squares and reduced major axis are the best methods for determining the true underlying linear relationship between the two variables. Working on the assumption that errors exist in X and Y, these methods use statistics to estimate error-free counterparts of X and Y and establish the relationship between these unobservable variables.

Step 3. Calculate the Equation of the Line.

In addition to plotting a straight line, each of the aforementioned fitting routines calculates the equation of the line. The equation for a straight line is as follows:

$$Y = a + bX \qquad \text{(II-1)}$$

Where:
***X** and **Y** are the measured values of the two variables under consideration.*
***a** is the Y-axis intercept of the line when $X = 0$.*
***b** is the slope of the line – the number of units that Y changes for each one unit change in X.*

A line-fitting routine applied to logarithmically transformed data uses the logarithms of the data points, not the arithmetic values. The equation of the line must be written accordingly:

---

[1] See Troutman and Williams (1987, p. 118) for an explanation of the differences between structural and functional analysis.

$$\log Y = \log a + b \log X \qquad \text{(II-2)}$$

Where:
a** is now the Y-axis intercept of the line when X = 1. Some authors denote* **loga as simply* ***a***.
By ***a*** *they mean that the term is a constant – the log of* ***a***.

This equation can be rewritten in a simpler form by taking the antilogs of Y, X, and a. The new equation is in the form of a power law as follows:

$$Y = aX^b \qquad \text{(II-3)}$$

Where:
a** is now a proportionality constant. It is the* log *of* ***a *in (II-1).*
***b** is an exponent in the nonlinear relationship.*

Step 4. Assess the Degree to Which the Line Fits the Data.

A standard part of every line-fitting routine should be to mathematically, rather than just visually, determine how well the line fits the data set. This can be done by calculating the correlation coefficient and examining the residuals.

Correlation coefficient. The correlation coefficient (r) is a measure of the linear association between X and Y or how well X predicts Y. Coefficient correlations will be $-1.0 \leq r \leq 0$ or $0 \leq r \leq +1.0$. When $r = 0$, there is no linear association between X and Y. An r of -1.0 or +1.0 means perfect correlation. A direct relationship between X and Y or an equation with a positive slope yields a positive r. Negative values occur when an equation has a negative slope or the two variables have an inverse relationship.

Correlation coefficients should be interpreted according to the following guidelines:

1. When various line-fitting routines are applied to a data set, the line with the highest correlation coefficient is not necessarily the best fit (see **Step 3. Calculating the Equation of the Line**).

2. When comparing different pairs of variables from the same data set, remember that coefficients have relative, not absolute, value. An r of 0.9 for variables X and Y is not twice as good as an r of 0.45 for Y and Z.

3. Technically, correlation coefficients from different data sets should not be compared.

4. A high correlation coefficient implies nothing about the statistical or geological significance of the linear association. All it signifies is that the two variables have a high degree of linear association (Mann, 1987).

A more useful comparison may be made using the coefficient of determination (r^2). It gives the fraction of data spread which is accounted for by the fitted line (Etnyre, 1984a).

Residual analysis. Residual analysis is another excellent method of checking the quality of a fitted line. A residual (d) is the difference between an observed value and the predicted value. The equation is as follows:

$$d = Y - \hat{Y} \qquad \textbf{(II-4)}$$

Where:
d is the residual.
Y is the observed value.
$\hat{Y}$ *is the predicted value as determined by the equation of the fitted line.*

There are several types of residuals and various ways to display them (Mann, 1987, p. 99). One technique is to plot raw residuals against X, Y, or $\hat{Y}$ and examine the magnitude and pattern of the residuals (Figure AII-3). The closer the line fits the data, the closer the residuals cluster randomly on a narrow band along d = 0. The nature of the distribution of the residuals about d = 0 also helps to identify outliers, reveal trends, and verify the two most often violated linear regression assumptions: linearity and constant variance of errors (Mann, 1987, p. 79).

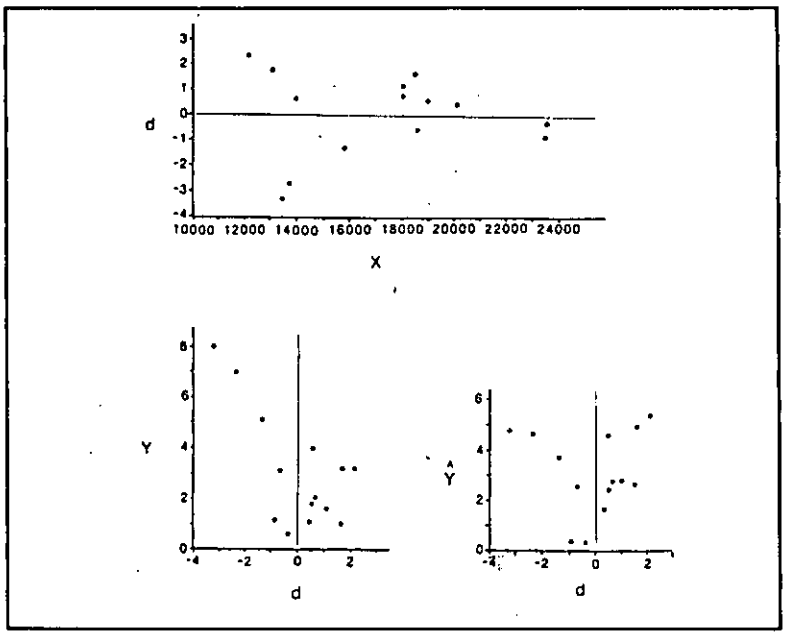

Figure AII-3. Example of three ways to plot raw residuals: against predictor variable X (top), regressor variable Y (lower left), and predicted values Y (lower right) (Mann, 1987).

Step 5. Properly Use the Data.

Extrapolating linear relationships beyond the range of the data set is very tenuous. When there is no alternative, one should at least be aware of two potential errors:

1. The trend and/or the relationship between the two variables may change in the region beyond the data base. For example, the relationship between TDS and Cw is linear for fresh water and curvilinear for saline waters.

2. Confidence in predictions decreases away from the center of the data and drops off even faster beyond the data set. Confidence intervals on a graph readily show this (Figure AII-4). This explains one reason why predicting Rw from Ro-Porosity plots is often unsuccessful (Etnyre, 1984a). Confidence intervals should be kept in mind when predicting the TDS of waters with either very high or very low conductivities (those at the extreme ends of the data set).

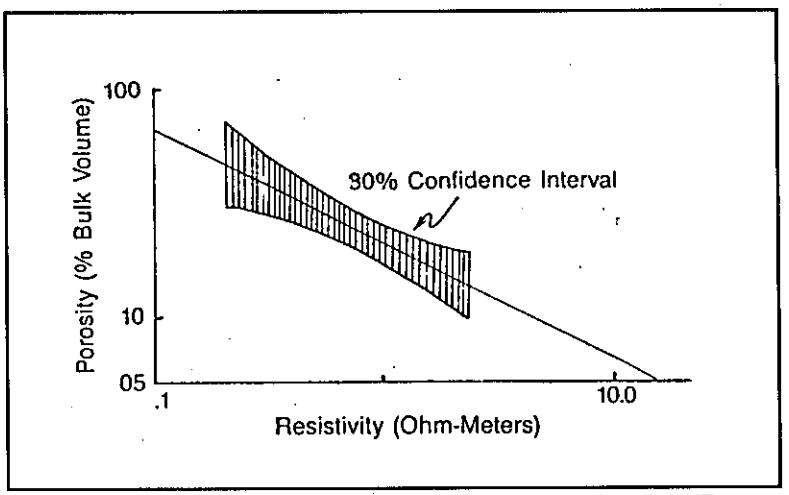

Figure AII-4. Confidence interval about the regression line (Etnyre, 1984a).

Step 6. Properly Handle Logarithmic Transformations.

Many data sets that have a curvilinear trend on an arithmetic scale can be converted to a linear trend by mathematically transforming the data. A transformation common in log analysis is to convert the values of the variables to their natural logarithms. This is the transformation discussed in this section.

Logarithmic transformations are usually performed by simply plotting the data on log-log paper, which is the method used in this study. An alternate technique is to calculate the logarithms for each data point and plot the logarithmic values on an arithmetic scale (see Fogg and Blanchard, 1986, for examples). However, this method is time consuming and cumbersome. Computer programs sometimes make the transformation, calculate the line, convert the data and the equation to their antilogs (arithmetic values), and then graph them without ever displaying a logarithmic plot. This procedure has a disadvantage in that no one ever visually inspects the logarithmic plot.

The advantage of logarithmically transforming data to a straight line is that all of the above mentioned line-fitting routines and quality checks are then applicable. After the appropriate line-fitting routine has been applied, then the data can be plotted on arithmetic or logarithmic scales.

As discussed in Step 3., the equation of the line can be written either of two ways:

$$\log Y = \log a + b \log X \qquad \text{(II-5)}$$

or

$$Y = aX^b \qquad \text{(II-6)}$$

Equation II-6, called a power law, is a little faster to solve and is more commonly used.

Logarithmic transformation involves an often overlooked pitfall -- the addition of an unavoidable weighting factor to the data. A weighting factor is introduced because the line-fitting routine deals with the logarithms of the data points, not the arithmetic values. Because of the logarithmic transformation, the relative weight or influence of small values on the fitted line is greatly increased and the relative weight given to large values is decreased.

To demonstrate why a logarithmic transformation introduces a weighting factor, consider two numbers: 100 and 10,000, and their logarithms, 2 and 4. The relative weight of 4 to 2 is considerably less than the relative weight of 10,000 to 100 and vice versa.[1] Consequently, during the line-fitting of logarithmic data, the line will be skewed toward the small logarithms. When a line is fitted to the arithmetic values, the large numbers will have more influence and the line will move in their direction. Thus, the best-fit line for a logarithmically-derived straight line, when recalculated into the untransformed equivalent (antilog) and plotted on an arithmetic scale, will plot lower than the line calculated from the arithmetic scale (Figure 4-3). Jansson (1985) has a good discussion of this subject.

Adding this weighting factor to the data may or may not be advantageous. When it is not advantageous, as is often the case, the remedy is to use weighted least squares. Etnyre (1984a,b) has an excellent treatment of how to apply weighted least squares to logarithmically transformed data.

---

[1] Etnyre (1984a, p. 14) mathematically derives the weighing factor for ordinary least squares that a logarithmic transformation creates.

Sometimes only one variable is converted to its natural log (i.e., a core porosity versus core permeablility graph). In this case the following procedures apply:

1. Regressing Y on the natural log of X does not affect the deviations of Y from the fitted line (Figure AII-5). The equation of the line is as follows:

$$Y = a + b\ln X \qquad \text{(II-7)}$$

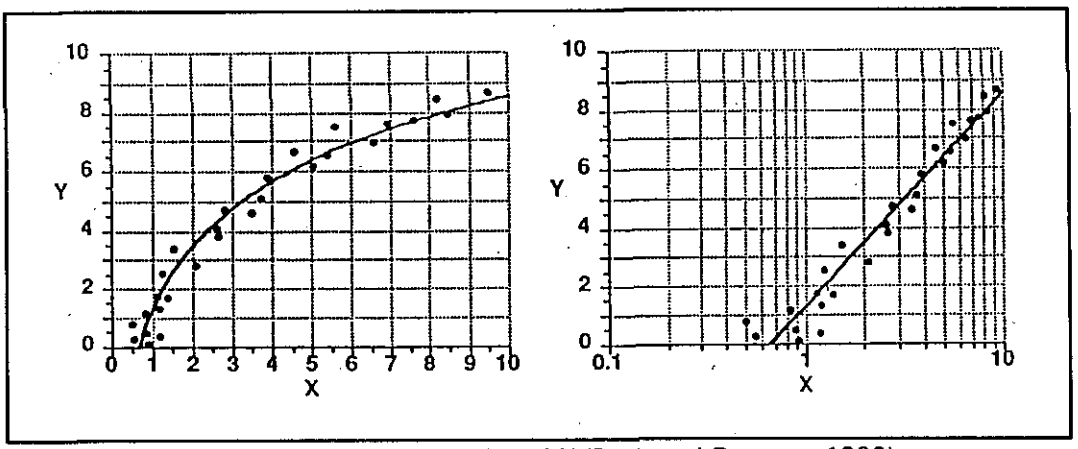

Figure AII-5. Regressing Y on the natural log of X (Davis and Doveton, 1990).

2. Regressing the natural log of Y on X will mean that the deviations of lnY from the line will be symmetrical, but the deviations of Y will not be (Figure AII-6). The equation of the line is as follows:

$$\ln Y = a + bX \qquad \text{(II-8)}$$

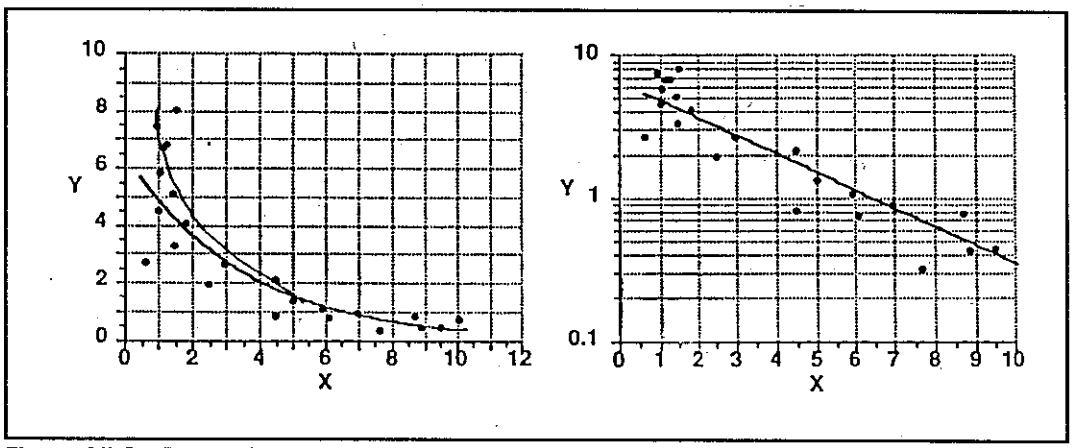

Figure AII-6. Regressing the natural log of X on X (Davis and Doveton, 1990).

3. All of the guidelines mentioned in this chapter for straight-line fitting routines also apply to semi-logarithmic plots.

TECHNIQUES TO EVALUATE THE QUALITY OF DRILLING MUD

Appendix III

Chapter 8 demonstrated that the chemical composition of the drilling fluid has an important bearing on the quality of the log responses. Drilling fluids also will effect drilling efficiency. Even more important, well productivity is directly related to the quality of the drilling fluid. Because drilling fluids are so critical to all aspects of the assessment and development of a water well, the addition of this appendix was deemed necessary. This material is from Baroid Drilling Fluids, Inc.'s 1991 seminar on Drilling Fluid Technology As Applied To Minerals Exploration, Water Well, and Geotechnical Drilling. Bob Pace of Baroid Drilling Fluids provided additional comments.

Drilling fluids perform a number of important functions that effect the drilling operation. They:

1. Cool and lubricate the bit and drill string.
2. Clean the cuttings from the bit and the bottom of the hole.
3. Suspend solids.
4. Transport cuttings and sloughings to the surface.
5. Minimize fluid loss into permeable formations.
6. Stabilize the well bore.
7. Prevent the flow of formation fluids into the well bore.
8. Minimize wear and corrosion of the drilling equipment.
9. Assist in gathering subsurface geological data and formation evaluation.

Good quality drilling fluid more efficiently performs the above functions. The performance of drilling fluid depends on four physical properties: mud weight (density), viscosity, filtration (filter cake and filtrate

volume), and sand content. It also depends upon the chemical properties of pH and ion concentrations. Ion concentrations determine which additives can be used to design specific properties into the drilling fluid.

Many people tend to forget that the primary purpose of a drilling fluid is to convey drilled solids from the hole to make room for the production casing and down hole pumps. A 10 inch hole drilled to 200 feet moves approximately nine tons of drilled solids. The drilling fluid must deal with these solids chemically and physically. If the solids are not physically removed from the fluid then they must be treated chemically to minimize their effects on the fluid.

A drilling fluid may be as simple as clean, fresh water, or it may be designed to densities of greater than 18 pounds per gallon in order to tolerate temperatures greater than 500 degrees Fahrenheit. Most non-oilfield applications are not so complex, except for geothermal applications. The most common designs are simple fresh water, extended bentonite dispersions. Even so, it is a dynamic fluid in a constant state of change as active ingredients, mainly commercial bentonite, are constantly being diluted or replaced with inactive ingredients (solids from the formations). The only way to maintain a good mud quality is to routinely measure the mud properties and adjust the mud accordingly.

This chapter defines the most important physical and chemical properties of drilling mud and discusses their effect on drilling and logging operations. Recommendations on how to maintain the proper balance of each property are included.

PHYSICAL PROPERTIES

Mud Weight (Density)

Mud weight, or density, is the most important mud property. Density is measured in pounds per gallon (lb/gal) by weighing a known volume of mud with a mud balance. Density must be measured. Visual estimates will not be accurate.

For simple water-base muds, it is a measure of the percentage of suspended solids (Table 9-1). It also indicates the hydrostatic pressure of the mud column as follows:

$$\textit{Hydrostatic pressure (psi)} = 0.052\ (\textit{mud weight, lb/gal}) \times \textit{depth (ft)} \qquad \text{(III-1)}$$

TABLE III-1. RELATIONSHIP BETWEEN SOLIDS CONTENT AND MUD WEIGHT

Percent Solids*	Mud Weight lbs/gal
0	8.33
1	8.47
2	8.60
3	8.74
4	8.88
5	9.02
6	9.15
7	9.29
8	9.43
9	9.57
10	9.70
11	9.84
12	9.98
13	10.12
14	10.25
15	10.39
16	10.53
17	10.67
18	10.80
19	10.94
20	11.08

(Baroid course notes, 1991). * Assumed Solids Specific Gravity = 2.65 gm/cm^3

Mud weight is very important to both the drilling and logging process because excessive solids create a number of problems:

1. A pressure differential between the mud column and the formation water which is too high increases impregnation and can either reduce formation permeability or cause loss of circulation by fracturing the formation.

2. Excessively thick mudcake, which impairs water production, affects pad-type logging tools, and can stick pipe.

3. Excessive wear on the mud pump, drill string, and bit.

4. The settling of cuttings at the surface is retarded, so the mud pump does unnecessary work recirculating solids and the drilling rate is reduced.

For most water well drilling and coring, density should be kept below about 9 lb/gal. (Water is 8.33 lb/gal.) If the solids control equipment or settling pits are inadequate to control solids density, it may rapidly increase to 9.5 lb/gal or greater. In the case of artesian water pressure, mud weight will need to be increased (preferable with barite) to control the overpressured zone.

However, a low mud weight does not guarantee a good quality mud. The type, as well as the quantity, of solids in the mud determines mud quality. A 9.0 lb/gal natural mud will be composed of clays and other solids from the formations. It will not be nearly as effective in fulfilling the previously mentioned drilling mud functions as will a 9.0 lb/gal mud containing commercial bentonite and other additives.

With a poorly designed drilling fluid handling system, the density will increase as the hole is deepened. This means that at the most critical time, when the bit reaches the target aquifer at the bottom of the hole, the drilling fluid is at its highest density and poorest quality.

Several techniques can be used to control density. The most important ones are: have a good mud pit design, use a shale shaker with fine screens, use desander cones, keep the pump suction off the bottom of the mud pit, and add water to the mud.

Filtration (Filter cake and Filtrate)

A filtration test measures the filter cake thickness to the nearest $^{1}/_{32}$ of an inch and the mud filtrate in cubic centimeters (cm^3) produced by a filter press in 30 minutes at 100 psi under static conditions. The results are used to estimate the quality of the mud cake forming in the borehole and the amount of filtrate invading the formations.

A good mudcake is essentially impermeable (low filtration rate), thin, slick, pliable, and easily removed during well development. The quality of the mudcake is a function of the type and the concentration of solids in the mud. A good mudcake requires commercial bentonite rather than native clay and a low percentage of natural solids. Otherwise, problems may develop:

1. A high water-loss mud with excessive mud filtrate invasion will affect the resistivity response and increase the chance of differentially sticking of the drill pipe.

2. An abnormally thick mudcake that will affect pad-type logging tools, reduce well productivity, and create tight spots.[1]

3. Less stable borehole walls.

For water well drilling and coring the filter cake should be less than $^{3}/_{32}$ of an inch thick, slick, and soft. The filtrate loss during the test should be 15 cm^3 or less. Mud cake quality and filtrate loss are controlled by keeping the ratio of commercial bentonite to natural solids high.

Viscosity

Viscosity is the resistance offered by a fluid to flow. The term is loosely applied to drilling mud as a measurement of carrying capacity and gel strength. It is measured with a Marsh funnel in seconds/quart (which is commonly abbreviated to seconds). As a rule of thumb,

$$viscosity \approx 4(mud\ weight) \qquad (9\text{-}2)$$

Although the Marsh funnel is not a true viscosity measurement, its use is considered very useful for simple drilling fluids.

The viscosity and velocity of the drilling fluid determine how effectively cuttings are removed from the face of the bit and are carried to the surface. Low viscosity muds are best at these tasks if adequate pumping is available. However, higher viscosity muds may be needed to remove coarse sand from the borehole and to stabilize some unconsolidated sand and gravel formations that cave into the well bore.

---

[1] A natural mud with a viscosity of 45 seconds and a density of 10.3 lb/gal will form a volume of filter cake 36 times greater than a bentonite additive mud with a weight of 8.6 lb/gal (Baroid course notes, 1991).

When drilling fluid circulation ceases, the mud thickens or "gels". The force needed to break the gel when circulation resumes is the gel strength. For normal water-base muds viscosity is a good indicator of gel strength. Gel strength from commercial bentonite suspends cuttings in the borehole when circulation stops, thus preventing the drill pipe from getting stuck.

High viscosity and gel strength create the following problems:

1. Drilling rate is reduced because cuttings are not removed efficiently from the bit face and from the mud when it reaches the surface.

2. High pump pressure is required to break the gel, which can cause impregnation and loss of circulation.

3. Mud weight increases.

Viscosity should be as thin as practical and still clean cuttings from the hole. The recommended range is 32 to 38 sec/qt. (Water is 26 sec/qt.) However, for hole stability in very unconsolidated formations, viscosity may need to be much higher.

Viscosity is increased by adding more bentonite or a polymer. It is decreased by adding water or, in some cases, a phosphate deflocculant.

Sand Content

Sand content is defined as percent by volume of mud solids retained on a 200-mesh sieve. The recommended limit is less than 2 percent by volume.

Excessive sand content creates a number of problems such as:

1. Thickens the mud cake.

2. Increases the mud weight.

3. Abrades the pump, drill string, and bit.

4. Slows the drilling rate.

Sand content is controlled by utilizing a shale shaker, desanders, and a good mud pit design that maximizes settling time. Adding water to lower the viscosity will also decrease the sand content.

CHEMICAL PROPERTIES

pH

The term pH is defined as -log of the hydrogen ion concentration (H^+). In its simplest terms, 1 to 7 is acidic and 7 to 14 is alkaline. In fresh water it is easily measured with pHydrion paper or ColorpHast sticks. Most drilling fluids should have a pH of 8.3 to 9.5 (or moderately alkaline) because:

1. The effectiveness of bentonite is greatly reduced in acidic conditions (pH less than 7) and viscosity, gel strength, and filtration are adversely affected.

2. Drilling equipment exposed to acidic conditions may corrode rapidly.

3. A pH greater than 9.5 can accelerate clay dispersion and may cause thick drilling fluid and borehole deterioration, which can hamper both drilling and logging.

Drilling fluids should not be overtreated with alkaline materials (caustic soda, bicarbonate of soda, or soda ash). Cement contamination is the main cause of excessively high pH. The pH is lowered by adding sodium bicarbonate. When using fresh water add caustic soda to raise the pH. Soda ash should be added if the available water is considered hard (soluble calcium).

Alkalinity

Most non-oilfield drillers do not test their drilling fluids for any chemical property except pH. However, many drilling problems could be eliminated if they tested the mud alkalinity.

P_m. P_m is defined as the volume, in cm^3, of standard (N/50) sulfuric acid to reduce the pH of 1 cm^3 of whole mud from actual pH to pH 8.3 using phenolphthalein as the pH indicator. It quantifies the amount of soluble and

insoluble alkaline material in the mud (lime or cement, caustic soda, bicarbonate of soda, or soda ash.)

P_f - M_f. P_f is defined as the volume, in cm^3, of standard (N/50) sulfuric acid to reduce the pH of 1 cm^3 of mud filtrate from actual pH to pH 8.3 using phenolphthalein as the pH indicator.

M_f is defined as the volume, in cm^3, of standard (N/50) sulfuric acid to reduce the pH of 1 cm^3 of mud filtrate from the actual pH to pH 4.3 using methyl orange as the pH indicator. The relationship between P_f and M_f quantifies the amount of hydroxyl, bicarbonate or carbonate ions in the filtrate.

Total Hardness

There is a standard test for total hardness (calcium and magnesium ions.) The amount of total hardness is important because small amounts of either or both elements will effect the yield of commercial bentonite. The amount will dictate whether caustic soda, bicarbonate of soda, or soda ash should be used.

Chloride

There is a standard test for determining the amount of chloride. A knowledge of the amount of chloride is important for two reasons. First, the yield of commercial bentonite is affected by chloride in the mud, and second, the quality of the electric log responses is affected.

Field testing procedures for drilling fluids (API RP 13B) are available from the AMERICAN PETROLEUM INSTITUTE, Production Department, 211 North Ervay, Suite 1700, Dallas TX 75201.

MAKE-UP WATER

Make-up water should be tested and treated before bentonite is added. Most city drinking water is adequate. Water that is drinkable is adequate for drilling fluid. In some areas of the United States, the water in the local streams and creeks will have a total hardness that needs to be treated with soda ash to reduce it to an acceptable level before the commercial bentonite will yield properly.

Testing Program

All mud property measurements and any changes made to the mud system should be documented and included in the permanent well file. For water wells the testing normally will be done by the drilling crew. For petroleum tests, a representative of the mud company (mud engineer) periodically does a detailed analysis, in addition to those performed by the drilling crew. The mud sample should be taken from the flowline before the mud has traveled through any surface equipment (shale shaker, pits, etc.).

The more important mud properties, for characterizing the borehole environment for log analysis, are mud type, density, filtration, chloride ion, and any major changes to the mud system. The standard log heading has spaces for type fluid in hole, density, viscosity, pH, and fluid loss (same as filtrate loss). The logging company does not measure these properties, but only records what is provided to them. The information is usually present on petroleum logs. Water well logs usually contain the type fluid in the hole. Density and viscosity are sometimes noted but pH and fluid loss are seldom recorded. Log headings do not contain information regarding changes to the mud system. The mud properties on the heading should be those at the time of logging.

ABBREVIATIONS AND SYMBOLS

Appendix IV

a - Variable used in several equations in Chapter 4; meaning varies according to the equation
a - Tortuosity factor
A_1 - Guard electrode
A - Electrode
AC - Alternating current
a_{Ca} - Activity of the calcium ions
Al - Aluminum
AM - Electrode spacing of normal tools
AM ∞ - Antiquated term for AM
a_{mf} - Activity of the mud filtrate
a_{Mg} - Activity of the magnesium ions
a_{Na} - Activity of the sodium ions
AO - Electrode spacing of lateral tools
APHA - American Public Health Association
API - American Petroleum Institute
a_w - Activity of the formation water

b - Variable used in several equations in Chapter 4: meaning varies according to the equation
B_{cp} - Compaction correction factor (same as C_p)
BGT - Borehole Geometry Tool
B.H.V. - Borehole volume
BPB - British Plaster Board
Br - Bromide
BRC - Balcones Research Center

C - Conductivity
° C - Degrees Celsius
Ca - Calcium
Cali - Caliper
Ca_2SO_4 - Calcium SulFate
CDL - Compensated Density Log
CEC - Cation exchange capacity
CGR - Computed gamma ray curve minus the uranium count

CILD - Deep induction conductivity curve
Cl - Chloride
CNT-G - Epithermal-Thermal Compensated Neutron Log
CO_3 - Carbonate
Corr - Corrected
C_p - Compaction correction factor (same as B_{cp})
CPS Counts per second
CSNG - Compensated Spectral Natural Gamma Ray
Cw - Specific conductance or specific conductivity
$Cw_{Anion\ Sum}$ - Specific conductance calculated from the anion sum
$Cw_{Calculated}$ - Calculated specific conductance
$Cw_{Ion\ Conc.}$ - Specific conductance calculated from the ion concentration
$Cw_{Measured}$ - Measured specific conductance

DCAL - Differential caliper
DEC - Decimal
Δt - Travel time
Δt_f - Fluid travel time
Δt_{ma} - Matrix travel time
Δt_{sh} - Shale travel time
D.F. - Drill Floor
dh - Borehole Diameter (also d_h)
diff - Difference
DIL - Dual Induction Log
DIL-SFL - Dual Induction Log - Spherically Focused Log
DIS-EA - One version of Schlumberger's Dual Induction Tool
DLL - Dual Laterolog
DLS/DE - One version of Schlumberger's Dual Laterolog
DN - Density neutron
DNL - Dual Porosity Compensated Neutron Log
DNPOROS - Density-neutron crossplot
DPHI - Density porosity
DPT - Deep Propagation Tool
DRHO - Bulk density correction ($\Delta\rho$)

e - Bed thickness (in older literature)
E - Emitter
E_c - Electrochemical potential
E_k - Electrokinetic potential
EL - Electric log
E_{lj} - Liquid-junction potential

E log - Electric log
E_m - Shale membrane potential
emp - Equivalents per million
ENPH - Epithermal porosity
EPHI - Electromagnetic propagation porosity
EPT - Electromagnetic Propagation Tool
ES - Electrical Survey

F - A conversion factor
F - Flouride
F - Formation Factor
° F - Degrees Fahrenheit
F_c - Formation factor of the common porosity (depth) value
FDC - Compensated Formation Density
FFF - Field formation factor
FLUIDRES - Fluid resistivity
FoRxo Log - Flushed zone microelectrode tool
FR - First reading
FR - Fluid resistivity
F_R - Formation resistivity factor

g - Gram
G - Geometric factor
GAM - Gamma
g/l - Grams per liter
G.L. - Ground level
GLT - Geochemical Logging Tool
GR - Gamma ray
GRC - Gamma ray corrected
GR_{Cl} - Gamma ray response in a clean zone
Gr-ion/l -
GR_{Sh} - Gamma ray response in 100 percent shale
grain/gal - Grains per gallon

h - Bed thickness
H^+ - Hydrogen ion
HCO_3 - Bicarbonate

I - Survey current
IDPH - Phasor Deep Induction
IEL - Induction Electric Log

IES - Induction Electric Survey
IFG - Instruments for Geophysics
I_{GR} - Gamma ray shale index
I.H.V. - Integrated hole volume
ILD - Deep Induction Log
ILM- Medium Induction Log
IMPH - Phasor Medium Induction
ISF - Induction Spherically Focused Log
in - Inches, also (")

J - Pseudogeometric factor

K - Constant dependent on the electrode configuration
K - Constant that is a function of temperature
K - Potassium
K.B. - Kelly bushing
KCl - Potassium chloride
KGS - Kansas Geological Society
kg/m - Kilograms per meter
K_m - Constant that is a function of the mud weight
l - length
Lat. - Lateral
lb/gal - Pounds per gallon
LDT - LithoDensity Tool
LL - Laterolog
LL3 - Laterolog 3
LL8 - Laterolog 8
LLD - Deep laterolog
LLS - Shallow laterolog
LN - Long normal
LNS - Least Normal Squares
LONG NOR - Long normal

m - Cementation exponent
M_1, M_2, M_{11}, M_2' - Monitoring electrodes
md - millidarcy
MEAS - Measured
meq/l - Milliequivalents per liter
MeV - Million electron volts
Mg - Magnesium
mg/kg - Milligrams per kilogram

mg/l - Milligrams per liter
mm - Millimeters
mmhos/m - Millimhos per meter
μmhos/cm - Micromhos per centimeter
μsec/foot - Microseconds per foot
μs - microsiemens
MINV - Microinverse
ML - Microlog
MLL - Microlaterolog
MLS - Mineral Logging Systems
Mn - Manganese
MNOR - Micronormal
MRIL - Magnetic Resonance Imaging Log
mS/m - Millisiemens per meter
MSFL - MicroSpherically Focused Log
mv - millivolt

N - Electrode
NA - Not Available
Na - Sodium
NaCl - Sodium Chloride
$NaCl_{Equiv.}$ - Sodium Chloride equivalent
Na (diff.) - Sodium by difference
$NaHCO_3$ - Sodium bicarbonate
NAT - Natural
NGS - Natural Gamma Ray Spectometry Log (Schlumberger)
NGWA - National Ground Water Association
NO_3 - Nitrate
NPHI - Neutron porosity

O - Oxygen
O, O′, OO′ - Electrodes
Ω - Ohm
ohm-cm - Ohm-centimeter
ohm-m - Ohm-meter

P - Permeable bed
PC - Personal computer
Pe - Photoelectric factor
PEF - Photoelectric factor
ϕ - porosity (phi)

PHIE - Effective porosity
PI - Phasor Induction
PI - Petroleum Information Corporation
pi - π
PL - Proximity Log
ppm - Parts per million
psi - Pounds per square inch
PSP - Pseudostatic SP
pu - Porosity units
PUB - Public
PVC - Polyvinylchloride

R - Resistivity
R - Receiver
Ra - Apparent resistivity
redox- Oxidation-reduction
Ri - Resistivity of the invaded zone
R_{ID} - Deep induction resistivity
$(R_{IL})cor$ - Corrected induction resistivity
R_{ILD} - Deep induction resistivity
R_{IM} - Medium induction resistivity
Rm - Mud resistivity
Rmc - Mudcake resistivity
Rmf - Mud filtrate resistivity
Rmfe - Equivalent mud filtrate resistivity
RMA - Reduced Major Axis
Ro - Resistivity of the uninvaded formation when it is 100% saturated with water
Ro_c - Corrected resistivity of the uninvaded formation when it is 100% saturated with water
Ro_H - High Ro value
Ro_L - Low Ro value
Rs - Resistivity of shoulder beds
R_{SFL} - Resistivity of the spherically focused log
Rt - Resitivity of the uninvaded formation
Rw - Water resistivity
Rwa - Apparent water resistivity
Rwe - Equivalent water resistivity
Rxo - Resistivity of the flushed zone

S - Siemens

SBR - Shoulder bed restivity
SDL - Spectral Density Log
SFL - Spherically Focused Log
SFLA - Averaged Spherically Focused Log
SFLU - Unaveraged Spherically Focused Log
SGR - Spectral Gamma Ray
SGR - Total gamma ray count, including uranium
SH - Shale
SH NORM - Short Normal
SI - International System
SiO_2 - Silica
SMIN - Synthetic microinverse curve
SMNO - Synthetic micronormal curve
SN - Short normal
SO_4 - Sulfate
SP - Spontaneous potential or self potential
SPR - Single-point resistance
SPWLA - Society of Professional Well Log Analysts
SRG - Natural Gamma Ray Spectral Log (Gearheart)
SSP - Static SP

TD - Total depth
TDH - Texas Department of Health
TDS - Total dissolved solids
TDS_{actual} - Actual total dissolved solids
$TDS_{calculated}$ - Calculated total dissolved solids
TDS-Cw - Total dissolved solids - specific conductance
TDSMEEQU - TDS calculated using the equation of the line fitting the TDS-Cw graph and CW MEAS
Temp - Temperature
TENS - Tension
Th - Thorium
TNPH - Thermal neutron porosity
TNRIS - Texas Natural Resources Information System
TWC - Texas Water Commission
TWDB - Texas Water Development Board

U - Uranium
USGS - United States Geological Survey

var. - variation

VCAL - Volume of calcite
VCL - Volume of clay
Vmea - Voltage measured
V_{sh} - Volume of shale
VQTZ - Volume of quartz

W - Water
WC & ID - Water Control & Improvement District
WIDCO - Well Investment Development Co.
WLS - Weighted Least Squares
WSC - Water Supply Corporation

X - Variables in formulas

Y - Variables in formulas

Z - Atomic number
ZDL - Compensated Z-Densilog

2Z - Halliburton designation, electrode spacing for normal
3iZ - Halliburton designation, electrode spacing for lateral
6FF28 - Schlumberger slimhole induction tool
6FF40 - Schlumberger deep induction curve
8FF34 - Schlumberger medium induction curve

LOGGING BOOKS

Appendix V

Modern Logging Books

Aguilera, R.: **Naturally Fractured Reservoirs**, Penn Well (1980), 703 pp. (800) 627-3212

Allaud, L. A. and Martin, M. H.: **Schlumberger, The History of a Technique**, John Wiley & Sons, Inc., New York City (1977), 333 pp.

Asquith, G. B.: **Log Analysis by Microcomputer**, Penn Well (1980), 104 pp.

Asquith, G. B. and Gibson, C.R.: **Basic Log Analysis for Geologists**, Methods in Exploration Series, AAPG, Tulsa (1982), 215 pp., AAPG, Box 979, Tulsa, Oklahoma 74101, (918) 584-2555.

Asquith, G. B.: **Handbook of Log Evaluation Techniques for Carbonate Reservoirs**, Methods in Exploration Series No. 5, AAPG, Tulsa (1985), 47 pp.

Atlas Wireline Services: **Fundamentals of Diplog Analysis**, Gulf Publishing Company, Houston (1988), 216 pp., Book Division, Dept MA, Box 2608, Houston, Texas 77252-2608, (713) 520-4444.

Bateman, R. M.: **Cased-Hole Log Analysis and Reservoir Performance Monitoring**, IHRDC Press, Boston (1984), 380 pp., IHRDC, 137 Newbury Street, Boston, Massachusetts 02116, (617) 536-0202.

Bateman, R. M.: **Log Quality Control**, IHRDC Press, Boston (1984), 398 pp.

Bateman, R. M.: **Open-Hole Log Analysis and Formation Evaluation**, IHRDC Press, Boston (1985), 647 pp.,

Brock, J.: **Analyzing Your Logs; Vol. I: Fundamentals of Open Hole Log Interpretation**, Petro-Media, Inc., Tyler (1984), 270 pp., 1729 Rose Road, Tyler, Texas 75701 (214) 592-8348, (also has video tapes).

Brock, J.: **Analyzing Your Logs, Vol. II: Advanced Open Hole Log Interpretation**, Petro-Media, Inc., Tyler (1984), 186 pp.

Brock, J.: **Applied Open-Hole Log Analysis**, Contributions in Petroleum Geology and Engineering, vol. 2, Gulf Publishing Company, Houston (1986), 292 pp.

Cased-Hole Logging, Oil and Gas Production Series, No. 5, The University of Texas at Austin, Austin (1981).

Crain, E. R.: **The Log Analysis Handbook, Vol. I--Quantitative Log Analysis Methods**, PennWell, Tulsa (1986), 684 pp.

Desbrandes, R.: **Encyclopedia of Well Logging**, Gulf Publishing Company, Houston (1985), 585 pp.

Dewan, J. T.: **Essentials of Modern Open-Hole Log Interpretation**, Penn Well, Tulsa (1983), 360 pp.

Doveton, J. H.: **Log Analysis of Subsurface Geology--Concepts and Computer Methods**, John Wiley & Sons, Inc., New York City (1986) 273 pp.

Ellis, D. V.: **Well Logging for Earth Scientists**, Elsevier Science Publishing Company, Inc., New York City (1987) 532 pp.

Etnyre, Lee M.: **Finding Oil and Gas from Well Logs**, Van Nostrand Reinhold (1989), 305 pp.

Foster, Norman H. and Beaumont, Edward A. (editors): **Formation Evaluation I: Log Evaluation**, AAPG, Tulsa, Treatise Reprint Series. 742 pp.

Foster, Norman H. and Beaumont, Edward A. (editors): **Formation Evaluation II: Log Interpretation**, AAPG, Tulsa, Treatise Reprint Series. 600 pp.

Galperin, E. I.: **Vertical Seismic Profiling and Its Exploration Potential**, P. Kennett, editor, E. Reidel Publishing Company, Dordrecht, Holland (1985).

Glossary of Terms & Expressions Used in Well Logging, second edition, Society of Professional Well Log Analysts, Houston (1984), 74 pp.

Gore, N.: **Wireline Operations**, Oil and Gas Production Series, J. Paxson, editor, The University of Texas at Austin, Austin (1984), 80 pp.

Gruner, Schlumberger, A.: **The Schlumberger Adventure**, Arco Publishing, Inc., New York City (1982).

Hallenburg, J. K.: **Geophysical Logging for Mineral and Engineering Applications**, Penn Well (1984), 264 pp.

Hearst, J. R. and Nelson, P. H.: **Well Logging for Physical Properties**, McGraw-Hill Book Company, New York City (1985), 576 pp.

Helander, D. P.: **Fundamentals of Formation Evaluation**, Oil and Gas Consultants International (OGCI) Publications, Tulsa (1983), 344 pp., OGCI, 4554 South Harvard, Tulsa, Oklahoma, 74135, (918) 742-7057.

Hilchie, D. W.: **Advanced Well Log Interpretation**, Douglas W. Hilchie Inc, Golden Co. (1989), variously paginated. 37 Perkins St., Prescott, Arizona 86301.

Hilchie, D. W.: **Applied Openhole Log Interpretation for Geologists and Engineers**, Douglas W. Hilchie Inc., Golden, Co. (1978), variously paginated.

Hilchie, D. W.: **The Geologic Well Log Interpreter**, Douglas W. Hilchie, Inc., Golden, Co., (1987), variously paginated.

Hilchie, D.W.: **Wireline: A History of the Well Logging and Perforating Business in the Oil Fields**, Boulder, Co. (1990), 200 pp.

Hill, A. Daniel: **Production Logging--Theoretical and Interpretive Elements:** Society of Petroleum Engineers, Monograph Volume 14, Dallas (1990), 154 pp., SPE Box 833836, Richardson, Tx. 75083 (800) 527-6863 (Texas) (214) 669-3377.

Hurst, A., Lovell, M. A. and Morton, A. C., editors: **Geological Applications of Wireline Logs**, Geological Society of London Special Publication (1990), No. 48, 357 pp. Order from AAPG.

Johnson, David E. and Pile, Kathryne E.: **Well Logging for the Nontechnical Person**, Penn Well (1988), 200 pp.

Jorden, J. R. and Campbell, F. L.: **Well Logging I--Rock Properties, Borehole Environment, Mud and Temperature Logging**, Society of Petroleum Engineers, Monograph Volume 9, Dallas (1984), 167 pp.

Jorden, J. R. and Cambell, F.L.: **Well Logging II--Electric and Acoustic Logging**, Society of Petroleum Engineers, Monograph Volume 10, Dallas (1986), 182 pp.

Kerzner, Mark: **Image Processing in Well Log Analysis**, IHRDC Press, Boston (1986), 140 pp.

Keys, W. Scott: **Borehole Geophysics Applied to Ground-Water Investigations**, USGS Open-File Report 87-539 (1988), 305 pp. NGWA Bookstore, Box 182039, Dept. 017, Columbus, Ohio 42018. TWI O2-E2

Kobranova, V.N. , English Translation by V.V. Kuznetsov: **Petrophysics**, Springer Verlag, New York (1990), 375 pp.

Labo, J.: **A Practical Introduction to Borehole Geophysics--An Overview of Wireline Well Logging Principles for Geophysicists**, Society of Exploration Geophysicists (1987), 330 pp., Box 702740, Tulsa, OK 74170-2740 (918) 493-3516.

Merkel, R. H.: **Well Log Formation Evaluation**, Continuing Education Course Note Series No. 14, AAPG, Tulsa (1983), 82 pp.

Open-Hole Logging, Oil and Gas Production Series No. 4, The University of Texas at Austin, Austin (1984), 87 pp.

Paillet, Frederick L. and Cheng, C.H.: **Acoustic Waves in Boreholes**, CRC Press, 000 Corporate Blvd. Boca Raton, Florida, 33431 407/994-0555 176 pp. $89.95

Pirson, S. J.: **Geologic Well Log Analysis**, third edition, Gulf Publishing Company, Houston (1983), 476 pp.

Repsold, H.: **Well Logging in Groundwater Development**, International Association of Hydrogeologist, International Contributions to Hydrogeology, v. 9, 136 pp. Verlag Heinz Heise GmbH & Co. KG (1989) 136 pp. Hannover, West Germany. Box 610407, D-3000 Hannover 61, West Germany.

Rider, M. H.: **The Geological Interpretation of Well Logs**, John Wiley & Sons, New York (1986) 175 pp.

Schlumberger: **Log Interpretation Principles/Applications**, Schlumberger Educational Services, Houston (1989), Document No. SMP-7017, variously paginated.

Schlumberger: **Cased Hole Log interpretation principles/Applications**, Schlumberger Educational Services Houston (1990), Document No. SMP-7025, variously paginated.

Sengel, E. W.: **Well Logging Handbook**, Institute for Energy Development (IED), Oklahoma City (1984), 168 pp.

Serra, O.: **Fundamentals of Well-Log Interpretation, Vol. I: The Acquisition of Logging Data**, Elsevier Science Publishing Company Inc., Developments in Petroleum Science, No. 15A, New York City (1984), 423 pp.

Serra, O.: **Fundamentals of Well-Log Interpretation, Vol. II: The Interpretation of Logging Data**, Elsevier Science Publishing Company Inc, Developments in Petroleum Science, No. 15B, Amsterdam (1986), 684 pp.

Serra, O.: **Sedimentary Environments From Wireline Logs**, Schlumberger Technical Services, Paris, Document No. M-081030/SMP-7008 (1985), 211 pp.

Theys, Phillips P.: **Log Data Acquisition and Quality Control**, Gulf Publishing, Houston (1991), 380 pp.

Tittman, J.: **Geophysical Well Logging**, excerpted from **Methods in Experimental Physics Vol. 24: Geophysics**, Academic Press, Inc., New York (1986), 175 pp.

Ward, Stanley H., editor: **Geotechnical and Environmental Geophysics, v. 1, Review and Tutorial**, Society of Exploration Geophysicists.

Ward, Stanley H., editor: **Geotechnical and Environmental Geophysics, v. 2, Environmental and Groundwater**, Society of Exploration Geophysicists.

Ward, Stanley H., editor: **Geotechnical and Environmental Geophysics, v. 3, Geotechnical**, Society of Exploration Geophysicists.

Well Log Response Chart, Penn Well (1983).

Wireline Logging Tool Catalog, second edition, Gulf Publishing Co. (1984) 450 pp.

Wireline Operations and Procedures, second edition, Vocational Training Series, American Petroleum Institute, Dallas (1983) No. 5.

Wyllie, M. R. J.: **The Fundamentals of Well Log Interpretation**, third edition, Academic Press, Inc., New York City (1963).

Old Electric Log Books

The Art of Ancient Log Analysis, Houston SPWLA (1979), 131 pp., plus reprints of 22 classic papers.
Society of Professional Well Log Analysts
6001 Gulf Freeway, Suite 129
Houston, Texas 77023 (713) 928-8925

Handbook of Well Log Analysis for Oil and Gas Formation Evaluation, Sylvain J. Pirson, Prentice-Hall, Inc.: Englewood Cliffs, New Jersey (1963), Chapters 7-12.

Old (pre-1958) Electrical Log Interpretation, Douglas Hilchie (1979), 163 pp.
Douglas Hilchie, Inc.
37 Perkins St.
Prescott, Az. 86301

Practical Log Analysis, a series of reprints from the Oil and Gas Journal, pp. 45-56 are on old logs.
Penn Well
Box 21288
Tulsa, Oklahoma 74121 800/627-3212

Prospecting with Old E-Logs, R. W. Frank (1986), 161 pp.
Schlumberger Educational Services
Box 2175
Houston, Texas 77252 (713) 928-4920

Printed on recycled paper

EQUAL OPPORTUNITY EMPLOYER

The Texas Water Development Board does not discriminate on the basis of race, color, national origin, sex, religion, age, or disability in employment or the provision of services, programs, or activities.

1-800-RELAY TX *(for the hearing impaired)*

Well Name: TWDB SITE F 88-59-411

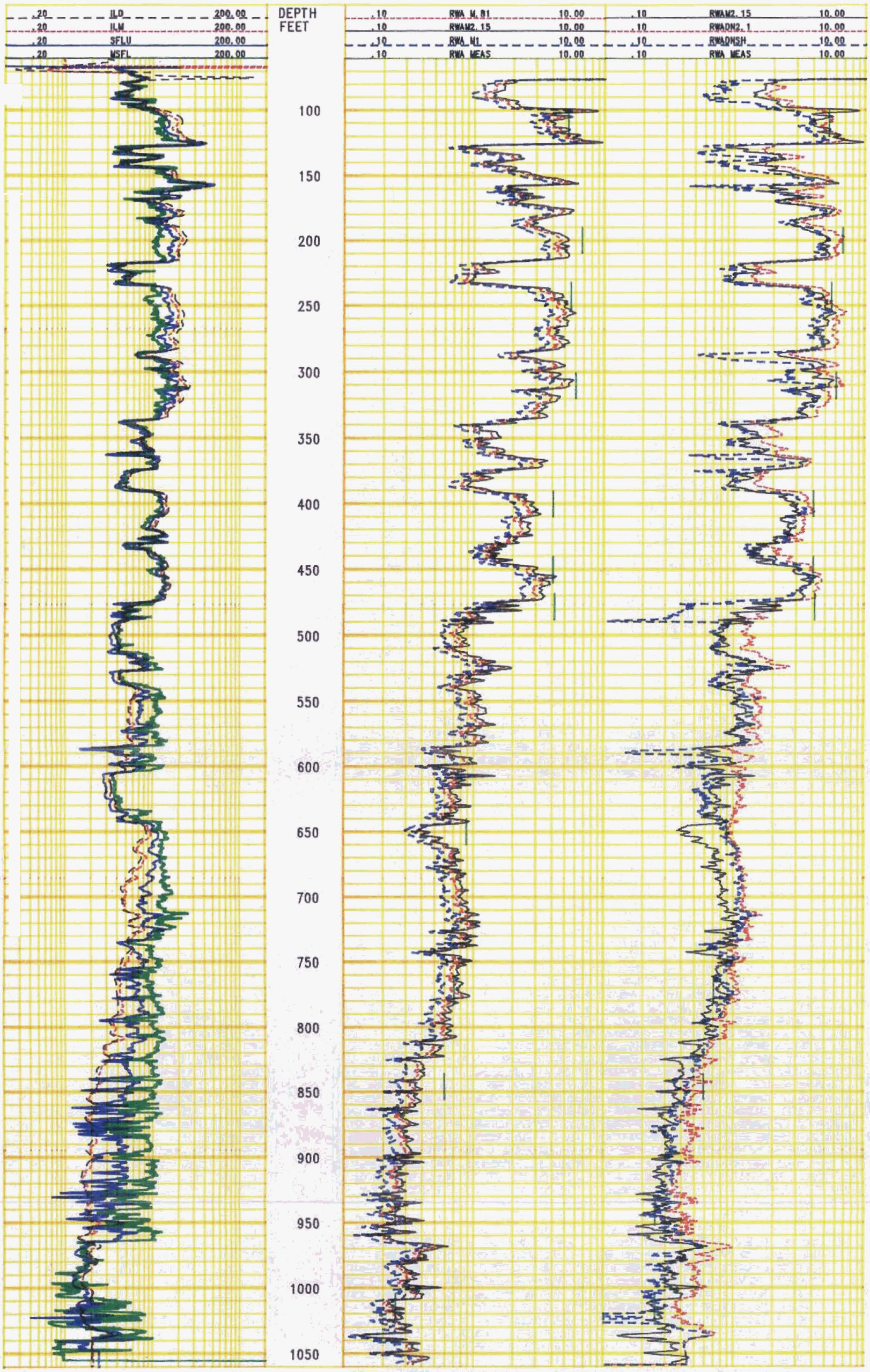

PLATE 1. Rw calculated by the Formation Factor method using different a, m, and porosity values. Track 1 contains deep induction (ILD), medium induction (ILM), unaveraged spherically focused (SFLU), and microspherically focused logs (MSFL). The MSFL has been borehole corrected. Tracks 2 and 3 contain Rwa curves calculated by the Formation Factor Equation using five different sets of variables and Rw values calculated from the ionic concentrations of water samples taken during pump tests (RWA MEAS). There were discrepancies in the measured conductivity values, so calculated values were used instead. All curves in tracks 2 and 3 have been normalized to 77 ° F. The Rwa curves in track 2 were calculated from density porosity (2.65 g/cm^3 matrix density) using either $1/\phi^{.81}$ (RWA M.81), $.62/\phi^{2.15}$ (RWAM2.15), or $1/\phi^2$ (RWA M1). The RWAM2.15 curve is the most accurate of the three. This is because the aquifers are high porosity unconsolidated sandstones, which is the appropriate geological environment for $.62/\phi^{2.15}$. As predicted by Figure 14-15, the RWA M.81 curve has Rw values that are close but slightly lower than the RWAM2.15 curve and the RWA M1 values are even lower. All three Rwa curves in track 3 were calculated with $.62/\phi^{2.15}$ and different porosity curves: density porosity (RWAM2.15 from track 2), density-neutron crossplot porosity (RWADN2.1) and density-neutron crossplot porosity corrected for shale (RWADNSH). Overall, the RWADN2.1 curve has the most accurate Rw values. The curve utilizing only density porosity has Rw values nearly as accurate as the two lithology corrected curves. This is because the density curve is affected very little by shale. Thin section analysis of core samples and the PEF curve (Plate 4) revealed that the mineralogy includes calcite and shale. The spiky nature of the curves, due to thin beds and washouts, illustrates the advantage of calculating Rw over entire formations rather than at a few specific depths. It is much easier to determine the best Rw value for a formation by scanning the curve for the entire interval. Track 1 shows that the invasion profile changes down the borehole from Rw > Rmf to Rw = Rmf to Rw < Rmf. Bottomhole temperature is 110° F at 1060 feet. The well is the TWDB PUB Test Well Site F, Cameron County, Texas (state well number 88-59-411). Plates 2 to 4 and Figures 13-12, 14-13, and 14-20 contain additional data on this well.

Well Name: TWDB SITE F 88-59-411

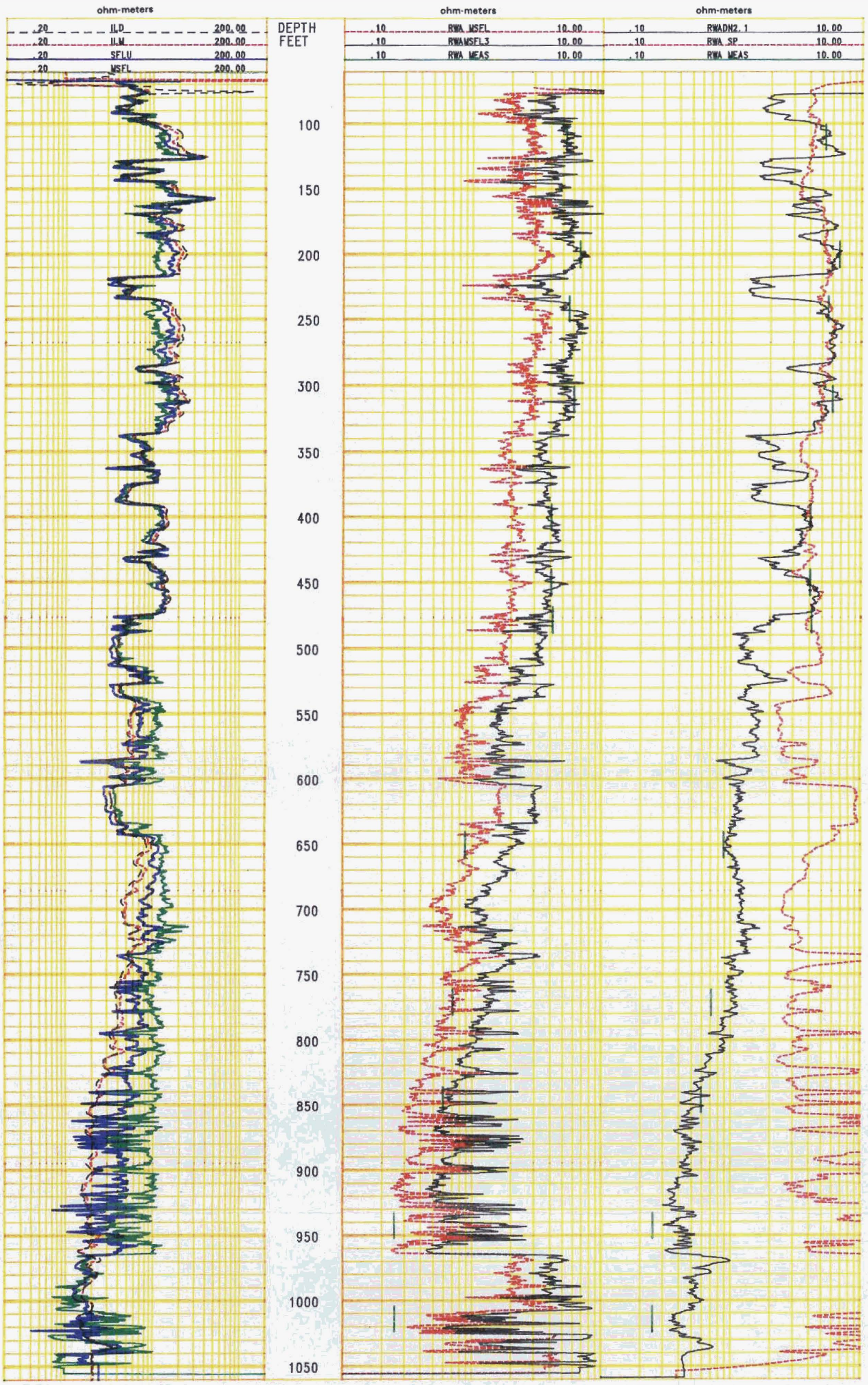

PLATE 2. Rw calculated by the Resistivity Ratio and SP methods. Track 1 contains Dual Induction and Microspherically Focused resistivity (MSFL) logs. Track 2 contains Rw curves calculated by the Resistivity Ratio method using the MSFL curve for Rxo. The drilling report and the log header reported different Rmf values, so Rw curves were calculated for each Rmf value: 1.77 ohm-meters @ 77° F from the log header (RWA MSFL) and 3.3 ohm-meters @ 77° F from the drilling report (RWAMSFL3). Neither curve is accurate for the bottom 100 feet of the borehole. This is to be expected since there is little invasion over this interval (refer to the invasion profile in track 1). Overall, the RWA MSFL curve is very accurate. Track 3 contains Rw curves calculated by the Formation Factor Equation (RWADN2.1, refer to Plate 1 for details) and SP (RWA SP) methods. The RWADN2.1 curve is very accurate for most of the borehole. The RWA SP is very accurate down to 500 feet, but it reads much too high below 500 feet and is very spiky. The sandstones are very thinly bedded below 700 feet, which means that the SP curve is reading much less than SSP. This would result in calculated Rw values that are much too high, just as are present on the RWA SP curve. Correcting the SP curve for thin bed effects would significantly improve the calculated Rw values. The error may also be due, in part, to significant differences in the water chemistry between the two intervals (confirmed by the water analyses) and/or differences in the membrane potential of the shales. The radioactive interval at 480 feet, which may be an unconformity, lends support to the idea that the shales on each side of 480 feet are diffferent. Rw values (RWA MEAS) are calculated from the ionic concentrations of water samples taken during pump tests . All curves in tracks 2 and 3 have been normalized to 77 ° F. The well is the TWDB PUB Test Well Site F, Cameron County, Texas (state well number 88-59-411). Plates 1, 3, and 4 and Figures 13-12, 14-13, and 14-20 contain additional data on this well.

Well Name: TWDB SITE F 88-59-411

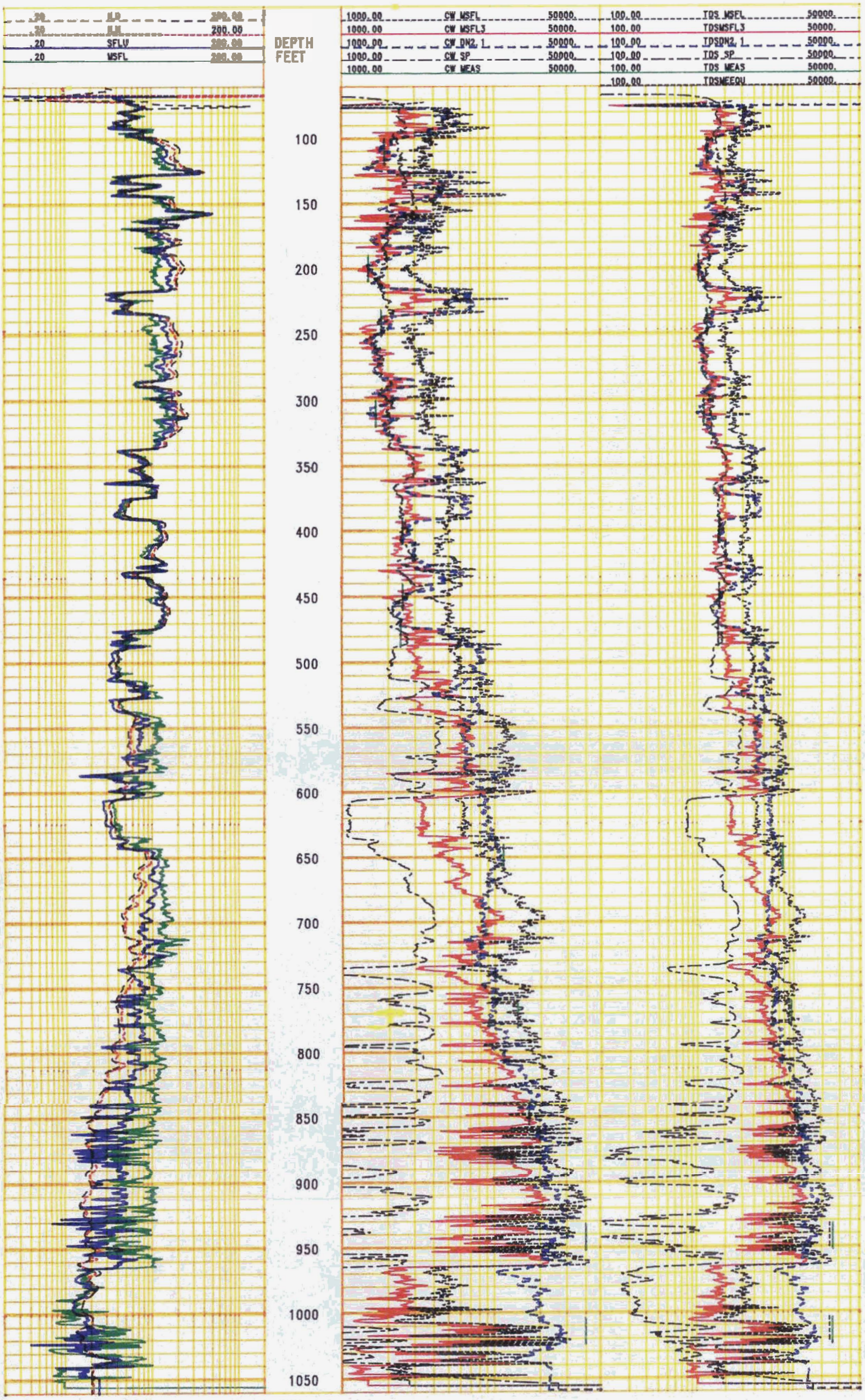

PLATE 3. Comparison of water conductivity (Cw) and TDS curves calculated by Resistivity Ratio, Formation Factor Equation, and SP methods. Track 1 contains Dual Induction and Microspherically Focused (MSFL) logs. Track 2 contains four Cw curves calculated from Rw curves on Plates 1 and 2. CW MEAS was calculated from the RWA MEAS data. Track 3 contains TDS curves calculated from the Cw curves in track 2 using the equation of the line fitting a TDS-Cw graph that includes Cameron County (Figure 14-17). The TDS curves in track 3 demonstrate that accurate TDS values can be calculated from logs and that the accuracy increases if several methods are used and the entire well is evaluated. The TDS MEAS values are from the water analyses, and the TDSMEEQU values were calculated using the equation of the line fitting the TDS-Cw graph and CW MEAS values. Comparison of the TDS MEAS and TDSMEEQU values confirms that accurate TDS values can be calculated from TDS-CW graphs. TDSMEEQU is greater than TDS MEAS below 480 feet, which is the depth at which the water chemistry changes. All curves in tracks 2 and 3 have been normalized to 77 ° F. The well is the TWDB PUB Test Well Site F, Cameron County, Texas (state well number 88-59-411). Plates 1, 2, and 4 and Figures 13-12, 14-13, and 14-20 contain additional data on this well.

Well Name: TWDB SITE F 88-59-411

SP in mv, GR in API units, CALI in inches

ohm-meters

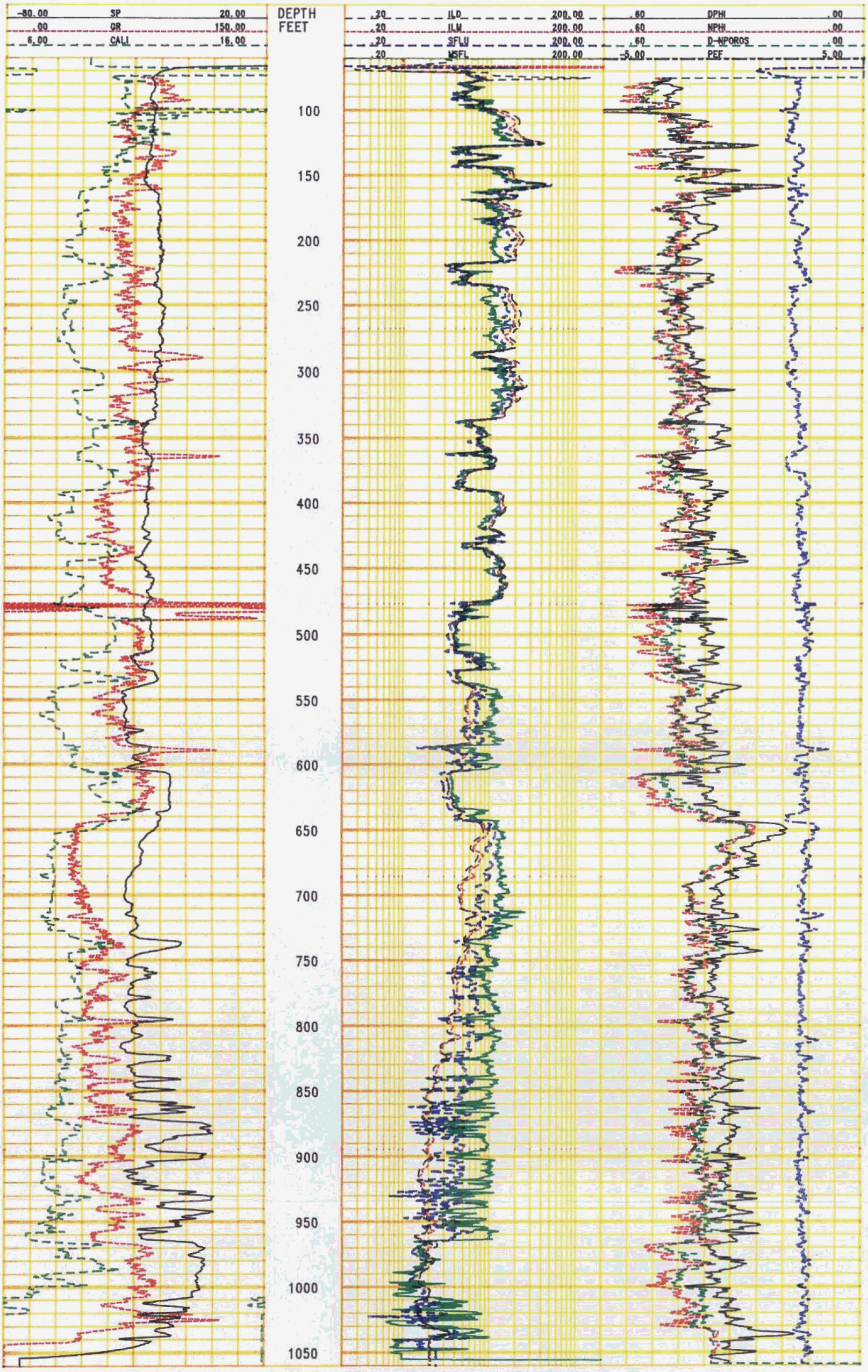

PLATE 4. Logging suite used to calculate water quality. Track 1 contains SP, gamma ray corrected for borehole effects (GR), and caliper (CALI). Track 2 contains Dual Induction and Microspherically Focused resistivity (MSFL) curves. The MSFL has been corrected for borehole effects. Track 3 contains density porosity (DPHI), neutron porosity (NPHI), density-neutron crossplot porosity (D-NPOROS), and photoelectric factor (PEF) curves. The porosity curves are calculated on a sandstone matrix. The well is the TWDB PUB Test Well Site F, Cameron County, Texas (state well number 88-59-411). Plates 1 to 3 and Figures 13-12, 14-13, and 14-20 contain additional data on this well.

Well Name: NEW BRAUNFELS A-1

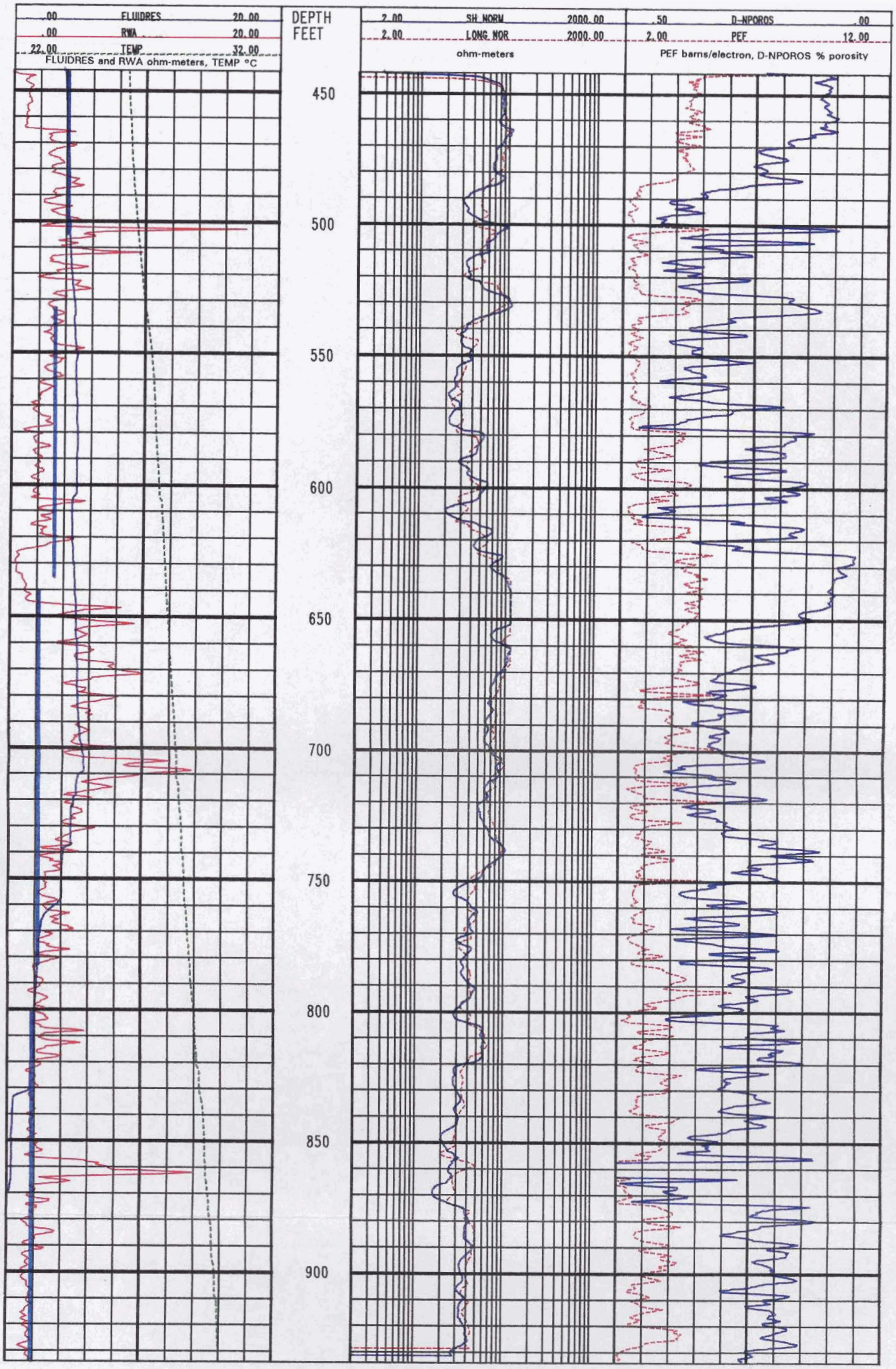

PLATE 5. Rw calculated by the Formation Factor method. Track 1 contains fluid resistivity (FLUIDRES) and temperature curves, along with an RWA curve calculated by the Formation Factor method using $1/\phi^2$, unaveraged spherically focused resistivity values (not shown), and lithology corrected porosity values (track 3). The blue vertical lines are measured Rw values from water samples taken during pump tests. There is excellent agreement between the RWA curve and measured Rw values. Spikes in the RWA curve are due to thin intervals that cannot be accurately measured by the resistivity and porosity tools, resulting in inaccurate RWA calculations for these intervals. However, averaging the RWA curve for a large interval gives an accurate picture of Rw. RWA is less than RW above 650 feet. This may be due to surface conductance. This interpretation is supported by the fact that as water salinity decreases below 650 feet, the RWA and Rw overlay. The RWA curve may be accurately reflecting an increase in water salinity below 650 feet, which the composite water sample taken over the entire interval cannot show. The RWA curve clearly shows transitions in water quality throughout the entire borehole. Track 2 contains short normal (SH NORM) and long normal (LONG NOR) curves. The two curves agree so well because the drilling fluid was formation water and there is no invasion. Differences in the normal curves are due to the different vertical resolution of each tool. Track 3 contains density-neutron crossplot porosity (D-NPOROS) and photoelectric factor (PEF) curves . The lithology is alternating limestone and dolomite, so only a crossplot porosity curve will be accurate. At 635 to 652 feet on the normal logs the curves show a false flat top because the curves went off scale on the hard copy of the log from which the curves were digitized. This is a well in the Edwards aquifer, New Braunfels, Texas. The well is the Edwards Underground Water District, A-1 (state well number 68-23-616). The bit size is 7 ⅞ inches. Figures 13-32 and 14-19 contain additional information on this well. Poteet, Collier, and Maclay (1992) contains a detailed petrophysical analysis of this well.